Gezamenlijke opleiding Universiteit Hasselt en KU Leuven

2016•2017
FACULTEIT INDUSTRIËLE INGENIEURSWETENSCHAPPEN
master in de industriële wetenschappen: bouwkunde

Masterproef

Impact of cyclic loading on shear screwed connections used in steel cold-formed structures

Promotor :
Prof. dr. Jose GOUVEIA HENRIQUES

Copromotor :
De heer Dan DRAGAN

Promotor :
ing. MARK BROUWERS

Chris Gielen , Karsten Moreels
Scriptie ingediend tot het behalen van de graad van master in de industriële wetenschappen: bouwkunde

2016•2017

Faculteit Industriële ingenieurswetenschappen

master in de industriële wetenschappen: bouwkunde

Masterproef

Impact of cyclic loading on shear screwed connections used in steel cold-formed structures

Promotor :
Prof. dr. Jose GOUVEIA HENRIQUES

Copromotor :
De heer Dan DRAGAN

Promotor :
ing. MARK BROUWERS

Chris Gielen , Karsten Moreels

Scriptie ingediend tot het behalen van de graad van master in de industriële wetenschappen: bouwkunde

Introduction

The end of our academic journey, as well as an important chapter of our lives, is approaching. The completion of a masters includes a thesis. We completed this thesis in combination with an educational internship in one semester. During the writing process of this thesis, we examined the behaviour of a screwed connection of a LSF-structure under the influence of both a monotonic and a cyclic load. The main reason we chose this subject is the growing interest in the subject ‘’steel’’ while taking the classes ‘’Hout en staal 2’’ and ‘’Bouwkundig project’’ in the last year of our masters.

In particularly, we would like to thank prof. dr. ir. José Gouveia Henriques for the excellent guidance during the writing of our thesis. Ir. Dan Dragan, PhD student at Uhasselt also deserves a word of thanks for the support during the execution of the tests. We would also like to express our gratitude towards Mark Brouwers, engineer in IT at the company CBZ, to provide us with the necessary test materials which were needed to execute the experimental tests. Finally, we would like to thank our parents for giving us the opportunity to start this study and also finish it.

Thank you!

Chris Gielen & Karsten Moreels
Master Industriële Ingenieurswetenschappen
Universiteit Hasselt & Universiteit Leuven

Woord vooraf

Het einde van onze opleiding, alsook een belangrijk hoofdstuk uit ons leven, is in zicht. Bij het afronden van een masteropleiding hoort uiteraard ook een thesis, deze hebben we in combinatie met een leerrijke stage in één semester afgerond. Tijdens het maken van dit eindwerk onderzochten we het gedrag van een schroefverbinding bij een LSF-structuur onder invloed van zowel monotonische als cyclische belasting. De motivering om te kiezen voor dit onderwerp is gegroeid naarmate onze interesse voor staal vorig jaar gegroeid is tijdens de lessen van ‘’Hout en staal 2’’ en tijdens ons bouwkundig project.

Graag zouden we in het bijzonder prof. dr. ir. Jose Gouveia Henriques willen bedanken voor de uitstekende begeleiding tijdens het schrijven aan onze thesis. Ook ir. Dan Dragan, doctoraatstudent aan Uhasselt, verdient via deze weg een dankwoordje voor de begeleiding tijdens het uitvoeren van de testen. Daarnaast willen we ook nog onze dank betuigen aan Mark Brouwers, ingenieur in de ICT bij het bedrijf CBZ, om ons de nodige testmaterialen te verschaffen die nodig waren voor de uitvoering van de testen. Tot slot willen we graag onze ouders bedanken, zij hebben ons immers de kans gegeven om deze studie te beginnen en te beëindigen.

Hartelijk Dank!

Chris Gielen & Karsten Moreels
Master Industriële Ingenieurswetenschappen
Universiteit Hasselt & Universiteit Leuven

Table of contents

List of figures

List of tables

List of graphs

Abstract - English

Light steel framing (LSF) has been increasingly used in the last couple of years. The appliance of LSF has been evolved from secondary elements, as the construction of interior walls and false ceilings, to primary applications, as the construction of facades of multi-story buildings and the main structure of houses. Up to today, the behaviour of LSF-connections under cyclic loading has not been described explicitly. The general purpose of this master thesis is to analyse and to describe the behaviour of the screwed connection of an LSF construction subjected to cyclic loading.

The analysis of the screwed connection is executed in three approaches, namely: the analytical approach, the experimental approach and the numerical approach. For the first, the Eurocode 3 was used as a reference document. The experimental approach was accomplished through the execution of laboratory tests and for the numerical approach the software ABAQUS was used to reproduce the experimental tests.

From this research there can be concluded that the influence of cyclic loading on a screwed connection of and LSF structure is nil, the strength and the stiffness of the connection are nor substantially affected by the introduction of a cyclic loading. However, this result had still room for improvement, it is possible to use better equipment (fully automatic) and to use other profiles (C-profiles) to finally achieve a more uniform result.

Abstract - Nederlands

Light steel framing (LSF) wordt tegenwoordig steeds vaker gebruikt in de constructiewereld. De toepassing van LSF is in de laatste jaren geëvolueerd van secundaire toepassingen zoals het maken van binnenmuren, valse plafonds… naar primaire functies zoals het uitvoeren van volledige gevels voor gebouwen van meerdere verdiepingen. Over het gedrag van de verbindingen tussen LSF-structuren onder cyclische belasting is tot op heden nog zeer weinig geweten. Deze masterproef heeft als doel om het gedrag van de schroefverbinding onder zowel monotone als cyclische belasting te analyseren en te beschrijven.

De analyse van de verbinding gebeurt door middel van 3 methodes, namelijk: Een analytische methode, een experimentele methode en een numerieke methode. Voor de analytische methode wordt er gebruik gemaakt van de formules uit Eurocode 3, de experimentele werd uitgevoerd door middel van testen en bij de numerieke methode werd er gebruik gemaakt van het softwarepakket ‘’ABAQUS’’.

Uit dit onderzoek is gebleken dat de invloed van cyclische belasting op een schroefverbinding bij LSF nihil is, de sterkte en de stijfheid van de verbinding worden vrijwel niet aangetast door het invoeren van een cyclische belasting. Dit resultaat is echter nog voor verbetering vatbaar, door het gebruiken van beter testmateriaal (vol automatisch) en andere profielen (c-profielen) is het mogelijk om uiteindelijk een meer uniform resultaat te bekomen.

I. General introduction

1.1 Introduction to the subject (LSF structures)

Cold-formed light steel framing is sheet steel that is formed into shapes and sizes similar to wooden lumber. Light steel framing structures (LSF) have been increasingly used due to its good thermal performance (when insulation and other materials are added) and structural performances. This building technology has entered the market several years ago and has gained great popularity and credibility in the past few years. Its growing popularity is attributed to its low-cost transportation, easy installation and its lightweight design. [1] Cold formed steel framing makes the steel shapes by passing steel sheets between large rollers to deform the steel. The rolling process deforms and stretches the steel, hardening it in its process. Most cold rolled steel is either 227,53 MPa or 344,74 MPa yield strength. [2] The profiles that can be made are the following:

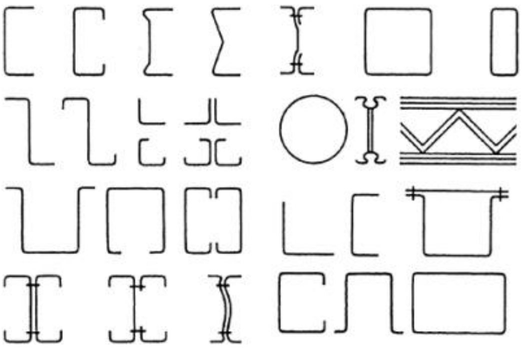
[3]

Figure 1: List of cold-formed profiles

After the production of the cold formed light steel framing profiles, the profiles can be used to construct multi-story buildings. For the construction of the building, the profiles are connected using mostly screws.

To make a connection between the LSF-profiles (to use them while constructing a multi-story building) self-drilling screws are being used. The walls are prefabricated in the factory, that's why the connections of the profiles need to withstand a certain cyclic loading (because of the vibrations while transporting the profiles). This cyclic loading can also appear when there's an earthquake (See chapter 2.5 for more information about cyclic loading) or wind action.

1.1.1. Advantages of cold formed light steel framing

1) Steel framing can lower the construction cost because of its high warranty: Steel cannot split, shrink or warp.
2) Steel can be recycled without losing its properties; these savings also translate into a lower cost.
3) Steel framing is easy to handle because it weighs 1/3 less than wooden studs and can also be installed at 6cm on centre.
4) There has always been a market advantage of steel because customers recognise steel as a superior framing product for its fundamental characteristics:
    - Long term maintenance costs are reduced because steel is resistant to rot, mold, termite and insect infestation.
    - Good indoor air quality (IAQ) is promoted because steel does not emit volatile organic compounds (VOCs).
    - Steel is "Green" because it contains a minimum of 25% recycled steel and is 100% recyclable.
    - Steel framing has proven performance in high wind and seismic zones.

5) LSF have a big corrosion resistance because of its construction system. Steel itself has a very bad performance when subjected to elevated temperature but when it’s used with other high quality materials, the total system can have high performances such as a big corrosion resistance.
6) LSF have a big fire resistance.
7) LSF is resistant to termites.
8) LSF have a high seismic and lightning resistance. [4]

1.2 Research Approach

1.2.1. Background

Our research will cover the behaviour of screwed connections in shear, undergoing a cycling loading in a cold-formed steel (CFS) structure. To make it more understandable each part of our test setup will briefly be explained in the following paragraphs.

“Cold-formed steel (CFS) is the common term for products made by rolling or pressing steel into semi-finished or finished goods at relatively low temperatures (cold working)” [5]. This thesis will focus on one material in particular, light-steel farming also known as LSF. Light-steel framing is part of the ‘cold-formed family’ because it is made in the same way but the thickness of the materials is rather small varying from 0,5 to 3 mm. The thin steel sheets are bent, pressed or rolled in a way so it can be used in construction. LSF has found its way on the construction market in several countries. In Belgium however it is not yet a known standard product for construction. The specimens used for this research are all LSF-products with a thickness of 1,5 mm.
The connection between the thin steel sheets will be made using self-tapping screws. For each test a different setup of screws will be applied. In total 4 different tests will be executed with 1-, 2- and 4-screw connections.

The main purpose of testing procedures in the near future is the appliance of cycling loading. A lot of constructions in modern day life are influenced by this type of load. Cyclic loads can be found all around us ranging from wind loads to earthquakes and even vibrations induced by transportation and heavy machinery. Cycling loading is a way of applying loads onto the test specimen in such a way that the specimen is undergoing stresses at one point in time and not being exposed to loads at another point in time.

1.2.2. Question

However, nowadays the behaviour of shear screwed connections in steel cold formed structures subjected to a monotonic loading is well known, there is less knowledge about the behaviour of the connections subjected to cyclic loading. Because of the lack of knowledge about the latter, this thesis was performed.

The strength of the connections will be analysed in 3 different approaches, in particular:
1. Theoretical calculation of the test specimens
2. Testing
3. Finite element modelling (FE-modelling)

The 3 approaches will be compared throughout the thesis.

1.2.3. Objectives

The general aim of this study is to check the behaviour of screwed connections used in steel cold-formed structures, subjected to cyclic loading.

The first objective is the analytical estimation of the test specimens (screw connections subjected to monotonic shear loading) according to Eurocode. Both the dimensions of the test specimens and the strength of the types of connections are going to be determined, as described in the Eurocode.

Secondly, the connections are going to be tested through experimental characterization of the screwed connections subjected to monotonic and cyclic shear loading. These loads will affect the different types of connections. After the tests have been performed, the calculation of the first objective will be compared with the results of the tests.

Finally, a finite element simulation to reproduce first the monotonic behaviour and secondly, in case the time is sufficient, begin the simulation under cyclic loading. The program which is being used to develop the finite element method is ‘Abaqus’. The results of this finite element method will also be compared with the other results.

1.2.4. Method and materials

To bring this thesis along with its experiments to a successful conclusion it is important to follow a well-organized and fairly simple schedule. This schedule, see ‘Planning Thesis.pdf’, is constructed in such a way that it is easily visible on when a certain task needs to be finished or how long we have to finish each task. The guideline throughout our schedule consists out of ‘tasks’. For this part, we have 4 major tasks to consider.

The first task is the ‘pre-research’. Pre-research is a term used for every part of the research which happens in advance of the actual testing and calculation of our specimens. This includes a literature study, an on-sight inspection of the available equipment and a meeting with the company who will provide us the necessary materials. This company is called CBZ NV and is located in Zutendaal, Belgium.

The next step in the process is the ‘theoretical approach’. This includes every calculation according to Eurocode and the specimen drawings. This is a rather important step in the process as every part after this is based on what we have calculated and drawn in this step.
The ‘experimental stage’ is the 3rd step in our research. This includes the actual testing of the specimen but also the ordering of our specimen. The testing will take place in 2 different setups. The first one is with a static load on each different specimen. The results of the static loading tests will then be compared with the results of the cyclic loading tests. A detailed examination between the two setups will be made along with a conclusion.

At this point we have two results to work with, the results from the theoretical approach and the ones from the actual experiments. To make this research even more reliable a 3rd approach will be added, the ‘numerical approach’. Here we will use software specifically designed to calculate the results of our test setups using finite element methods. The software that will be used is called ‘Abaqus’ by ‘Dassault Systemes’.

1.3 Thesis outline

The goal of this thesis is to create a document which gives a global view of the behaviour of screwed connections subjected to a cyclic loading. First, the behaviour of the screwed connection subjected to a static load is going to be described. Secondly, the behaviour of the screwed connection subjected to a cyclic load is going to be described. Then, a global comparison between the two behaviours is going to be made. This comparison will give a global view of a connection subjected to a cyclic load.

II. Literature review on screw connections

2.1 Different types of connections in LSF

2.1.1. Screws

The main purpose of LSF-constructing is to keep it easy and simple to build prefabricated systems, that's why fasteners are mostly being used to perform the steel-steel connections. Basically, there are three head styles and two point styles, namely:

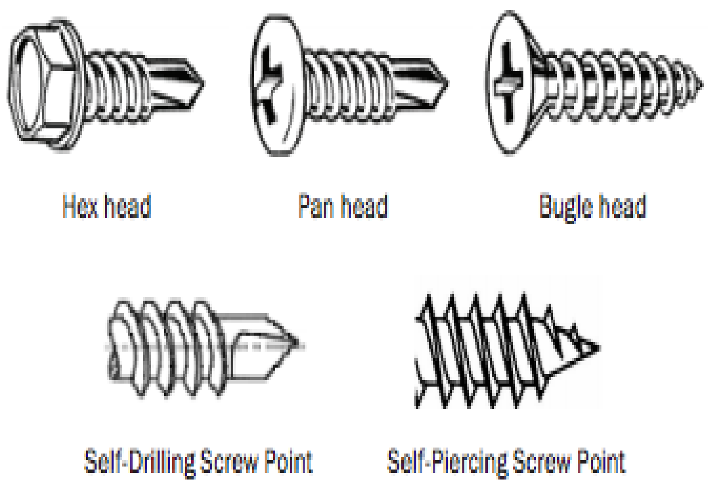

Figure 2: Types of fasteners

1) Hex heads: Hex heads are mostly used when the fasteners won't be covered by another material like a drywall. After the connection is made, you can see the head above the surface of the material.
2) Pan heads: Pan heads have almost the same application as the hex hades, only the shape of the head is different.
3) Bugle heads: Bugle heads are mostly used when the head needs to countersink into the material, the heads are not visible above the surface of the material.
4) Self- drilling screw point: Self- drilling screw points are being used when you are working with a thicker steel material. The screws have the ability to drill their own hole and form or cut their own internal mating threads without breaking during the assembly. Self-drilling screws are high-strength, one-piece, one-side-installation fasteners.
5) Self- piercing screw point: Self- piercing screw points are mostly being used when you need to penetrate thinner materials like interior drywall studs. The screws have the ability to penetrate the material and tap their own mating threads when driven. [6]

Other than the fasteners that are described above, there can also be used other fasteners. The only other alternative while working with steel-to-steel connections are pneumatically-driven fasteners, powder-actuated fasteners, crimping and riveting.

2.1.2. Pins

Pins fasteners are fairly new to the cold-formed steel framing industry. This technique of connecting is very similar to the nail connections of wooden structures; nail guns are also used to connect the steel pieces together. The advantage of pinned connections is that they are very easy to use, there is only needed a pneumatic nail gun and a pin to make the connection. Also, the pins can be installed up to 10 times faster than screws. The disadvantage of the pins is the holding strength; this strength is a lot greater when screws are being used. Loose pins can also create annoying squeaks in floor systems and the cost of the pins can be up to 5 times more than the cost of screws. Pins are rarely used to create a steel connection due to the small resistance against cyclic loading.

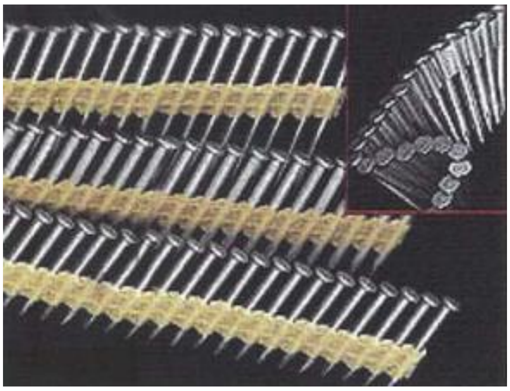

Figure 3: Collated pins

2.1.3. Clinching

Clinching is a method for connecting sheet materials and profiles without the use of screws, rivets or other fasteners. When clinching, one part of the steel is pressed into the adjacent steel, in a button or stitch configuration. The advantage of clinching is the fact that there are no consumables needed in the process (such as screws or pins). Also, the connection can be made in less than a second and it creates a relatively flat surface. The biggest disadvantage of clinching is the fact that it’s very difficult to use the big tools in the field, the tools are all rather bulky. Also, if a clinch is made in the wrong place, the connection had to be drilled or cut out. There are no easy ways to remove the connection without destroying the metal.

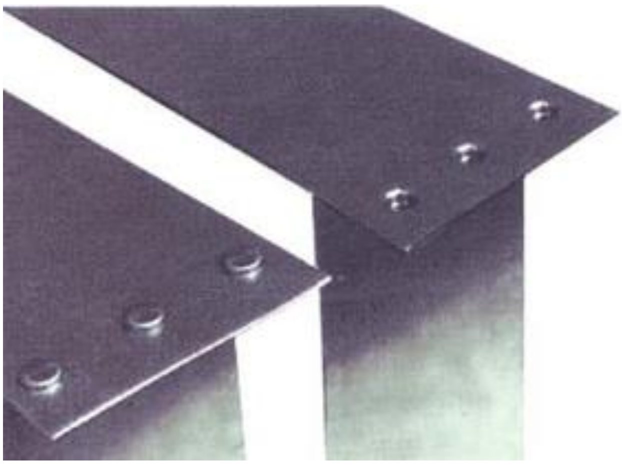

Figure 4: Clinching connection

2.1.4. Welds

Welding had been used very limited while making a LSF-connection. Most often this method is done in a fabricant plant with big plates/profiles. Weld can provide a very strong connection but it’s not very fast nor easy to create on the construction site.

2.1.5. Bolts

Just like the welded connection, the bolted connection is mostly used when connection heavy structural elements. The advantage of a bolted connection is the strength, the disadvantage would be that the connection requires three separate pieces of hardware (bolt, washer and nut).

2.1.6. Clip-together systems

Clip-together systems consist of specially formed components that are designed to lock into place without the use of fasteners such as screws. The use of these types of connections are limited to non-bearing walls and other non-structural elements because the strength of these is not very high. These connections have been very successful for partition walls. The advantage of these connection is the fact that they can be fastened very quickly and most can be dismantled very easy without destroying the metal. Most clip together systems are not approved for load bearing conditions unless additional fasteners are being used. [7]

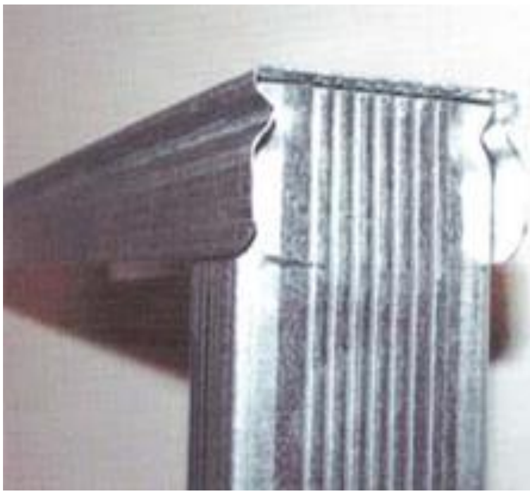

Figure 5: Clip-together connection

2.2 Advantages and disadvantages of screw connections

2.2.1. Advantages

The biggest advantage of screws is that they are widely available, standardized and the tool costs are very low. The installation also requires little training and mistakes can easily be fixed by withdrawing the screw out of the plate. Also, screwed connections have been recognised and included in most building codes and industry standards. The use of screw tools is also a positive influence on the ergonomic aspect of the construction of connections. [7]

2.2.2. Disadvantages

The biggest disadvantage of the screws is the fact that it takes longer to make the connection in comparison to some other techniques (see 2.1 types of connections) such as clinching and pinned connections. Also, because there is not used a washer, the load will be concentrated under the head. When applying the screw to a smooth surface, it can be possible that the screw will make a displacement and that makes it harder to make the connection (in comparison to a screw connection in wood where the screw will always be in place). [7]

2.3 Definition of screw connections in shear LSF

To get a better understanding of what a screwed connection in shear is, we can split this up into 2 subjects: the screwed connection and shear forces. A screw connection is typically a connection between two or more parts using a screw. This screw ensures that the fastened materials are kept in place and can withstand a certain force. As mentioned before there are a lot of different types of screws, each having its own qualities and usages. Next we have the factor shear. Shear forces are forces acting along on a surface of a material. These forces seize perpendicular to the surface of the material. The following image gives an example of a force acting on 2 steel plates (with a thickness t) in a screw connection. The forces (force F and reaction force in the rigid connection) are working in different directions but along the same axis which causes both plate and screw do be undergoing stresses, often called shear stresses.

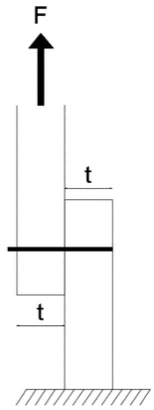

Figure 6: Applied forces on the system

These stresses however, can result in failures. The different failure modes will be explained in the following paragraph. Other detailed information about the behaviour of screws can be found in the Eurocodes. "The Eurocodes are the ten European standards (EN; harmonised technical rules) specifying how structural design should be conducted within the European Union (EU)." [8]

2.4 Behavior of screw connections under monotonic loading

2.4.1. General

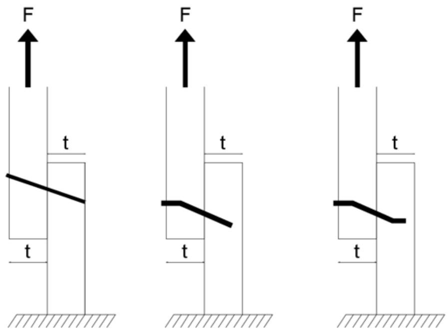

Figure 7: Screw failure modes

Monotonic loading, often referred to as static loading, are loads which exert a constant amount of force onto the material. There are different types of forces, but for our research the tensile and compressive strength are the most important ones. By applying these loads onto our test objects and increasing them will result in deformations. If the displacement of the objects exceeds its limits, then failures will occur. These failures can either be in the plates or in the connection (screw). The following images give a few examples of different failure modes. The most left connection is a typical example of a bearing failure of the plate. The plate being the weaker part of the connection will result in a deformation of the plate. Due to the widening of the hole, the screw is able to start tilting, the more force is being put on the connection. The other 2 images are an example of the screw being the weakest part of the connection. If the shear force exceeds the shear resistance of the screw, the screw will start deforming and eventually break. More detailed information can be found in the Eurocodes. The following paragraph will give an overview of some of the failure modes per Eurocode 'EN 1993-1-3: General rules - Supplementary rules for cold-formed members and sheeting.'

2.4.2. Code (Eurocode)

According to the official website, the EN Eurocodes serve as a reference documents and have the following purposes:

- *as a means to prove compliance of building and civil engineering works with the basic requirements of the Construction Products Regulation, particularly Basic Requirement 1 "Mechanical resistance and stability" and Basic Requirement 2 "Safety in case of fire";*
- *as a basis for specifying contracts for construction works and related engineering services;*

- *as a framework for drawing up harmonised technical specifications for construction products (ENs and ETAs).* [9]

Eurocode 3 is specifically developed to describe the design of steel structures using the limit state philosophy. Eurocode 3 consists of 20 documents each describing a different aspect of the design of steel structures. For our research purpose, the EN 1993-1-3: General rules – Supplementary rules for cold-formed members will be the most important document.

Table 8.2: Design resistances for self-tapping screws contains the necessary information about the different failure modes. Bearing resistance, net-section resistance and shear resistance are the values which will need to be examined. This is due to the fact that our system will be exposed to shear forces. The formulas for each resistance will be explained in a further paragraph. The following table gives a brief overview of the different failure modes according to Eurocode, clarified with an image. [10]

Failure mode	Description	Illustration
Bearing resistance	Bearing failure of the plate may occur when the strength of the plate is lower than the strength of the screw whilst the forces are increasing.	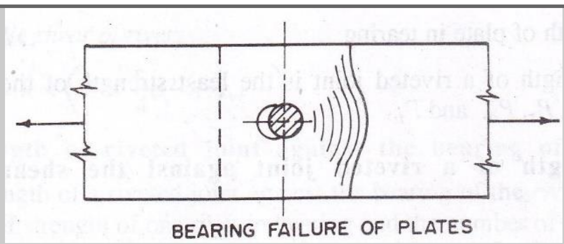
Net-section resistance	Net-section failure often referred to as tearing failure, may occur when the stiffness of the screws is higher than the stiffness from the plates. Can also occur when screw to edge distance isn't according to pre-calculated values.	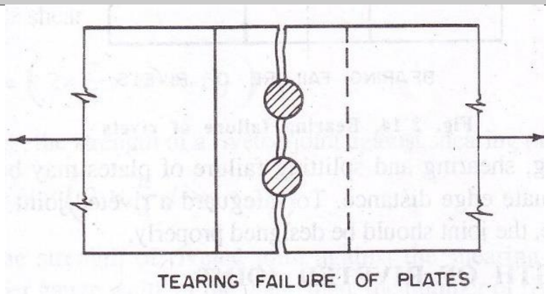
Shear resistance	Strength of the screw when exposed to perpendicular forces (shear forces). Screw may bend, break or rotate when increasing the forces.	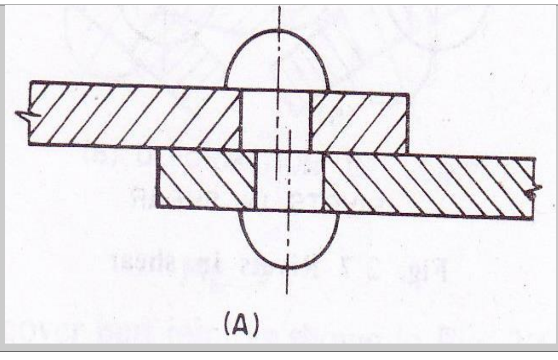

Table 1: Failure modes in screw connections subjected to shear

2.5 Behaviour of screw connections under cyclic loading

Cyclic loading is a way of applying forces onto the object that change over time but in a repetitive manner. This study is dedicated to see what the effect is of cyclic loading on screw connections. In pre-research however, not much has been found about the possible effect of cyclic forces. Other studies cover the effect of cyclic loading on bolted connections or the effect of cyclic loading on wooden structures. Since there is a lack of knowledge on this specific subject, it is therefore impossible to have a clear answer to what the effect of cycling loading on screw connections could be. By performing this study, the effect of cyclic loading will be covered and an unequivocal result will be given on how screws behave. This will be done using three different approaches; analytical, numerical and experimental.

2.6 Test procedure for cyclic loading

2.6.1. Introduction

To assess the behaviour of structural steel elements under cyclic loading, several tests were performed. This behaviour is important to know in the context of earthquake resistance design, because the real behaviour may be different than the response under monotonic loading.

A reference testing procedure for experiments considering cyclic loading of steel members or connections, is the procedure provided in the ECCS publication. [11] In the present research, this procedure was used as basis of the cyclic testing procedure. The ECCS cyclic testing procedure is described in detail hereafter.

2.6.2. Complete testing procedure

Each of the following tests are performed on a different specimen.

2.6.2.1. First test

The first test is a classical monotonic displacement test. The general purpose of this test is to define Fy^+ and ey^+ (Tension), with Fy^+ the positive conventional limit of the elastic range and ey^+ the positive displacement corresponding to that intersection. This test gives us the following F-e curve: [11]

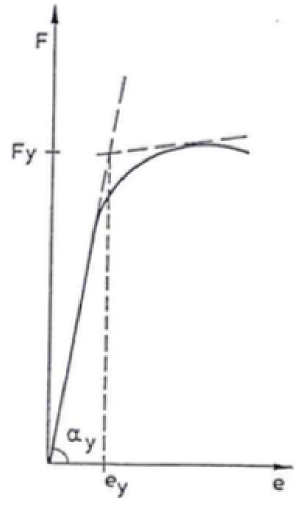

[11]

Figure 8: F-e curve

2.6.2.2. Second test

The second test that is going to be performed will also be a classical monotonic displacement increase test. In contrast to the first test, the second test will give us the negative conventional limit of the elastic range (Fy^-) and the positive displacement corresponding to that intersection (ey^-) (Compression). [11]

2.6.2.3. Third test

The third test is a cyclic test with an increase of the displacement. This test had the following characteristics:

1. One cycle in the $ey^+/4$, $ey^-/4$ interval
2. One cycle in the $2ey^+/4$, $2ey^-/4$ interval
3. One cycle in the $3ey^+/4$, $3ey^-/4$ interval
4. One cycle in the ey^+, ey^- interval
5. Three cycles in the $2ey^+$, $2ey^-$ interval
6. Three cycles in the $(2 +2n)ey^+$, $(2 +2n)ey^-$ interval with n=1,2,3,…. [11]

2.6.2.4. End of test

The test is ended at a certain level of force, this force was defined before the tests were executed. When there are other research requirements, the tests can also be stopped at a certain level of displacement. [11]

2.6.2.5. Combination of loads

The principles used in tests for combined loads are as follows:

The seismic load should be considered an accidental situation. Therefore, the values which are assigned to the actions of long duration should be the values which are most probable, while the short them duration actions, such as wind, should not be considered.
When there is an unsymmetrical demand on structural elements due to the combination of seismic action with long duration actions, the test can be performed with a partial reversal of displacement. This partial reversal should be defined in a proper matter. [11]

2.6.3. Alternative method

Because the test specimens can't withstand compression due to the low buckling resistance of the specimen, the ECCS procedure can't be performed. That's why an alternative testing method needed to be performed, a tension only test.
The applied force of the cycles in this test are determined after the monotonic tests are performed. The number of cycles was determined in other research papers, the average cycle of an earthquake is between 15 and 30 cycles, that's why there were performed 20 cycles in this alternative method.

2.6.3.1. Complete testing procedure (used in the experimental approach)

1. Fmax/4 (kN) Cycle 1
2. Fmax/4 (kN)
3. Fmax/2 (kN) Cycle 2
4. Fmax/2 (kN)
5. 3*Fmax/4 (kN)
6. 3*Fmax/4 (kN)
7. Fmax
8. Fmax
9. Fmax
10. Fmax
11. Fmax
12. Fmax
13. Fmax
14. Fmax
15. Fmax
16. Fmax

17. Fmax
18. Fmax
19. Fmax
20. Fmax
21. Fmax
22. Fmax
23. Fmax
24. Fmax
25. Fmax
26. Fmax
27. Fmax
28. Fmax
29. Fmax
30. Fmax
31. Fmax
32. Fmax
33. Fmax
34. Fmax
35. Fmax
36. Fmax
37. Fmax
38. Fmax
39. Fmax
40. Fmax

Cycle 20

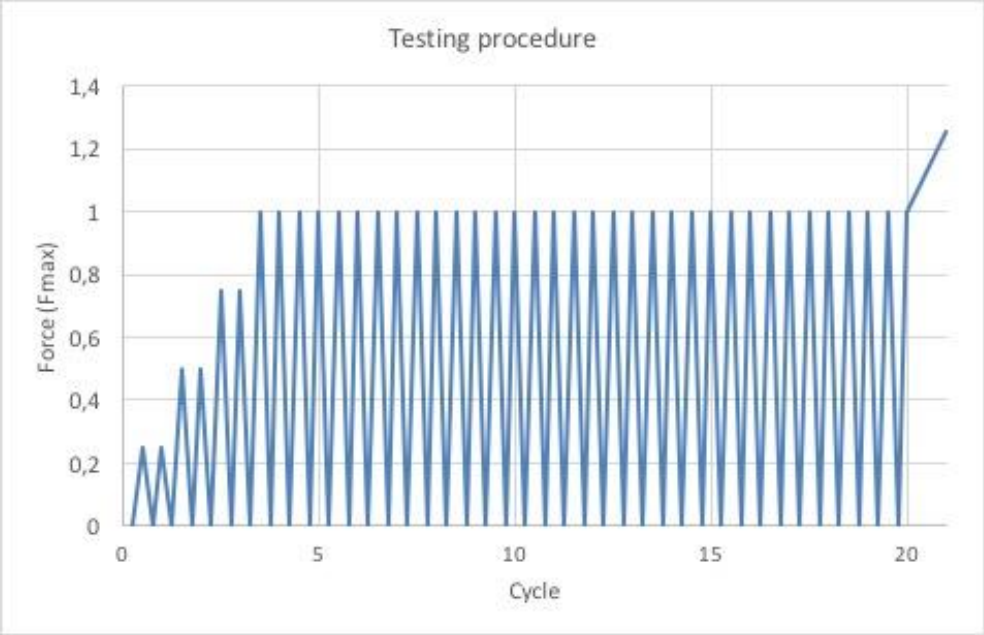

Figure 9: Testing procedure

41. Monotonic test until failure => Cycle 21

III. Theoretical approach

The theoretical approach is dedicated to the pre-research of the thesis. In this part the calculations and design were made according to the formulae drawn up by Eurocode. By using these formulas, we were able to make to the design of the different test specimens. The following paragraphs are dedicated to different formulas and design criteria. As an example, the 1-screw connection will be used to describe the calculation procedure.

3.1 Calculation of the connection resistance

There are a few different resistances that have an influence on the strength of a connection between materials. As explained in paragraph '*2.4.2. Code (Eurocode)'*, the code gives 3 different resistances; bearing resistance, net-section resistance and shear resistance. Because this study is dedicated to investigate the behaviour of a screwed connection in LSF-structures, *'Table 8.2 of the EN 1993-1-3'* [10] was used. The next step is to check if the screws are being loaded in shear or tension. For this study the test specimen will only be exposed to tensile forces on one side of the test setup. Therefor the screws will only be loaded in shear forces.

<u>*Bearing resistance*</u>
The first resistance that has to be verified is the bearing resistance of the plate. The bearing resistance can be calculated as following:

$$F_{b,Rd} = \alpha . f_u . d . t$$

The value for α is depending on the thickness of the plates. Since the plates have the same thickness of $t = t_1 = 1{,}5$ mm, α can be calculated as following:

$$\alpha = 3{,}2 . \sqrt{(t/d)} \text{ but } \alpha \leq 2{,}1$$

The only missing variable is the d, which is the nominal diameter of the fastener. The type of screw that was chosen for this study is the self-tapping screw with a diameter of 6,3 mm. By filling in previous equation, α = 1,56. The last variable is the ultimate tensile strength f_u. This information was given by the company who delivered the materials and f_u = 370 N/mm². By filling in the equation for $F_{b,Rd}$, we have calculated a bearing resistance of 5459,575 N ≈ <u>**5,46 kN**</u> per screw.

<u>*Net-section resistance*</u>
Net-section is the next resistance that has to be taken into account with. Net-section or often referred to as tearing failure of the plates is the failure mode in which the plate completely cracks along the axis of the screws. (See 'Table 1: Failure modes – screw connection' for the image of the failure type). The formula for the net-section resistance goes as follows:

$$F_{n,Rd} = A_{net} . f_u$$

The known variable in this equation is the ultimate tensile strength of the material (plate) f_u = 370 N/mm². A_{net} is the net cross-sectional area of the connected part. Depending on the number of screws this value can change. In this example, 1-screw connection, A_{net} can be calculated as following:

$$A_{net} = b.t$$
$$b = b\text{-}d$$

The width of the test specimen is depending on the number of screws. The width b = 50 mm for the 1-screw connection test specimen. For the 2- and 4-screw connections, a width of b = 70 mm will be used. The nominal diameter of the fastener stays the same on all of the tests, which is d = 6,3 mm. Filling in all of the parameters will give an A_{net} = 65,55 mm². This results in a net-section resistance of the plate of $F_{n,Rd}$ = 24253,5 N ≈ <u>**24,25 kN**</u>

Shear resistance

The last type of resistance according to the Eurocode, is the shear resistance. This value equals the strength of the fastener (screw) against shear forces. This value can only be determined by performing tests on the screw. Eurocode specifies the following formula:

$$F_{v,Rd} = F_{v,Rk}$$

In which $F_{v,Rk}$ can only be obtained by testing. The screws used in this study have a shear resistance of $F_{v,Rd}$ = **6,41 kN.** The diameter 6,3 mm screws were specifically chosen hence the fact that they have a higher resistance then the bearing resistance. This way theoretically the plate will start deforming first before the screws will fail.

Plasticity resistance

Plasticity resistance is the resistance of the material to plastic deformation. It gives the limit of stress at which point the material is no longer elastic but plastic. This resistance is not part of the strength of the connection and therefore not present in the same paragraph as the other resistances mentioned earlier. During the testing however, the displacement of the test specimen will be measured. To be sure that only the displacement of the connection is measured, the calculation of the plasticity resistance of the plate is made. The plasticity resistance is calculated using following method:

$$F_{pl} = \frac{Fy.A}{\gamma M0}$$

Where:

- F_y is equal to the yield strength of the plate material
- A is the surface of the plate material
- γ_{M0} is the partial factor and is equal to 1

For the 1-screw connection F_y = 318 N/mm² and A = 75 mm². The resistance to plastic deformation is therefore **F_{pl} = 23,85 kN**.

3.2 Calculation of the slip resistance

The test specimens are connected to the hydraulic jack and the steel framing using L-profiles. To avoid any deformation near the edges of the test specimens, the plates will be clamped between the L-profiles instead of using fasteners. This way of drilling the specimen can be avoided. This type of connection is based on the friction between the different materials. The tightening of the L-profiles with the test specimen in the middle will be done using bolts M16 class 8.8. The design slip resistance $F_{s,Rd}$ can be obtained as following:

$$F_{p,C} = 0,7.f_{ub}.A_s$$

Where f_{ub} is equal to the ultimate tensile strength of the bolt and A_s the cross-section of the bolt. For a class 8.8, f_{ub} = 800 N/mm² and A_s = 157 mm². Filling in the data gives $F_{p,C}$ = 87,92 kN. The design slip resistance $F_{s,Rd}$ can be obtained using the following formula:

$$F_{s,Rd} = \frac{ks\, n\, \mu}{\gamma M3} Fp, C$$

Where:

- k_s is given by 'Table 3.6: Values of k_s'
- n is the number of friction planes
- μ is the slip factor
- γ_{M3} is the safety factor

For the calculations the following values were taken:

- k_s = 1,0
- n = 1
- μ = 0,3

$\gamma_{M3} = 1,25$

After making the calculation, the slip resistance $F_{s,Rd}$ = 21,10 kN. This is the resistance of the plate assuming it was clamped using only one bolt. In our test setup 6 bolts will be used to tighten the plate between the L-profiles. The total slip resistance of the plate $F_{s,tot}$ = **126,60 kN**

3.3 Summary

The following table gives an overview of all the calculated resistances of the different connections. The calculations were made using the same method as described above. F_{pl} is the force of plasticity of the plates. It's the value at which the plate is going to start deforming in a plastic way. F_{con} is the lowest value from the calculated resistances. According to the calculations, this should always be the bearing resistance of the plates.

Number of connections				
Resistances	1	2	4	
$F_{b,Rd}$	**5,46**	**10,92**	**21,84**	
$F_{n,Rd}$	24,25	31,86	31,86	
$F_{v,Rd}$	6,41	12,82	25,64	
F_{pl}	23,85	33,39	33,39	
F_{con}	5,46	10,92	21,84	kN

Table 2: Maximum resistances

IV. Experimental program

4.1 General description

4.1.1. Objective

The research mainly focusses on the cyclic load-deformation of cold formed light steel connections, the deformation of the plates as well as the behaviour of the connections is going to be analysed. The objective of these tests is to observe the impact of the cyclic loading on the behaviour of the connection.

4.2 Experimental program

4.2.1. Number of tests

To perform the tests of the experimental program, 4 plates/profiles were used. The geometries to test are described in 4.2.2. First, each test specimen was exposed to a monotonic loading. These monotonic tests were performed two times on each test specimen. After the monotonic tests, there were performed three cyclic tests. In total there were performed 12 cyclic tests and 8 monotonic tests. The objective of the monotonic tests was to characterise the connection behaviour under monotonic loading to define the cyclic testing procedure and compare the specimen response under monotonic and cyclic loading. The order of the tests is like this:

Type of test specimen	Number of static tests - names	Number of cyclic tests - names
one-screwed connection	2 – 1S1 and 1S2	3 – 1C1, 1C2 and 1C3
Two-screwed connection	2 – 2S1 and 2S2	3 – 2C1, 2C2 and 2C3
Four-screwed connection	2 – 4S1 and 4S2	3 – 4C1, 4C2 and 4C3

Table 3: Number of tests

4.2.2. Geometries to test

To perform the tests, there were used 4 different test specimens. Because the height of the test set-up, the height of the test specimens needed to be the same for all the types of specimens. Because there was a free height of 760mm between the upper and the lower part of our test set-up, this was the height the test specimen needed to be.

An overview of the non-assembled test specimens (in mm) looks like this:

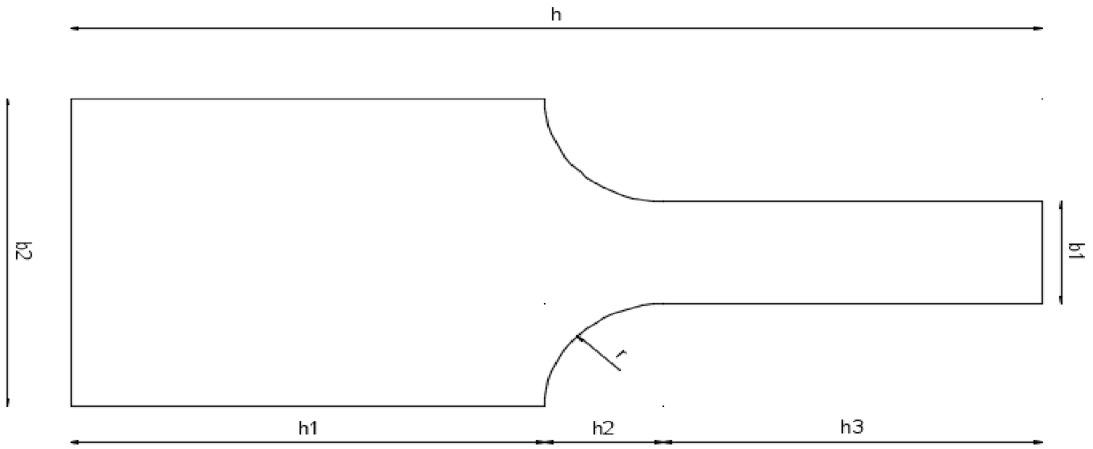

Figure 10: Non-assembled specimen

Type	H	B1	B2	H1	H2	H3	R
1 screw	410	50	150	200	50	160	50
2 screws	410	70	210	200	70	140	70
4 screws	425	70	210	200	70	155	70

Table 4: Properties of the different specimen

The screws that were used to assemble the plates have the following properties:

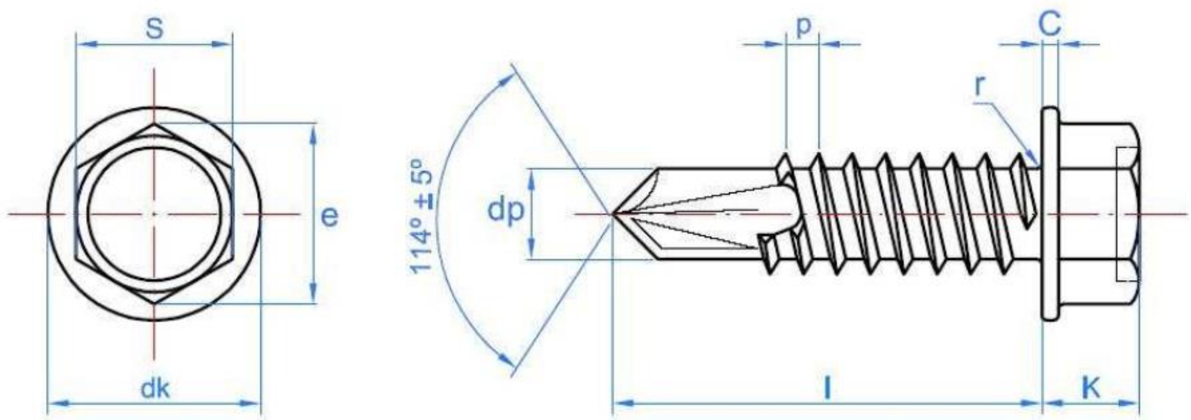

[12]

Figure 11: Properties of the screw

dk: Washer head diameter= 12,6mm
k: Head thickness= 6,3mm
c: Washer thickness= 2mm
s: Nut key= 10mm
D: Diameter outer thread= 6,25mm
d: Diameter inner thread= 4,88mm
p: Pitch= 1,8mm
l: Length of the screw= 16mm
[12]

Type	H	B1	B2	B3	B4	B5	H1	H2	H3	H4	H5	H6	H7	H8	H9
1 screw	760	150	150	25	0	25	200	50	100	30	0	30	100	50	200
2 screws	760	210	210	20	30	20	200	70	80	30	0	30	80	70	200
4 screws	760	210	210	20	30	20	200	70	65	30	30	30	65	70	200

Table 5: Properties of the assembled specimen

The assembly drawings look like this:

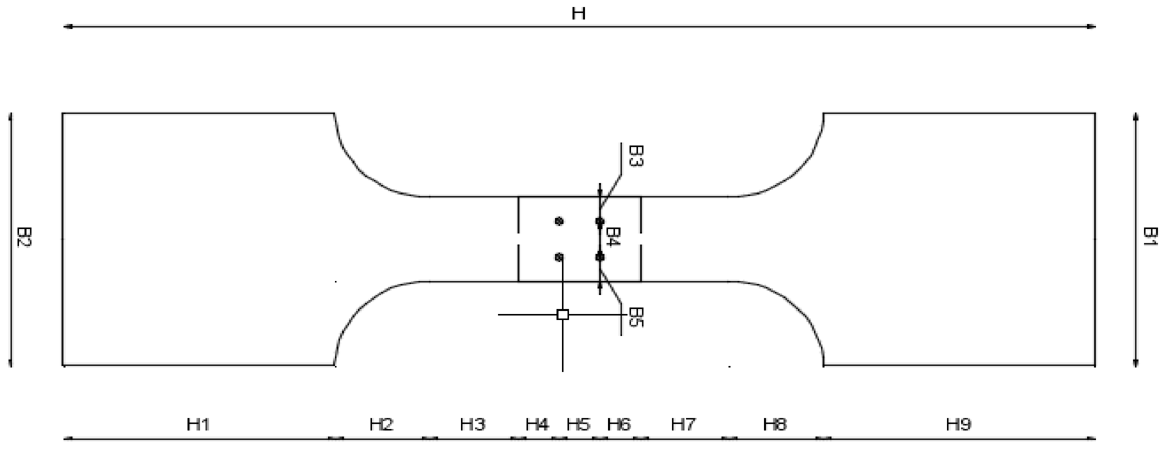

Figure 12: Assembly plate

4.3 Experimental layout and procedure

4.3.1. Scheme of the test setup

The total test setup consists of the following parts:

1) 4 x HEB300 -> Foundation
2) 4 x L-profiles
3) Test-specimen
4) Plate to fix the upper L-profiles
5) Load cell
6) Hydraulic jack
7) Plate to fix the hydraulic jack

The numbers can be found in the 3D-drawing of the test setup.

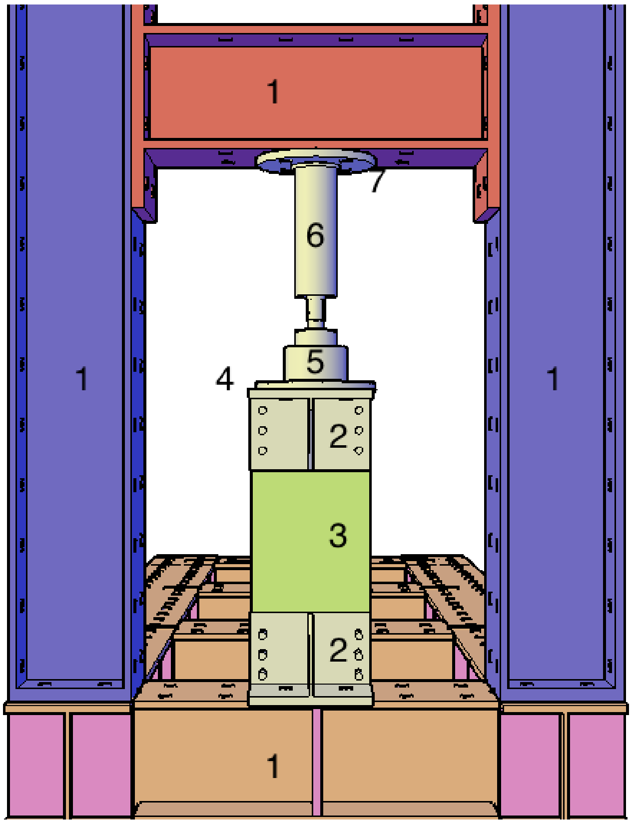

Figure 13: 3D test-setup

To perform the tests, a construction of HEB300-profiles is used to create the foundation. The prefabricated holes in the HEB300 have a diameter of 22mm, because of the pre-drilled holes, there were created L-profiles which can fit on the foundation to fixate the test-setup. The dimensions of the L-profiles are 200mmx200mmx20mm, such big L-profiles are being used to create a bigger friction between the test specimens and the profiles (bigger friction surface). No bolts were used to fixate the specimens. A detailed drawing of the L-profiles can be found in the attachments.
In between the 4 L-profiles, the test specimen can be found. This test specimen is fixed by friction. To create a connection between the upper L-profiles and the load cell, an aluminium plate with a thickness of 20mm is being used. A load cell was fixed to a hydraulic jack to simulate the forces, the load that is used is a U10-M with a height of 160mm. The hydraulic jack, which is fixed to the load cell, is a LDM 10-5/200 with a height of 330mm. To fixate the hydraulic jack to the HEB300, a circular plate of 20mm is being used.

4.3.2. Test procedure

The realization of the tests was based on four series of full-scale tests with specimens of different dimensions, based in practical solutions of steel screwed connections. Each series consisted of one of the four test specimens which are described in ‘’3.2.2. Geometries to test’’ and are tested both monotonic and cyclic. The specimens that are being used consist of 2 specimens of the same dimensions, connected with 1,2 or 4 self-tapping 6.3 screws with an overlap of 60mm-90mm. The full-scale testing program was done with tensile tests to determine the behaviour of the connections and the behaviour of the material. The experiments were conducted using a displacement tool (see 3.4.2 Placement of the monitoring devices) which measures the displacement of 2 stable points of the test specimen.

The cyclic testing methodology that was being used followed the ‘’alternative method’’ described in 2.3.3. The main outputs of the experiments were shear-force versus horizontal displacement.

4.4 Applying of the load

To apply the load on the test specimen, the following equipment was used:

1) A hand pump
2) A hydraulic jack
3) A load cell

A technical documentation of this equipment can be found in the attachments.

The way this setup works is like this:

1) The hand pump is connected to the hydraulic jack with 2 oil pipes. This oil is used to regulate the force of the hydraulic jack. [13]
2) The hydraulic jack, which is connected to the hand pump, is also connected to the load cell. The hydraulic jack can apply a load of up to 140T in both directions (tension and pressure). The maximum displacement that can be reached with the hydraulic jack is 200mm. [14]
3) The load cell, which is connected to the hydraulic jack, is also connected to the laptop and transduces the forces. In this way, the forces can be applied precisely on the test-specimen. [15]

4.5 Monitoring

4.5.1. Recording of the data

To record the data while performing the tests, linear variable differential transformers (LVDT) were used. An LVDT is a type of electrical transformer which can be used to measure the linear displacement between two points. The main principle of an LVDT is based on the principle of a transformer with three coils that are placed around a tube one after another. The center coil is primary, the two other coils are secondary and can be found at the outside of the LVDT. The two secondary coils need to have the same number of windings. A ferromagnetic core, for which the position needs to be measures, is attached to the object and slides along the axis of the tube. While moving, an alternating current goes through the primary coil and this causes an electrical voltage in each of the secondary coils which is proportional to the produced windings of the primary coil. The frequency of the LVDT is usually in the range 1 to 10 kHz. As the core moves, the voltage of the LVDT also changes. To measure the displacement, the voltage of the LVDT needed to be linked to a known displacement.

While performing the tests, two little L-profiles were connected to the test specimen. The two LVDT devices (a long and a short one) were placed against the L-profiles. While deforming, the spacing between the L-profiles was being measured by the LVDT devices which are connected to the laptop.

The results of the tests (force and displacement) were shown in a program. This software gave us an output in excel with all the recorded data. [16]

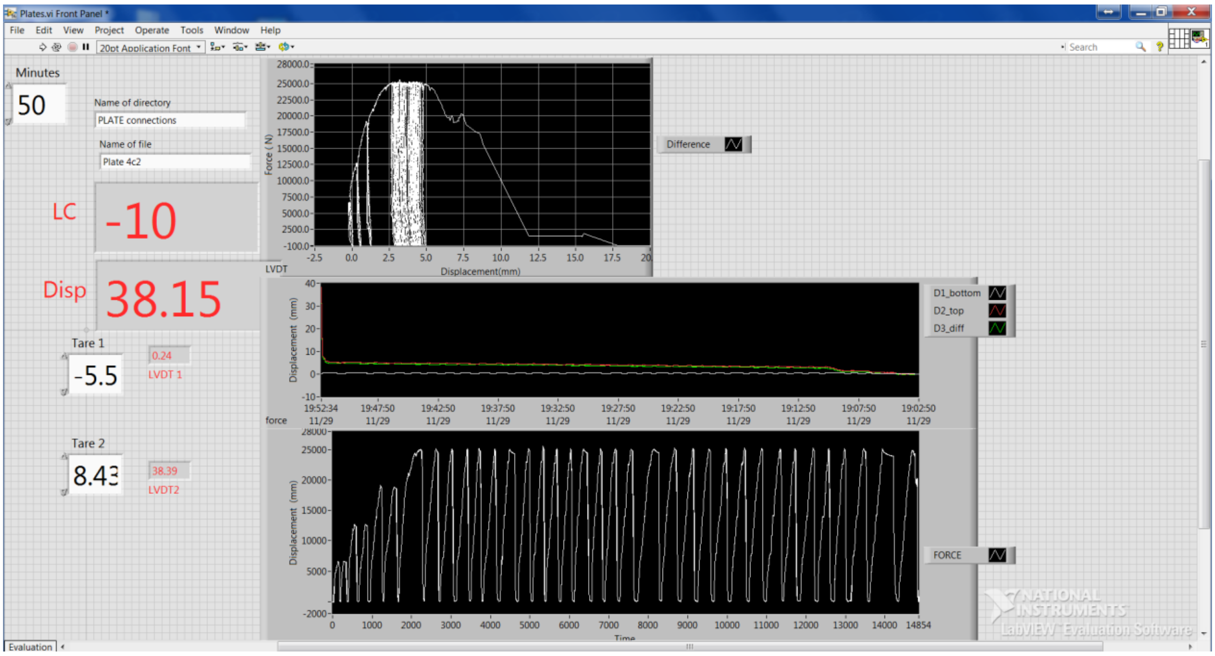

Figure 14: Labview printscreen

4.5.2. Location of the monitoring devices

The LVDT-devices were being placed at a steady construction next to the test setup. This construction needed to be very steady because every little displacement could affect the test results.

The calculation of the displacement and the placement of the monitoring devices is described in the following drawing:

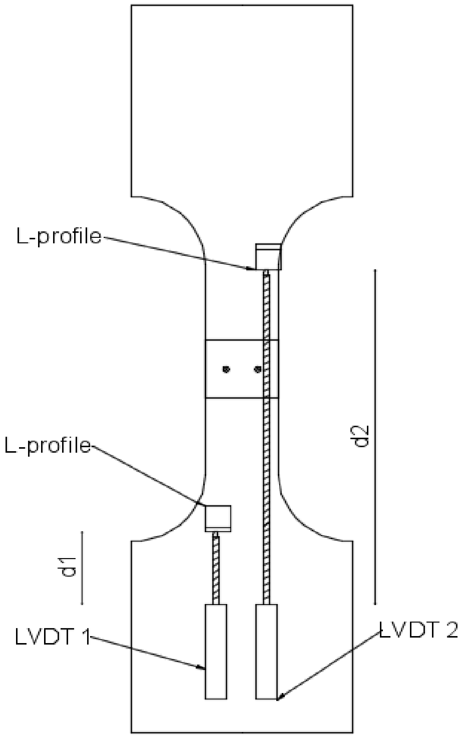

Figure 15: Placement of the LVDT's

To calculate the displacement of the connection, the displacement of the first LVDT was subtracted by the second LVDT: displacement d (mm)= d2 (mm) – d1 (mm).

4.6 Monotonic test results

After completing the tests, there was concluded that the behaviour of the connection was almost the same for all tests. The only big difference between the tests is the maximum resistance when the number of screws increases. Because of this fact, only the first test is described in detail, with pictures and comments. A Summary table of the other results can be found in paragraph 4.7.

4.6.1. One screwed connection

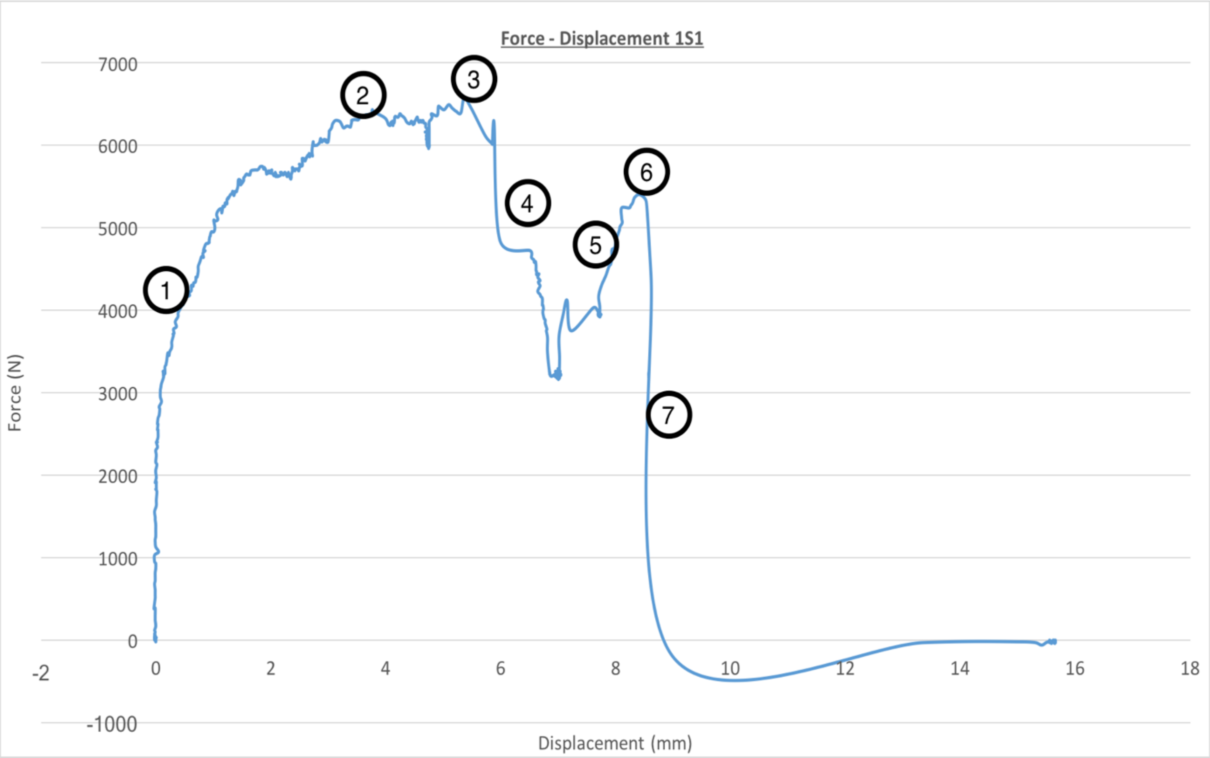

Graph 1: Force-displacement 1S1

The test results will be described based on the Force-displacement curves. The numbers on the graph correspond to the numbers down below. The connection behaved as follows:

1) The screw started tilting at 4,27 kN. => Picture 1
2) While tilting, the displacement of the system keeps increasing while the force is almost constant between 6kN and 6,5 kN. This represents the first plateau.
3) The connection reaches its maximum resistance of 6,57 kN. Once the screw reaches its maximum resistance, the material starts bearing. => Picture 2
4) Due to the bearing of the plate, there is a sudden decrease of the force.
5) After the maximum bearing is achieved, the screw starts tilting more. At a certain tilting level, the thread of the screw will be behind the plate. At that moment the force increases. => Picture 3
6) The screw reaches its maximum tilting resistance without getting out of the plate. => Picture 3
7) The connection fails and the screws get out of the plates. => Picture 4

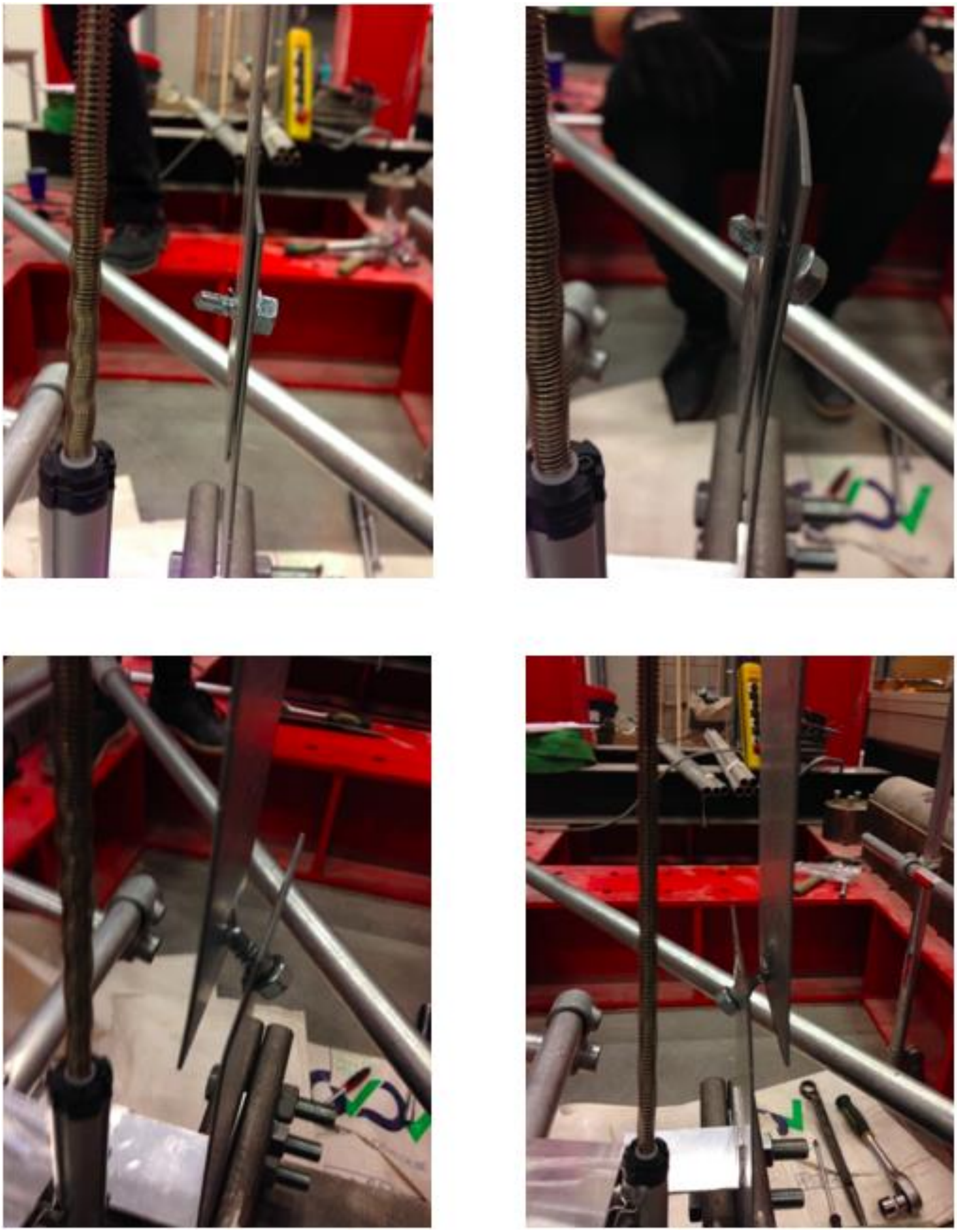

Figure 16: Pictures of the tests

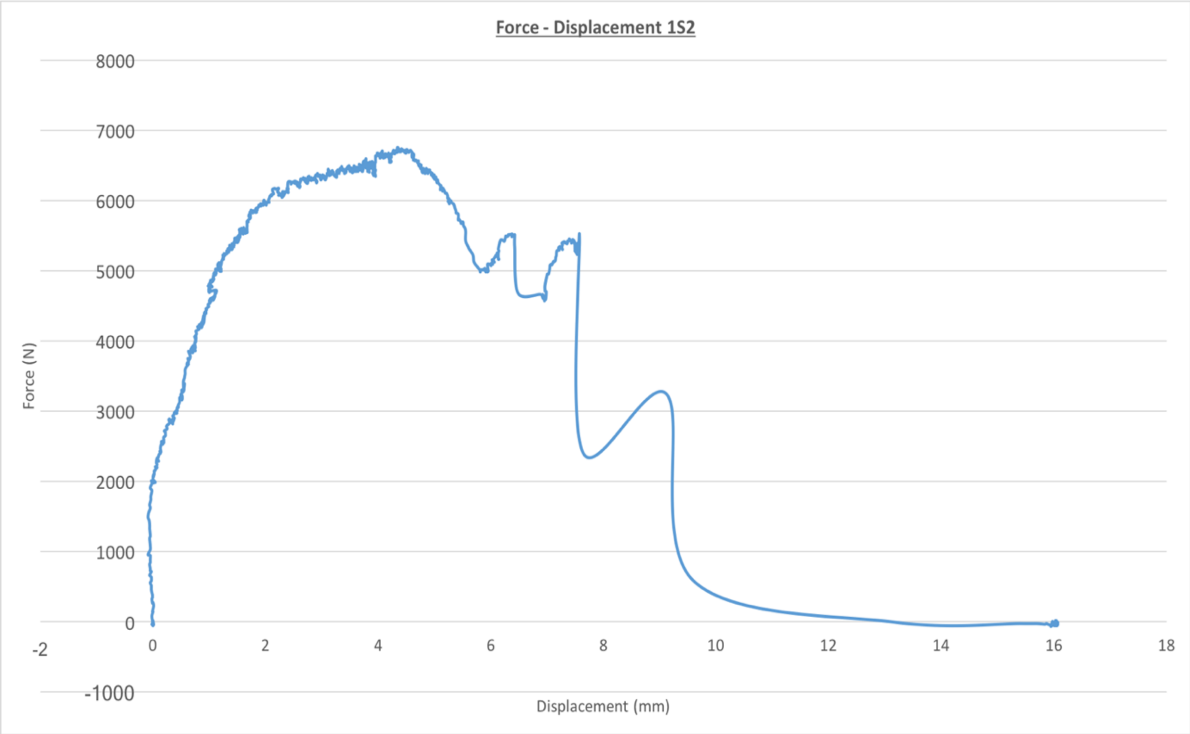

Graph 2: Force-displacement 1S2

4.6.2. Two screwed connection

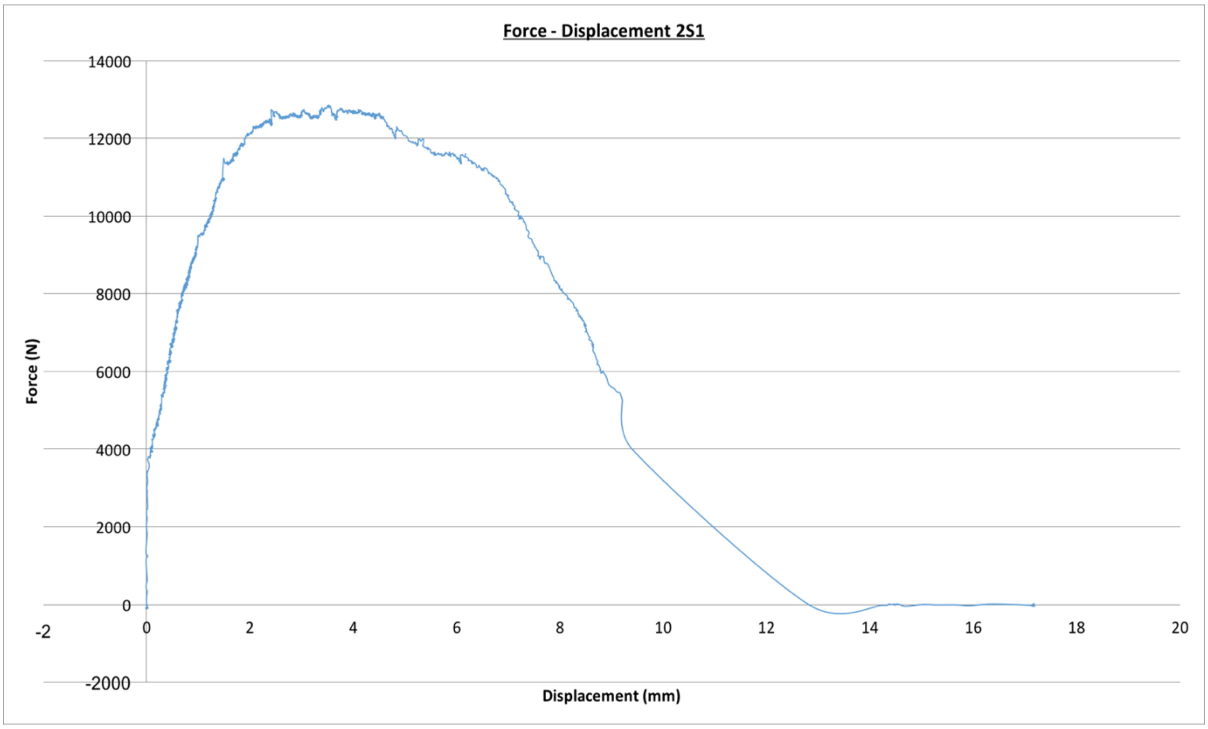

Graph 3: Force-displacement 2S1

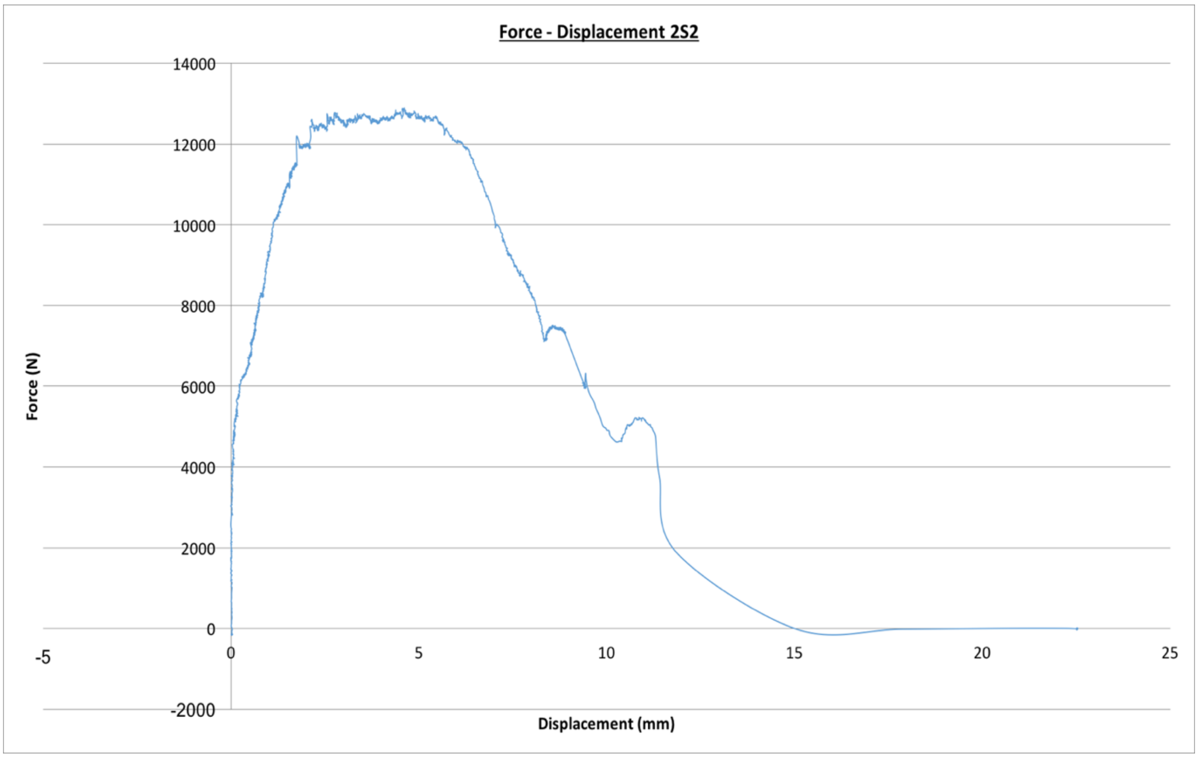

Graph 4: Force-displacement 2S2

4.6.3. Four screwed connection

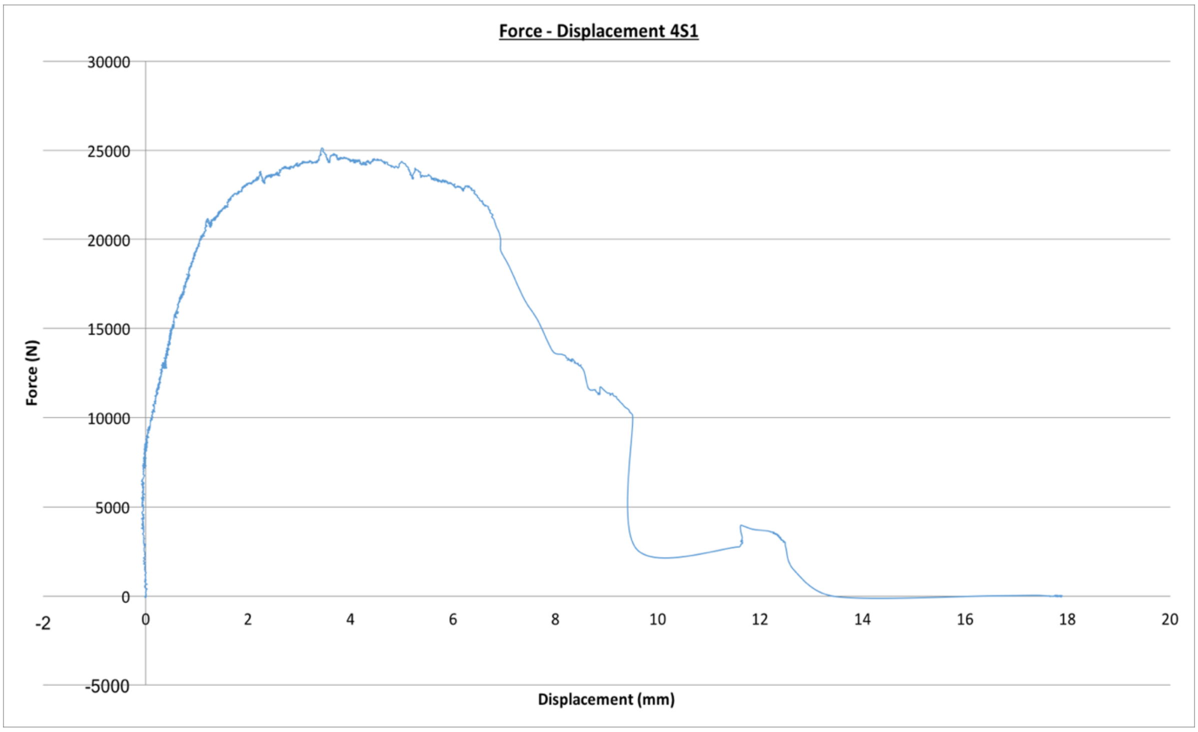

Graph 5: Force-displacement 4S1

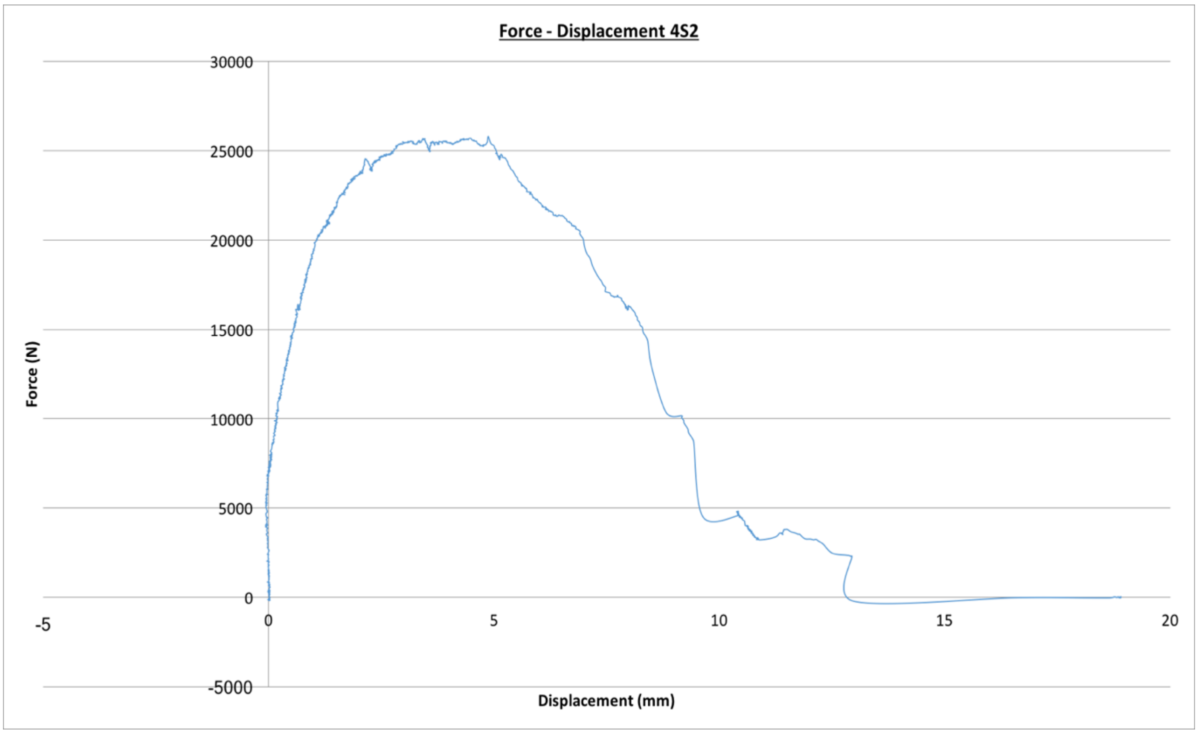

Graph 6: Force-displacement 4S2

4.6.4. First test vs. second test

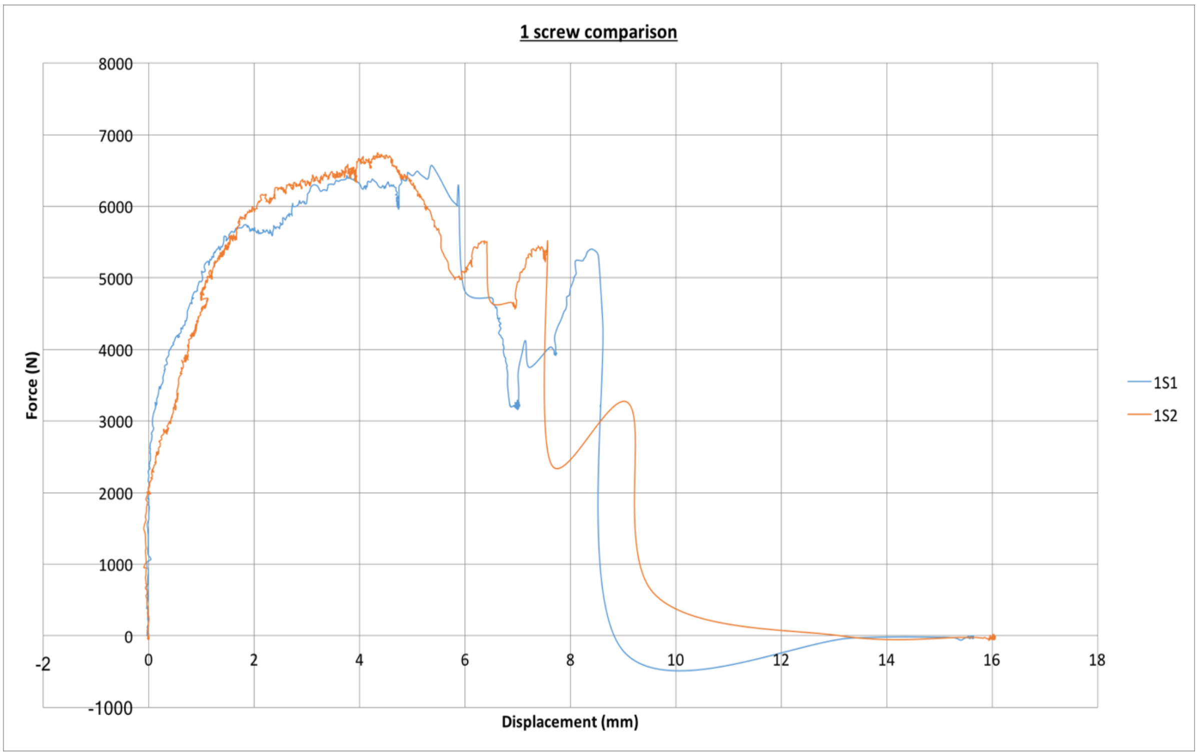

Graph 7: One screw comparison

4.6.5. Third test vs. fourth test

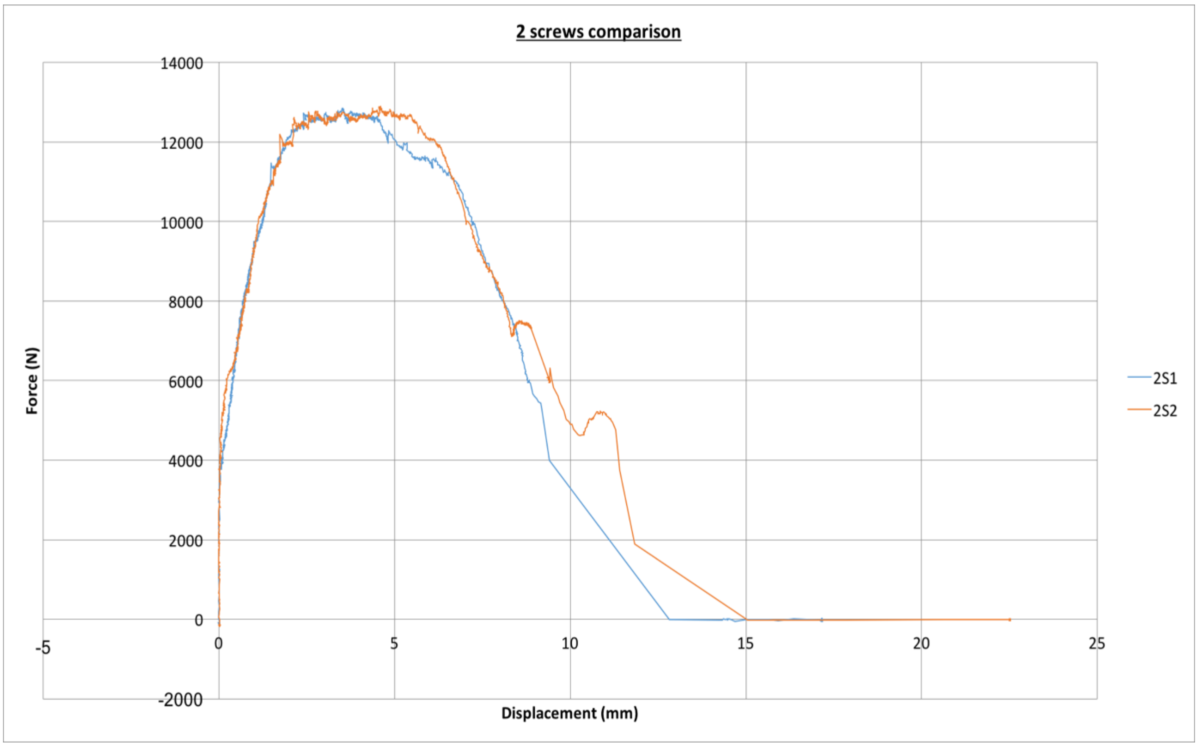

Graph 8: Two screws comparison

4.6.6. Fifth test vs. sixth test

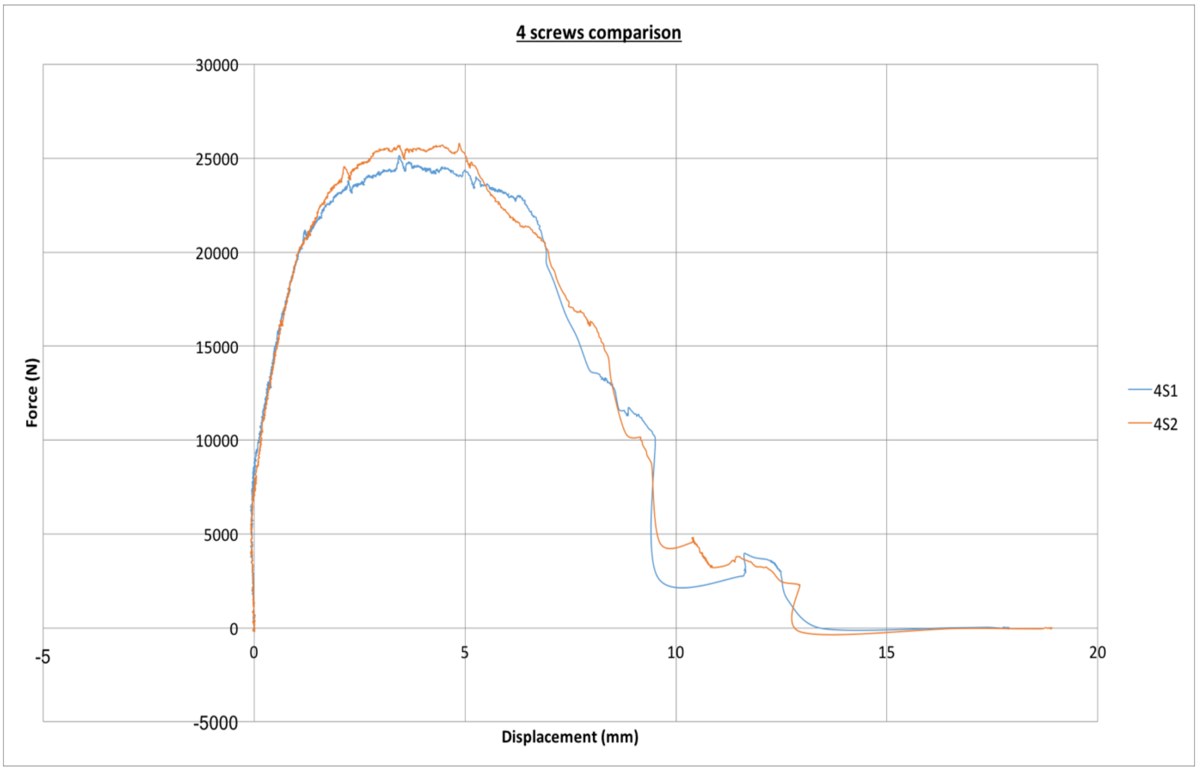

Graph 9: Four screws comparison

4.6.7. All monotonic results

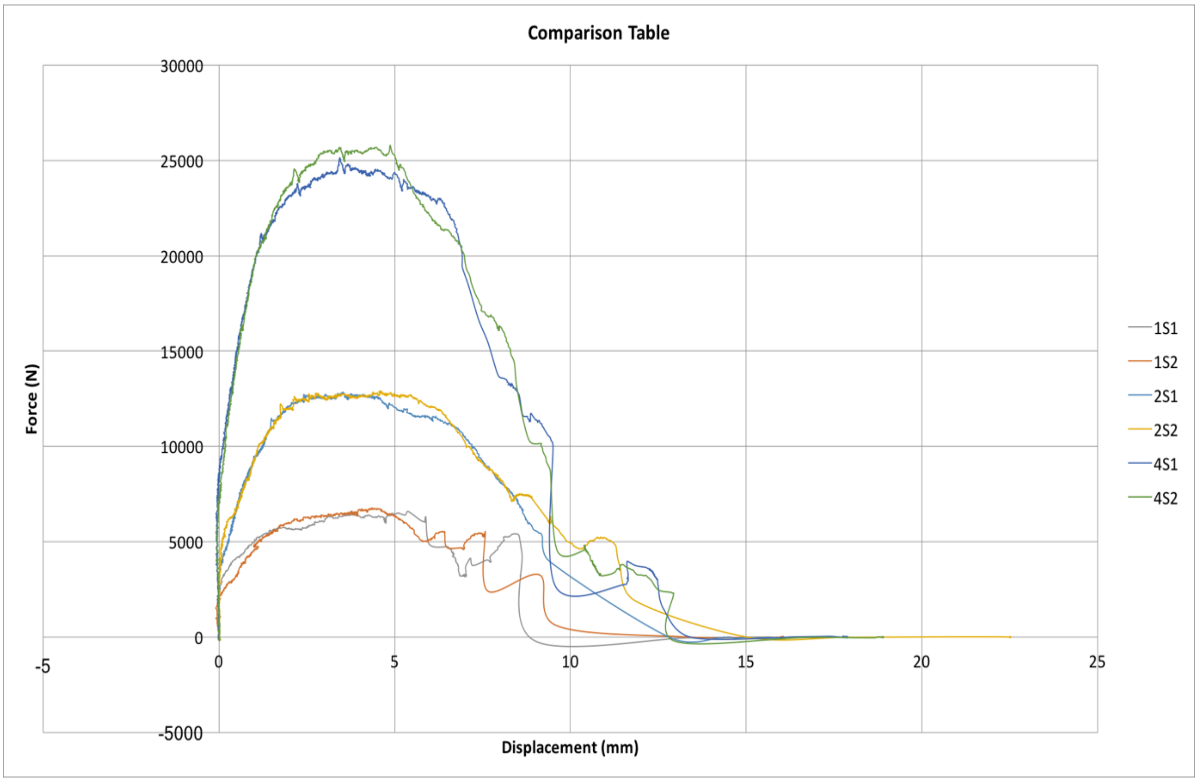

Graph 10: Global comparison monotonic tests

4.6.8. Group effect

The group effect of a connection decreases the strength of each screw, this means that the ratio between the strength will decrease if the number of screws increases. The following graph compares the analytical group effect with the group effect which was determined by testing the connections.

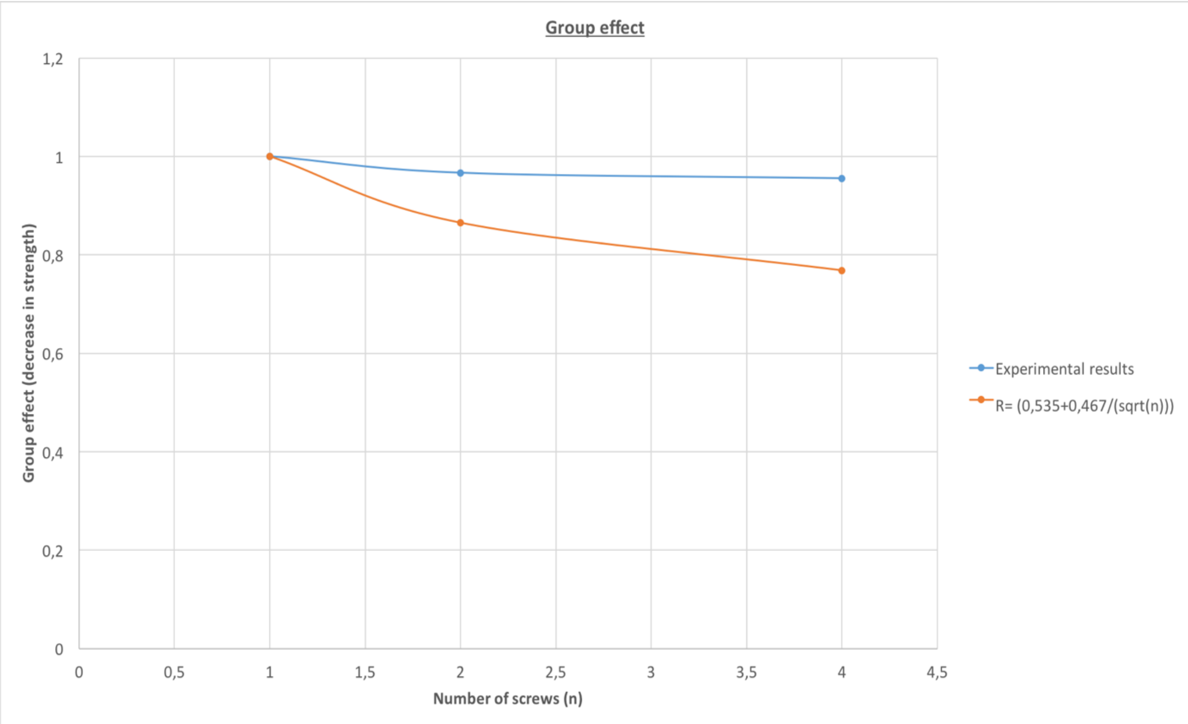

Graph 11: Group effect

As you can see in the graph, the analytical reduction factor is smaller than the reduction factor which is determined after the tests. This means that the connections behave much stronger in the experiments than which was predicted in the analytical procedure. [17]

4.7 Cyclic test results

4.7.1. One screwed connection

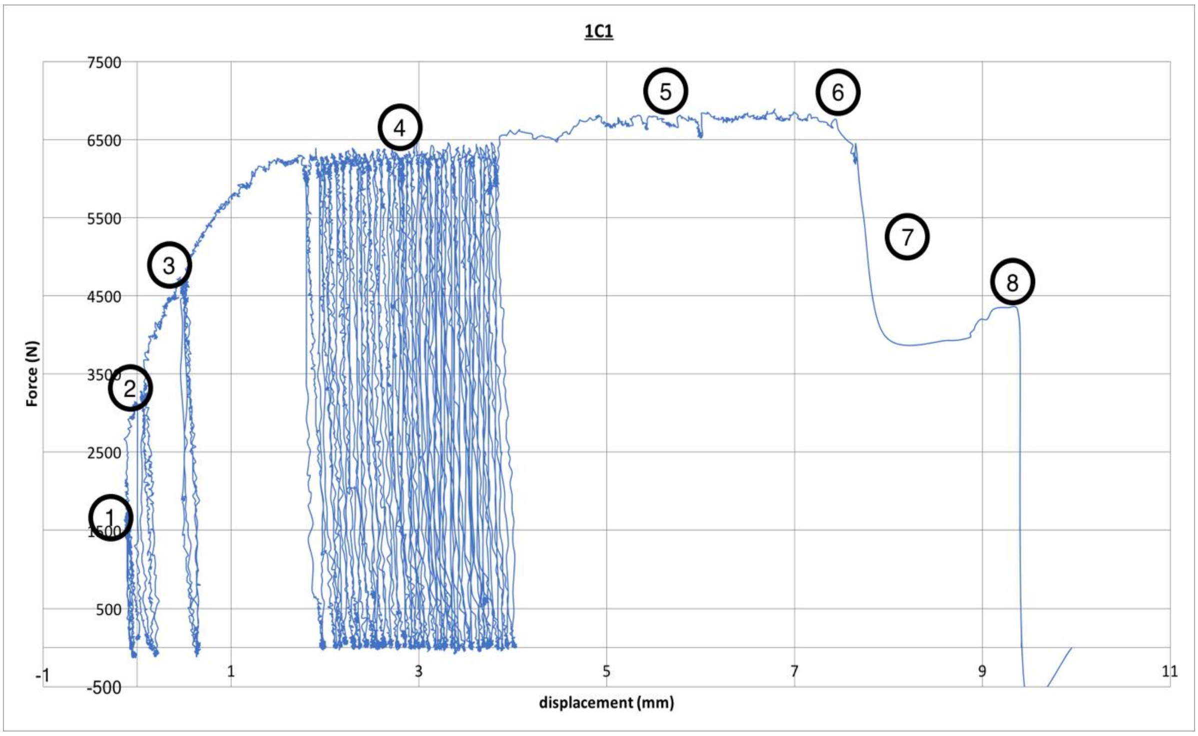

Graph 12: Force-displacement 1C1

The test results will be described based on the Force-displacement curves. The numbers on the graph correspond to the numbers down below. The connection behaved as follows:

1) The first cycle at Fmax/4= 1,56 kN
2) The second cycle at Fmax/2= 3,125 kN
3) The third cycle at 3*Fmax/4= 4,6875 kN
4) The fourth until the twentieth cycle at Fmax= 6,25
5) Performance of a monotonic test.
6) The connection reaches its maximum resistance at 6,89 kN.
7) After the screw reaches its maximum resistance, the connection fails.
8) At a certain moment, a thread of the screw touches the plate and creates an increase in Force. After this increase, the connection is going to fail completely.

From the fact that, when the cycles are completed, the force-deformation is almost vertical there can be concluded that the connection behaves very stiff. This means that the screw never goes back to its original place once the screw starts tilting. This is because there is no compression, only the tension is relieved and the force goes back to zero.

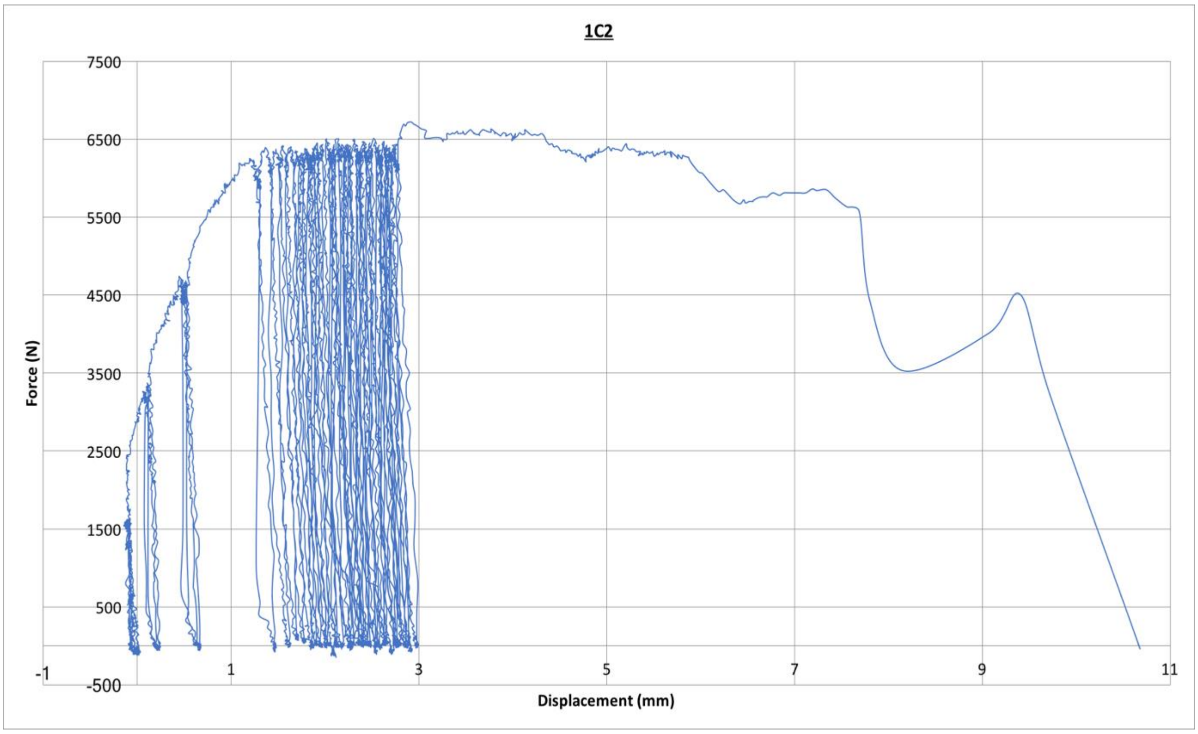

Graph 13: Force-displacement 1C2

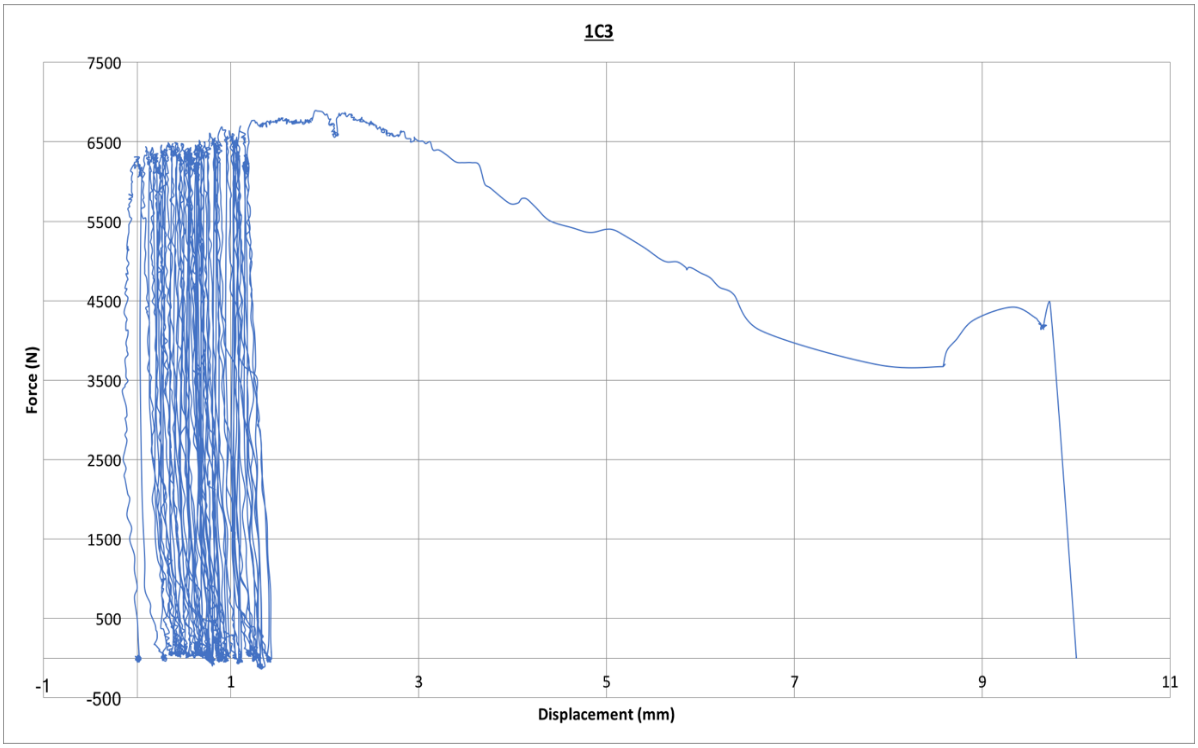

Graph 14: Force-displacement 1C3

The beginning of the third test looks different because there went something wrong while testing, the LVDT was blocked from the beginning. That's why these results needed to be deleted.

The general behaviour of the three one screwed tests was pretty much the same, except for the fact that the displacement of the plates was different for all tests. This can have multiple causes, namely:

1) The fact that the tests were performed manually and not automatically. Because of this, the tests progressed differently and this can cause the connection to behave differently.
2) The fact that the way of drilling the screws can be different.

4.7.2. Two screwed connection

The cycles of this series of tests is as follows:

1) Fmax/4= 3,125 kN
2) Fmax/2= 6,25 kN
3) 3*Fmax/4= 9,375 kN
4) Fmax= 12,5 kN

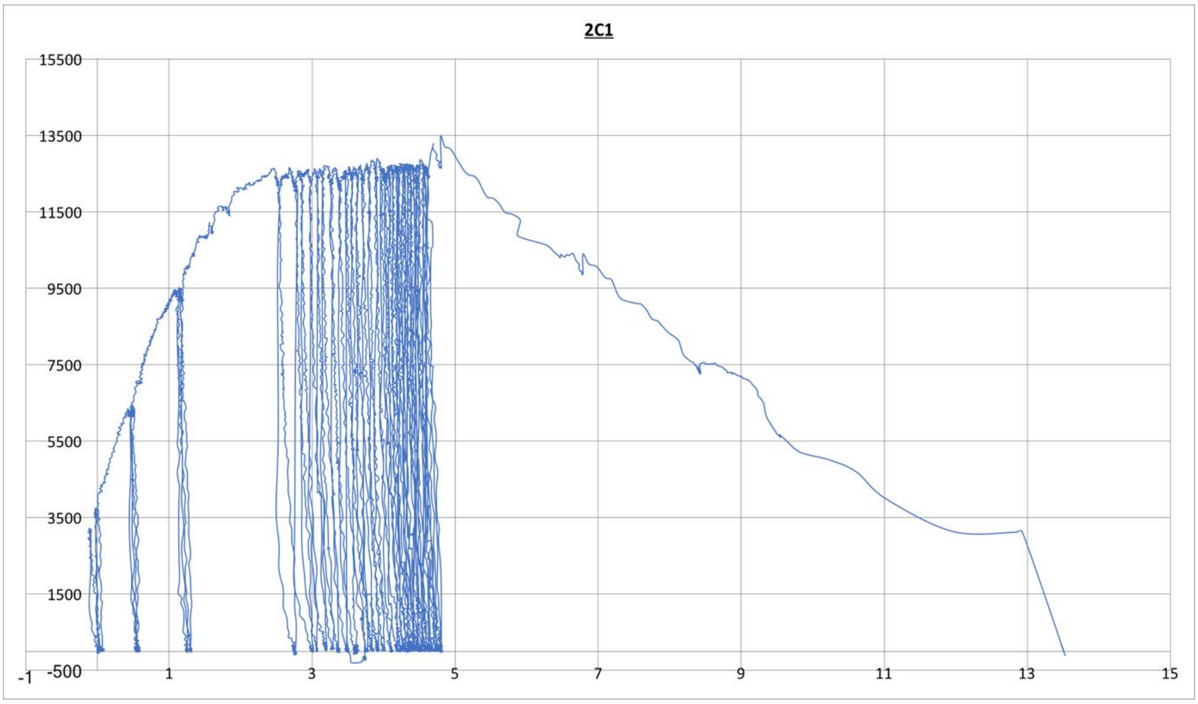

Graph 15: Force-displacement 2C1

After the 20 tests were completed, the monotonic procedure went to 13,5kN. The connection started to fail after reaching this maximum strength. This results is pretty similar to the results of the one-screwed connections, only the maximum resistance changes (almost doubles).

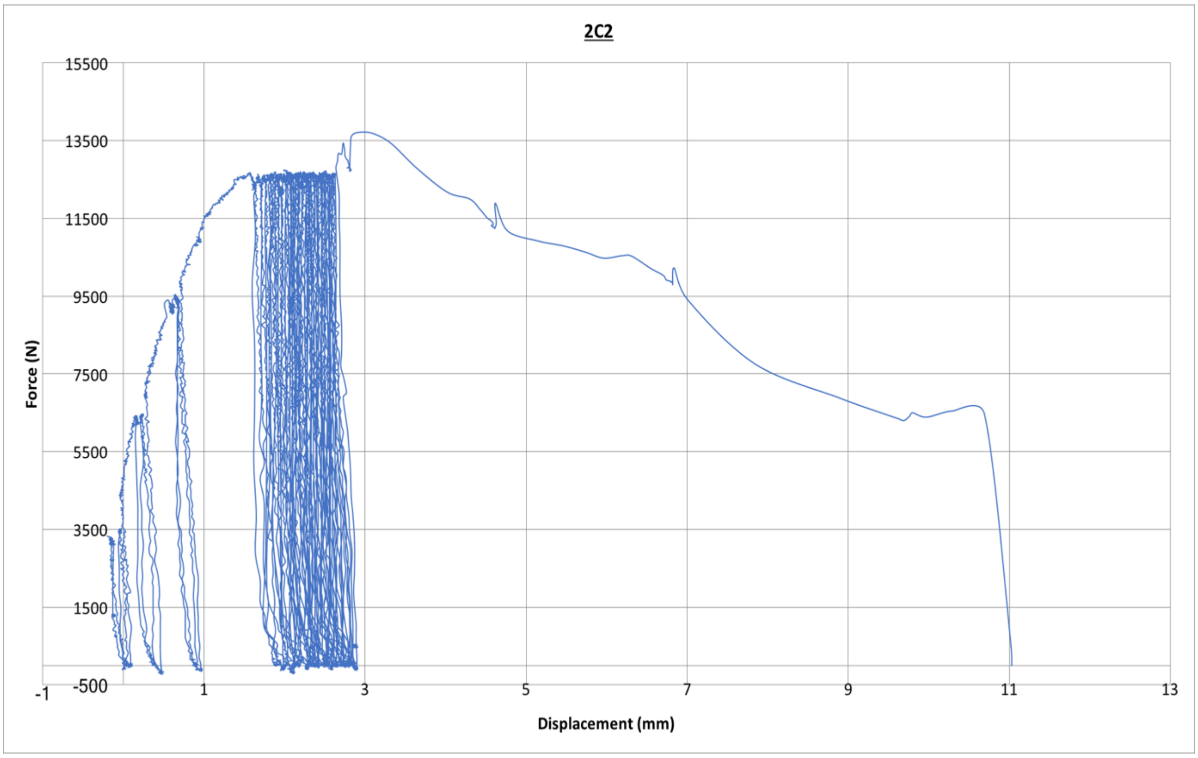

Graph 16: Force-displacement 2C2

After the 20 tests were completed, the monotonic procedure went to 13,55kN. The connection started to fail after reaching this maximum strength. Regardless of the displacement, the first and the second cyclic test were pretty much the same.

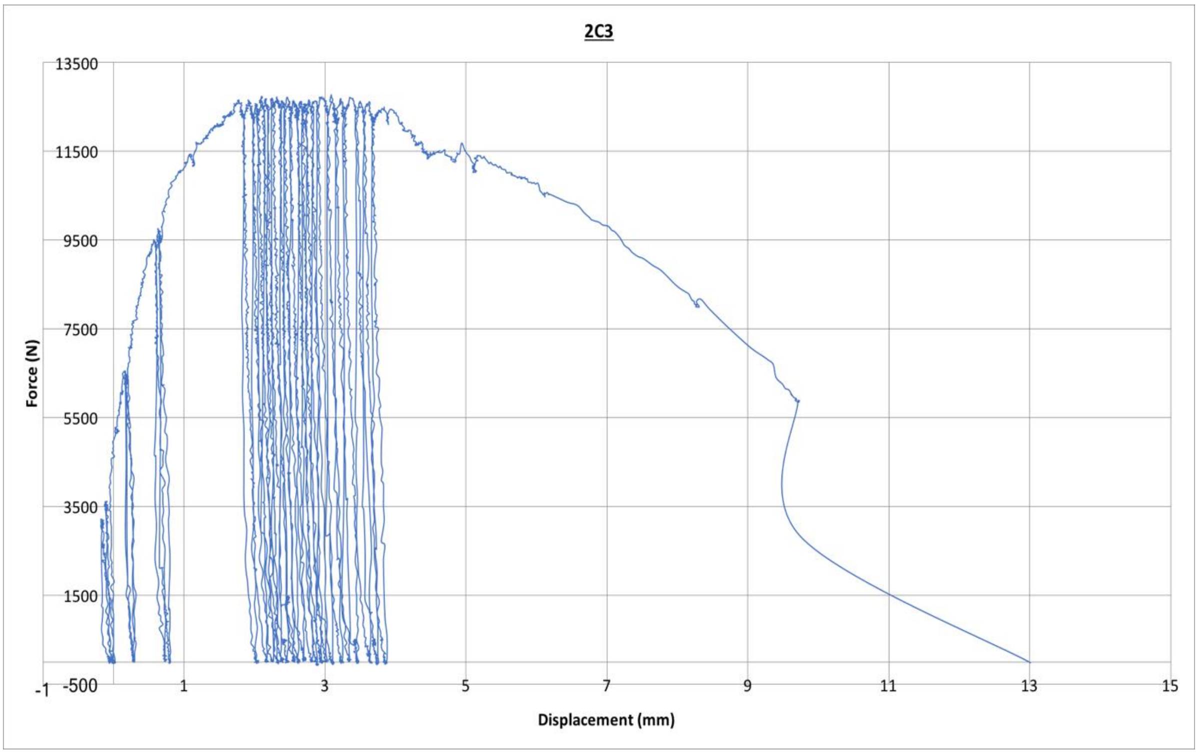

Graph 17: Force-displacement 2C3

At this test, only 11 cycles were reached. After these cycles, the connection started to fail at 12,5 kN.

4.7.3. Four screwed connection

In contrast to the previous tests, these tests all acted very differently from each other. The number of cycles as well as the displacement weren't similar.

The cycles of this series of tests is as follows:

1) Fmax/4= 6,25 kN
2) Fmax/2= 12,5 kN
3) 3*Fmax/4= 18,75 kN
4) Fmax= 25 kN

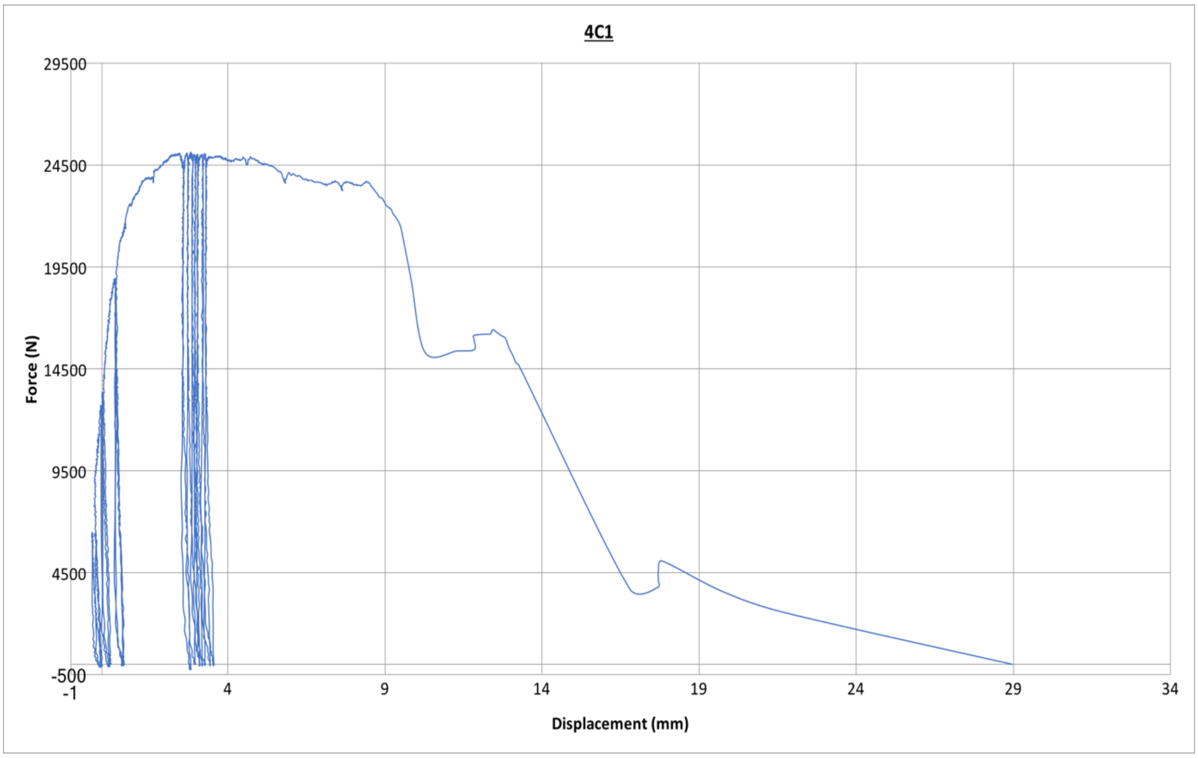

Graph 18: Force-displacement 4C1

In the beginning of the first cyclic test, the screw seemed to behave as expected. Even though, after 8 cycles, the connection started to fail at 25 kN. This sudden failure can be the result of several factors, for example:

1) The fact that the tests were performed manually.
2) The way the screws were drilled in the materials, with four screws it's more difficult to create a uniform connection because all the screws were drilled manually.
3) The strength of the steel.

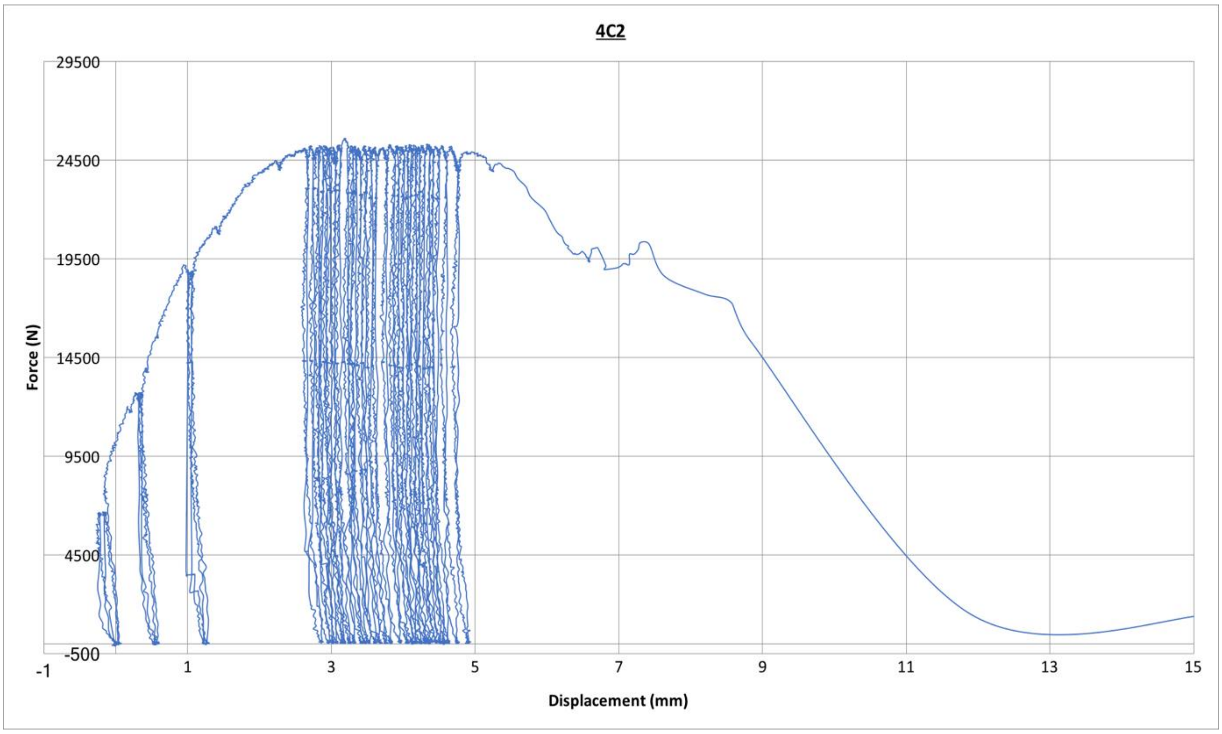

Graph 19: Force-displacement 4C2

In this test, the connection failed after completing 17 cycles. These 17 cycles are more close to the prescribed 20 cycles. The connection failed at a force of 25 kN.

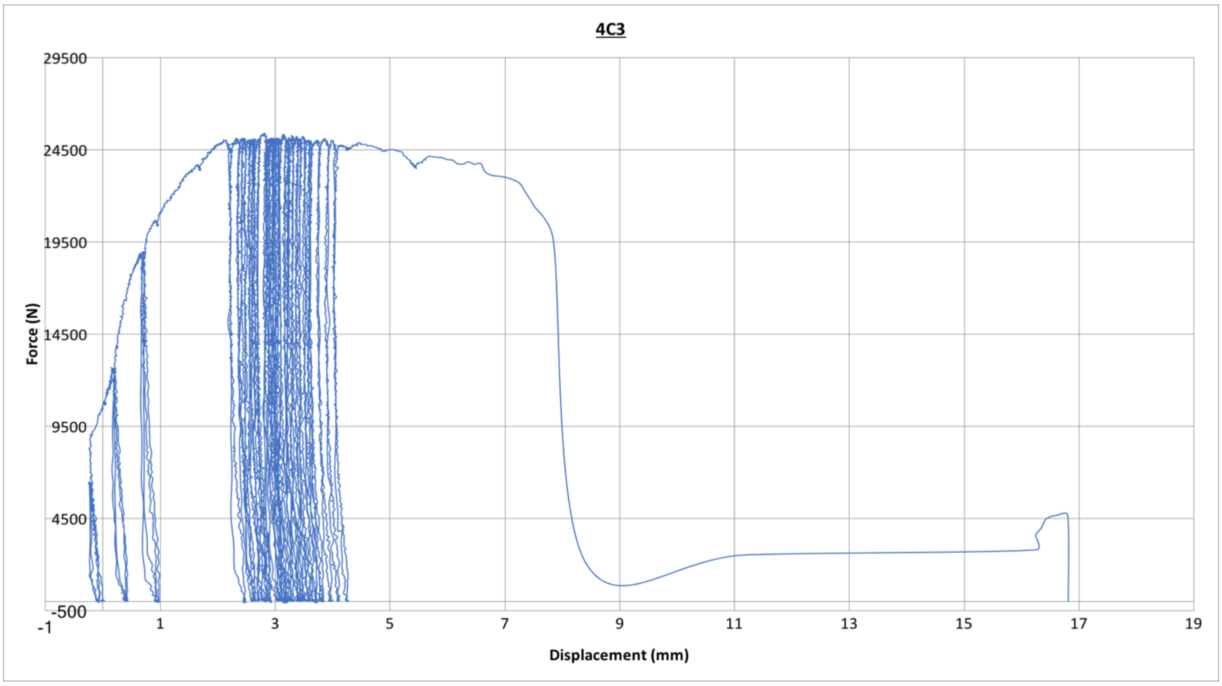

Graph 20: Force-displacement 4C3

In this test, the connection failed after completing 15 cycles. These 17 cycles are more close to the prescribed 20 cycles. The connection failed at a force of 25 kN.

4.7.4. Comparison one-screwed connection, cyclic test

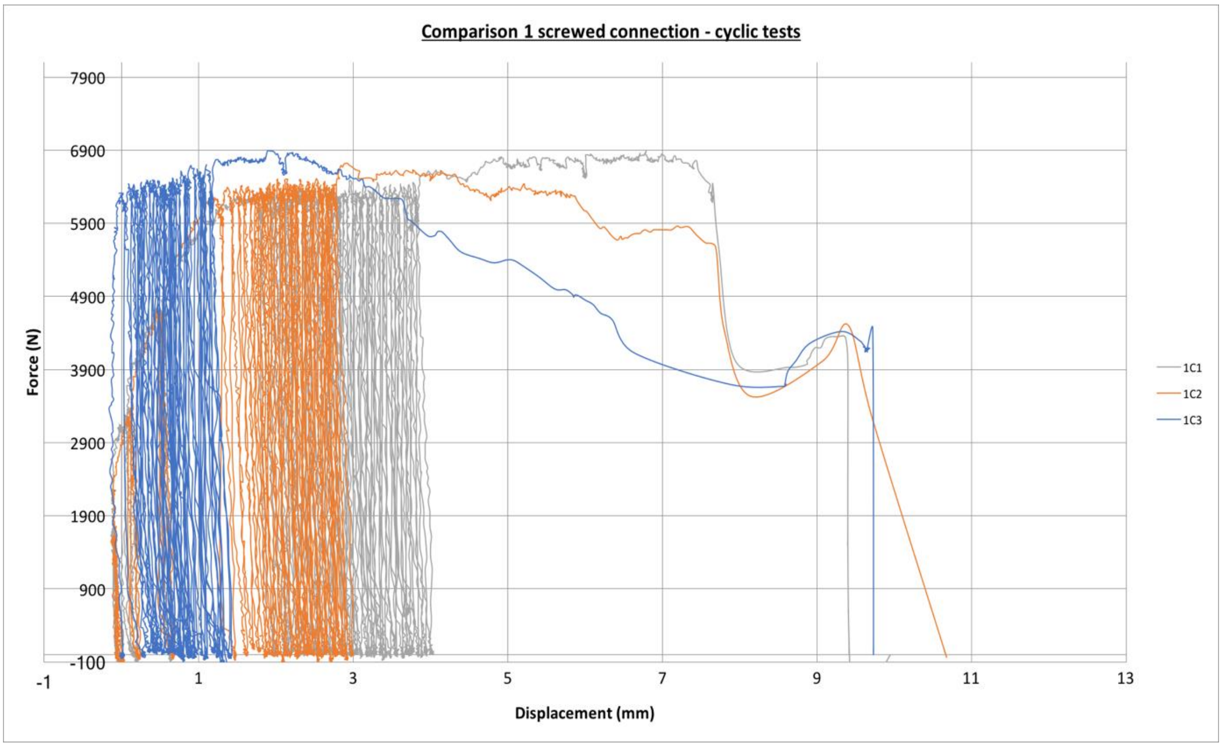

Graph 21: Comparison 1 screwed connection - cyclic tests

The tests with the one-screwed connection all behave the same way, in fact all the cyclic tests behave this way. They all have almost the exact same maximum strength. The only significant difference in these tests is the displacement of the system. The causes of this difference are most likely the fact that the tests were executed manually. When the tests would be executed automatically, the procedure would be the same for all tests and the deformation would most likely be the same for all tests. This difference is displacement can be found in all the cyclic tests. The manual testing doesn't have much influence on the results of the monotonic tests.

4.7.5. Comparison two-screwed connection, cyclic test

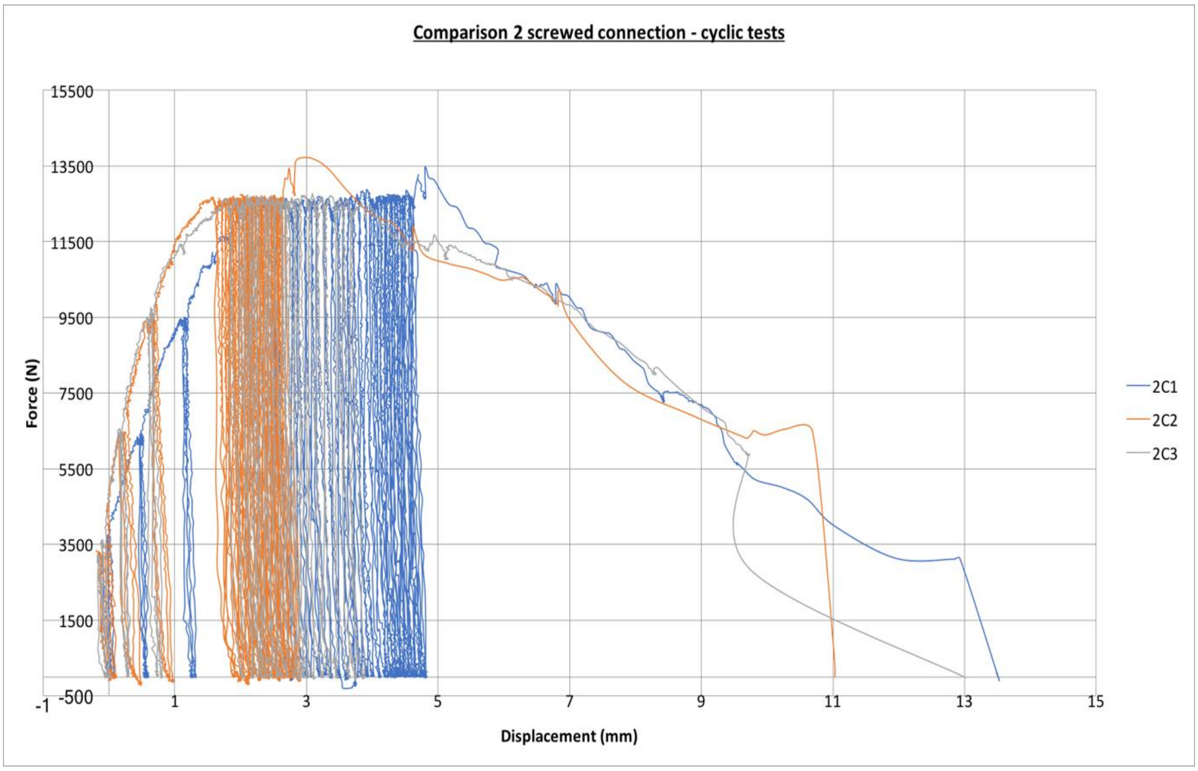

Graph 22:Comparison 2 screwed connection - cyclic tests

4.7.6. Comparison two-screwed connection, cyclic test

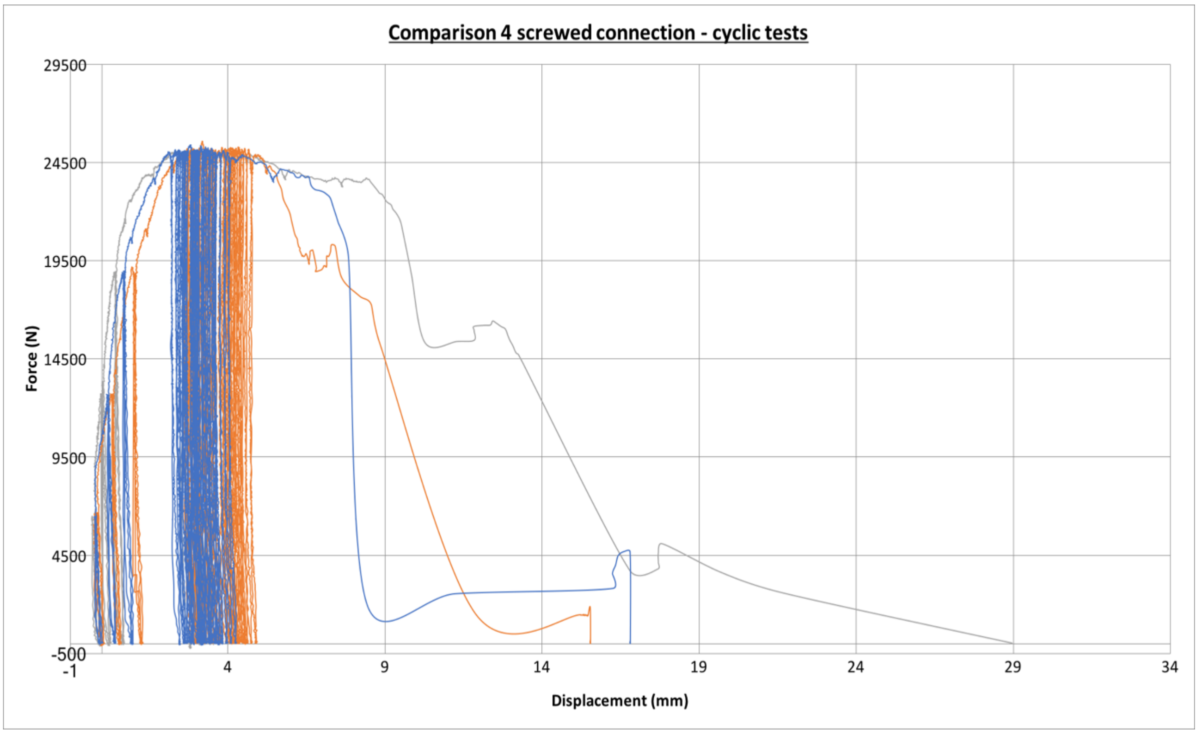

Graph 23: Comparison 4 screwed connection - cyclic tests

4.8 Summary table

4.8.1. Monotonic tests

Test specimen	Maximum resistance of the connection (kN)	Displacement (mm)	Ratio	Stiffness (N/mm)	Initial stiffness (N/mm)
1 screw, first test	6,57	5,36	1	817,1641791	1225,746269
1 screw, second test	6,75	4,34	1,02739726	1036,866359	1555,299539
2 screws, first test	12,85	3,52	1,95585997	2433,712121	3650,568182
2 screws, second test	12,9	4,61	1,96347032	1865,509761	2798,264642
4 screws, first test	25,12	3,435	3,823439878	4875,303251	7312,954876
4 screws, second test	25,78	4,865	3,923896499	3532,716684	5299,075026
Average 1 screw	6,66	4,85	1	915,4639175	1373,195876
Average 2 screws	12,875	4,065	1,933183183	2111,521115	3167,281673
Average 4 screws	25,45	4,15	3,821321321	4088,353414	6132,53012

Table 6: Summary table monotonic tests

4.8.2. cyclic tests

Test specimen	Maximum resistance of the connection (kN)	Displacement (mm)	Ratio	Stiffness (N/mm)	Initial stiffness (N/mm)
1 screw, first test	6,89	6,79	1	676,485027	1014,727541
1 screw, second test	6,72	2,92	0,97532656	1534,246575	2301,369863
1 screw, third test	6,89	1,89	1	2430,335097	3645,502646
2 screws, first test	13,47	4,8	1,955007257	1870,833333	2806,25
2 screws, second test	13,72	2,96	1,991291727	3090,09009	4635,135135
2 screws, third test	12,5	3,98	1,814223512	2093,802345	3140,703518
4 screws, first test	25,13	2,82	3,647314949	5940,898345	8911,347518
4 screws, second test	25,57	3,2	3,711175617	5327,083333	7990,625
4 screws, third test	25,39	2,8	3,685050798	6045,238095	9067,857143
Average 1 screw	6,833333333	3,866666667	1	1178,16092	1767,241379
Average 2 screws	13,23	3,913333333	1,936097561	2253,833049	3380,749574
Average 4 screws	25,36333333	2,94	3,711707317	5751,322751	8626,984127

Table 7: Summary table cyclic tests

V. FE-Modelling

Finite element modelling, also referred to as FE-modelling is *a numerical technique for finding approximate solutions to boundary value problems for partial differential equations*. [17] The software works by dividing the problem into smaller parts. These parts are called finite elements and are both smaller and simpler and therefore easier to calculate. For each finite element there are some simple equations. The smaller equations are then assembled into a lager system of equations for the entire problem. After solving the system of equations for the entire problem, the FEM-tool gives an approximate solution to the model. [17]

The program used for the numerical analyses is called Abaqus FEA (Finite Element Analysis). The workflow of the program including the design of the model, the different types of analysis and the convergence study are described in the following paragraphs. The goal of the FE-modelling is to have another approximation to compare the results of the experimental results. This type of modelling is also a good indication whether or not the experimental tests are performed correctly. Finally, there is a paragraph dedicated to possible future works. This part of the study will give an overview on the things that can be improved and how they should be improved to get (possible) better results.

5.1 Description of the model

For this research we have 3 different models which will compared; 1-, 2- and 4-screw model. In what follows the 1-screw model will be explained in detail. The other models follow the same workflow procedure and have the same properties. Abaqus FEA's work procedure consists out of different steps. Each step will be explained using visuals.

1. *Parts*

The first step in the process is to model the different pars which will be used. In this particular model, 2 different parts are present: plate and screw. The geometries of the test specimen can be found in paragraph '*4.2.2. Geometries to test'*. The only difference between the specimen used in the experiments and the models in the FEM is that the wider part is neglected. Since no force or displacement will occur on this part of the plate, it's neglected. Reason here for is that it will only take extra time for the model to calculate it yet there is nothing happening. Due to the plates being symmetrical it was only necessary to model 1 plate. The following images represent both the plate and the screw. Note that the extra lines on the parts are partitions. Partitions are made for each part so that in a later stadium it is easier to make the mesh fit better.

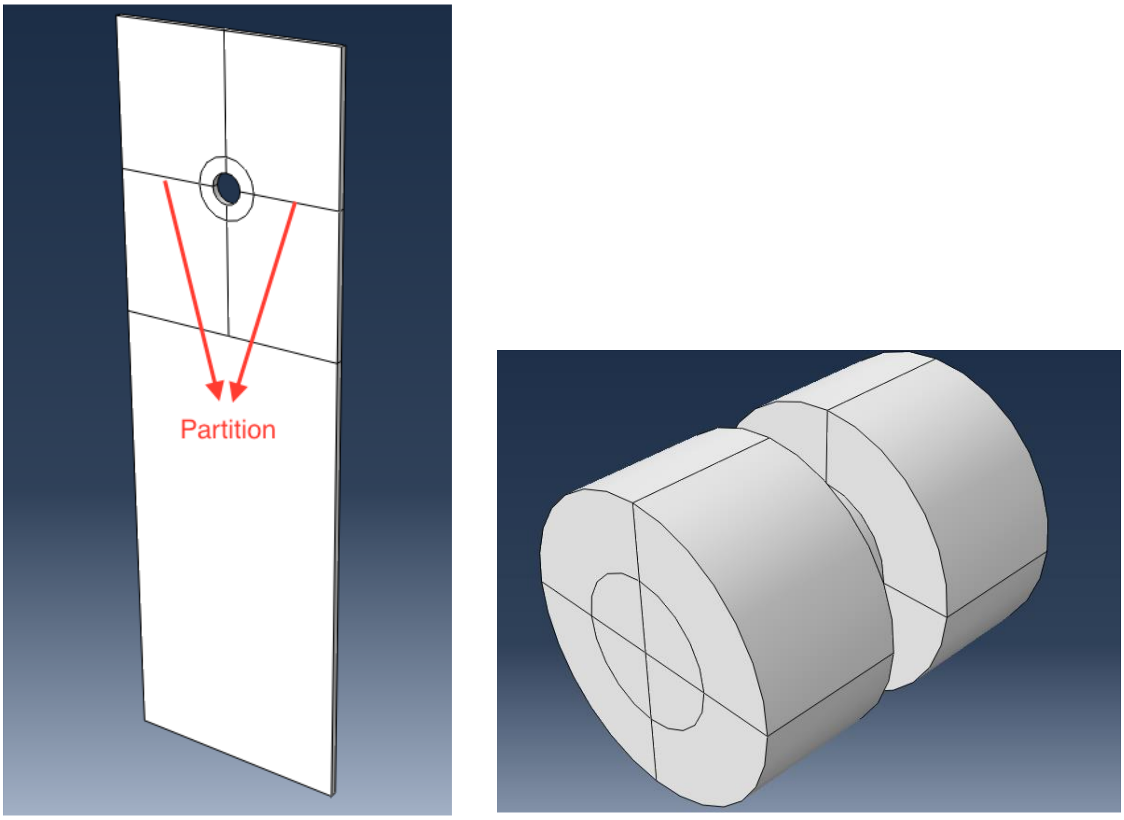

Figure 17: Modelling of the parts (plate and screw)

Due to the lack of knowledge and time at this stage of the study, the screw is modelled as a shaft with two heads. This is an easy model to have a first look on the behavior of the screw under a load. To have a more accurate resemblance with the tests, the screw should be modelled with a thread. Paragraph *'5.7 Future works'* gives a possible overview on how to model the screw with a thread.

2. *Property*

The next step is to assign the different material properties to each part made in step 1. When performing the tests, the screw is not allowed to plastically deform therefore it is modelled with only the elastic property. The plate however is assigned with both elastic and plastic values which makes it possible for the plate to either deform elastically or plastically. For the elastic behavior the following properties were used: E = 210GPa and υ = 0,3. The plastic behavior is concluded out of the stress-strain diagram in which the yield strength is equal to F_y = 318 MPa. Once the properties are assigned to the correct part, the parts are tinted as shown in the following image.

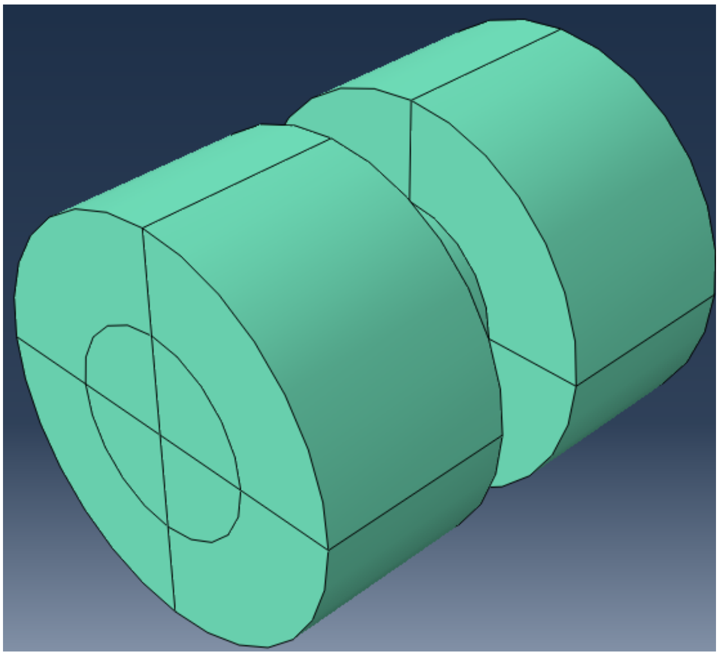

Figure 18: Property of the screw

3. *<u>Assembly</u>*

Assembly is the step in which the different parts made in step 1 are assembled together. The assembly is the test setup used in the experiments. The complete setup for the 1-screw connection is represented by the following image.

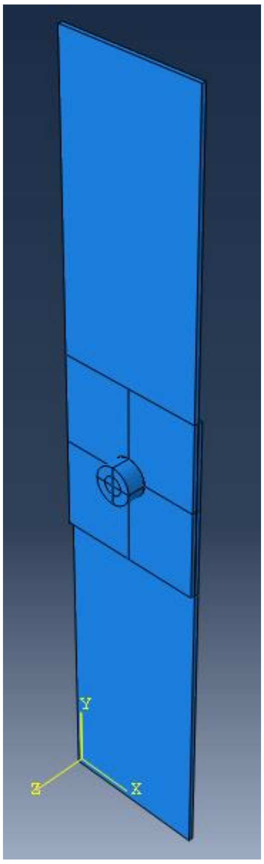

Figure 19: Assembly of the setup

4. *Interaction*

In this problem there are 2 different contact points. The first contact takes place between the 2 plates. The bottom plate and the top plate have a large contact surface. This surface needs to be assigned with a surface-to-surface contact. Abaqus FEA uses the terms 'master' and 'slave' to assign the different surfaces. In this configuration it does not matter which plate is assign as 'master' and which is assigned as 'slave'. Both plates work in the exact same way as they are symmetrical to each other. The last contact takes place between the screw and the plate. For this contact point it is necessary to assign the correct term to each part. The plates were assigned as 'master' surface and the screw as 'slave'. The interaction property was given a normal and tangential behavior.

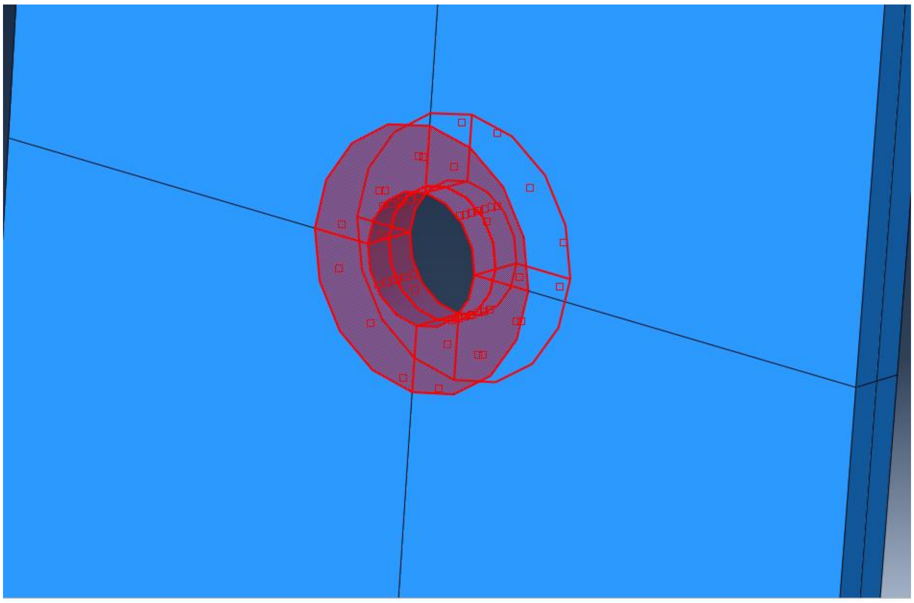

Figure 20: Interaction of the plates

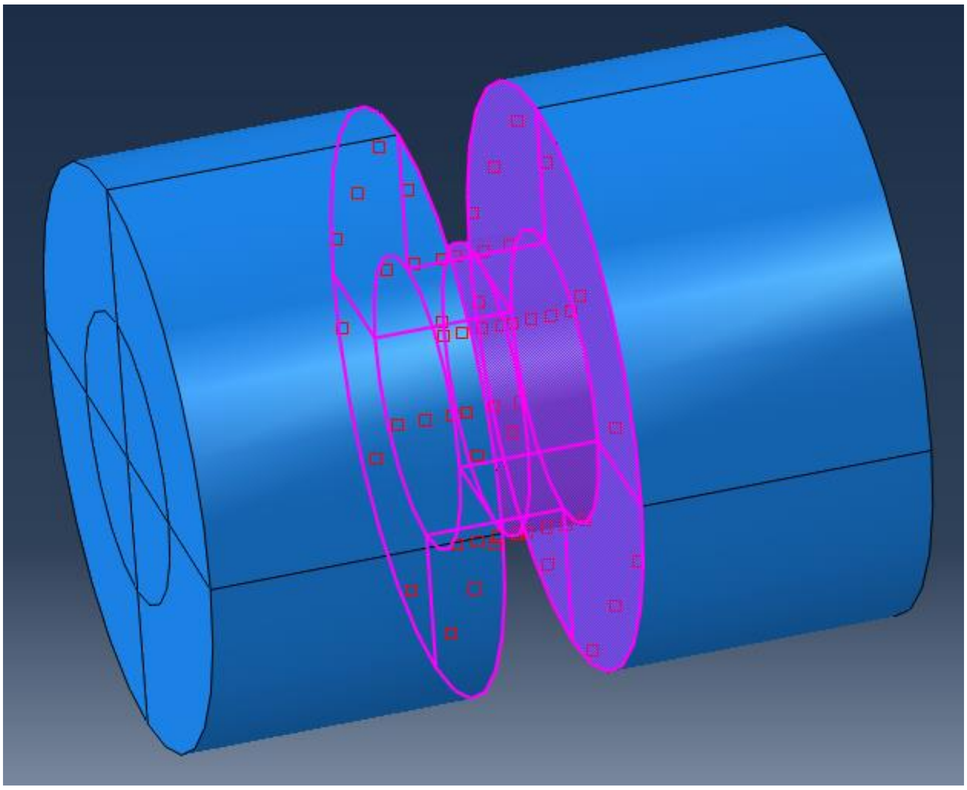

Figure 21: Interaction of the screw

The images above show the assignment of the 'master' and 'slave' surface. The red colored area is the area which is in contact with the screw. This surface is assigned as 'master'. The pink colored area on the screw is the area in contact with the plate and represents the 'slave' surface.

5. Load

Load is the step in which the forces are assigned to the model. For this model however there will not be any forces assigned. Instead, an obligated displacement will be assigned to the models. For each test, 3 different boundary conditions are drawn. The first boundary condition is to make the model rigid on the bottom part. Therefore, the boundary conditions U1, U2 and U3 (= x-, y-, z-axis) are all equal to 0. The top plate has also been set with some movement constraints. Because of the fact that there will only be pure vertical movement, the U1 and U3 (= x- and z-axis) are equal to 0. The last condition is the actual displacement of the system. Out of the performed tests a maximum displacement of 5 mm has been determined. This value has been adapted to the system as an obligated displacement in positive vertical direction.

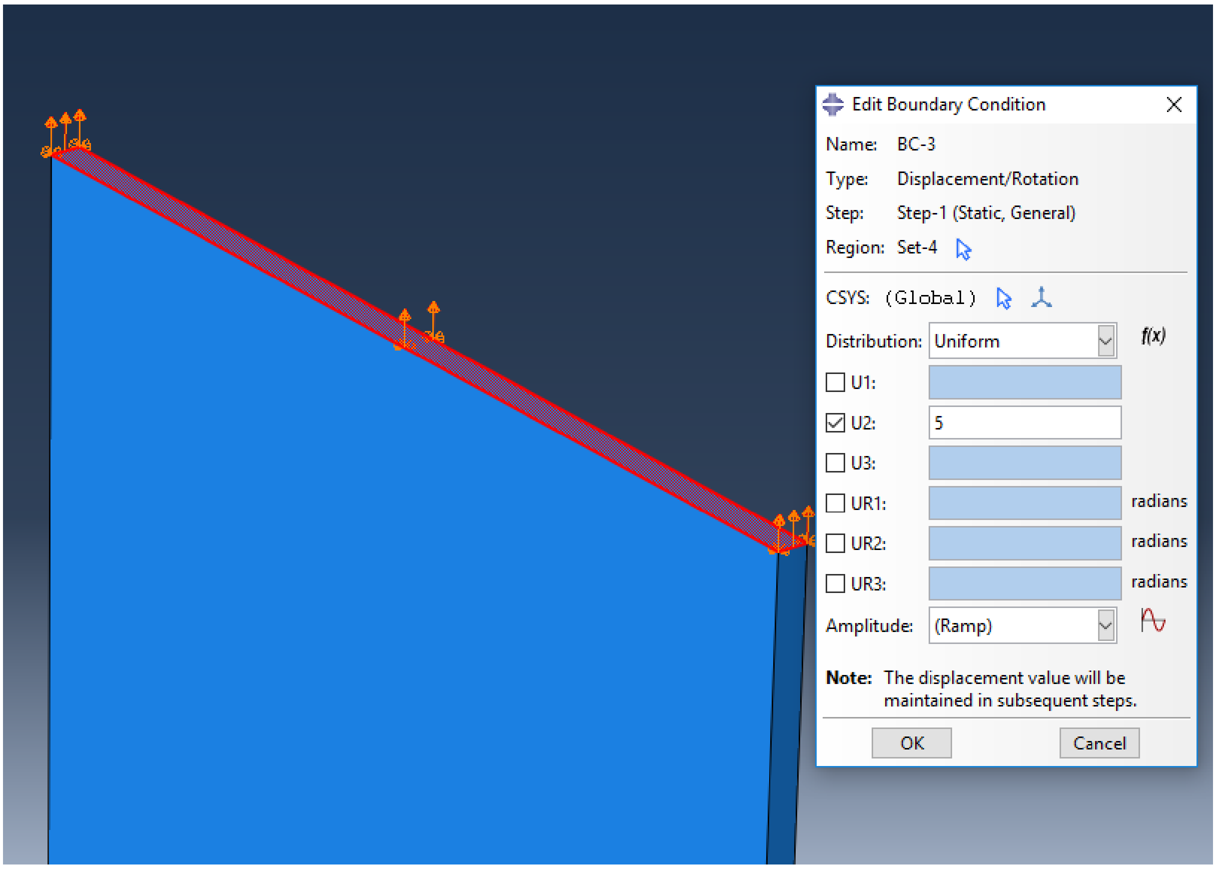

Figure 22: Applying of the load

6. Mesh

The mesh is a crucial step in a good finite element model. By refining the mesh to the best possible composition, the best results can be achieved. To have a better interaction between the meshes on the screw and the meshes on the plate is best that both are refined in such a way that a proper contact is made. The following image gives a total view of the mesh for the complete model.

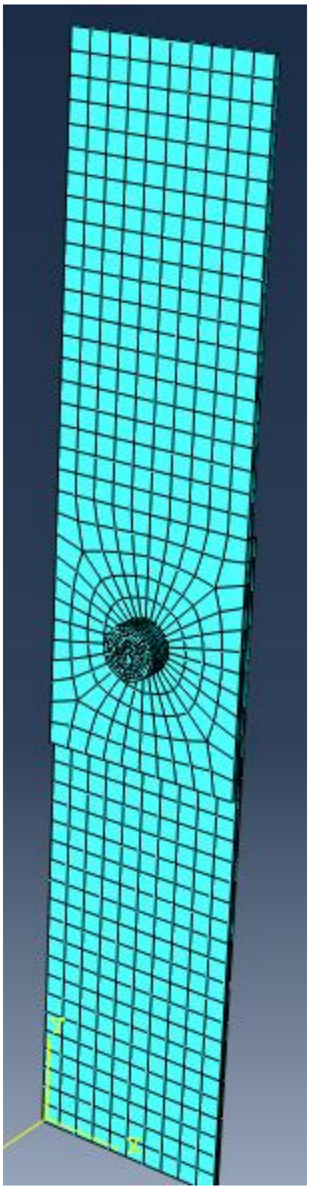

Figure 23: Meshes

The mesh has a near square surface on the bottom and top plate. Due to the circular form of the screw the meshes change in shape when closing in to the screw. However, for this model is smooth transition is made. The following image gives a detailed view on the connection between screw and plate. Here it is visible that meshes from both plate and screw fit perfectly.

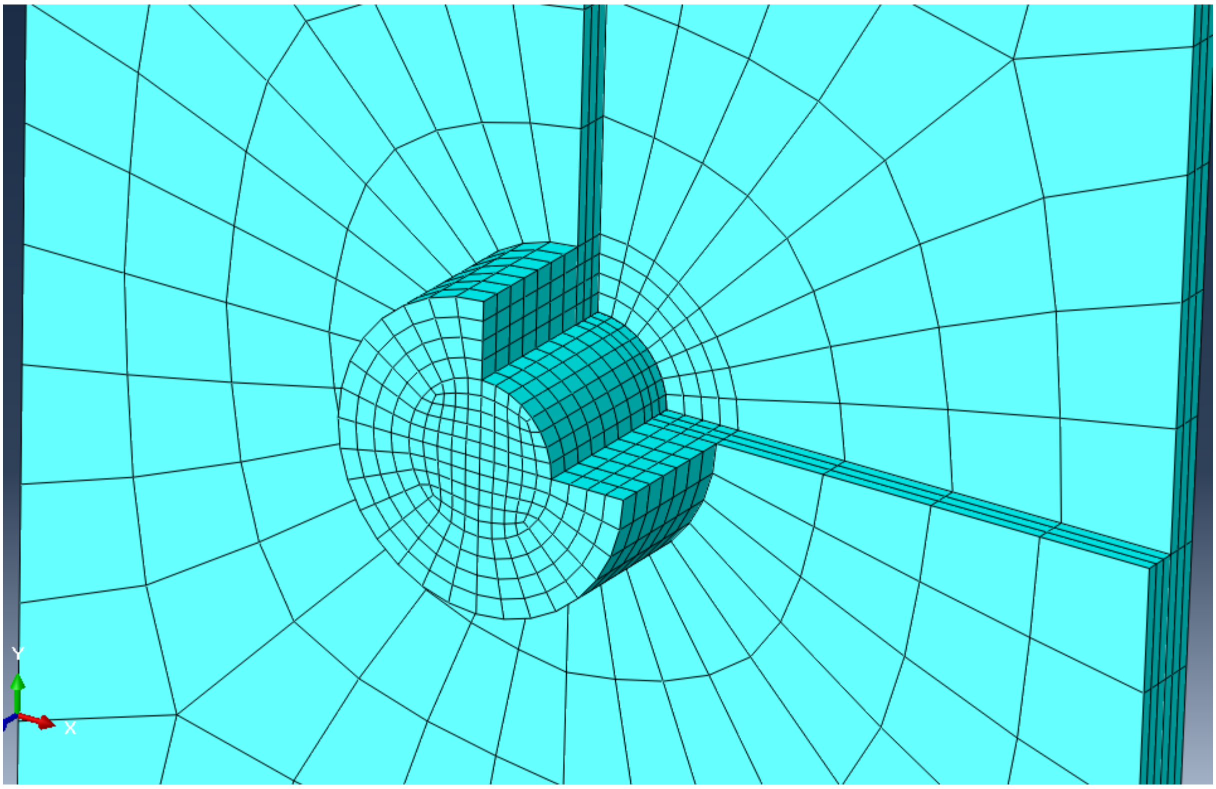

Figure 24: Mesh close-up

7. *Job*

At this stage the model is ready to be submitted for analysis. This is the last step in the process. When the model is done running, the results are ready to be consulted. The results of the 1-, 2- and 4-screw models are given in paragraph *'5.4 Simulation of the monotonic tests'*.

5.2 Types of analysis

Throughout the numerical modelling, several modifications were made. These modifications had the purpose to see which setup was giving the best results (= closest to experimental results). In total 4 different models were made. These models vary from the plate being pure elastic or both plastic and elastic and whether the nonlinear geometry is taken into account for or not. The following models have been calculated:

1) Plate is pure elastic (plasticity neglected) and nonlinear geometry was not taken into account (NLGeom = OFF)
2) Plate with both elastic and plastic conditions and NLGeom = OFF
3) Plate is pure elastic and NLGeom = ON
4) Plate has plastic behavior and NLGeom = ON

The results of the 4 different models have been compared on the following diagram.

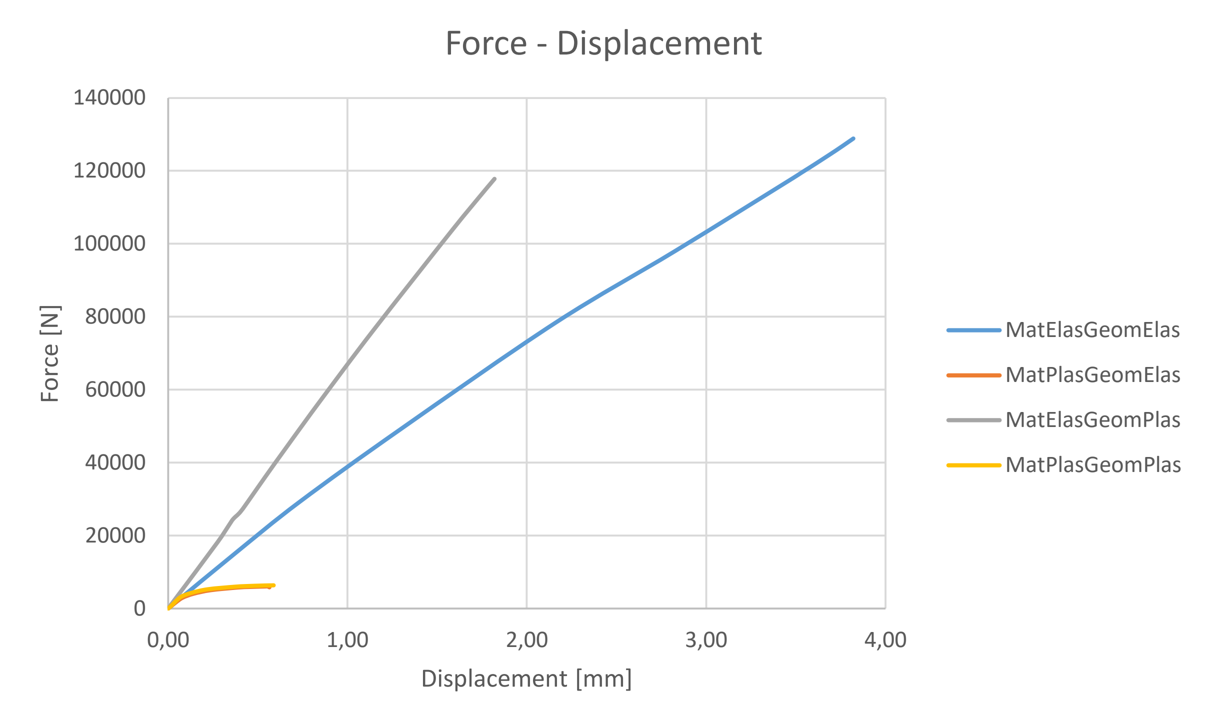

Graph 24: Force-displacement (type of analysis)

The difference between the blue and the grey and the orange and yellow curve is remarkable. This due to the material property of the plate being pure elastic. Since there is no plasticity in the plate, it is able to deform in much larger amount before failing compared to the tests executed when also taking the plastic behavior into account. By rescaling the x- and y-axis, the curves with only plastic behavior are more visible. The following diagram is a detailed shot of the previous diagram.

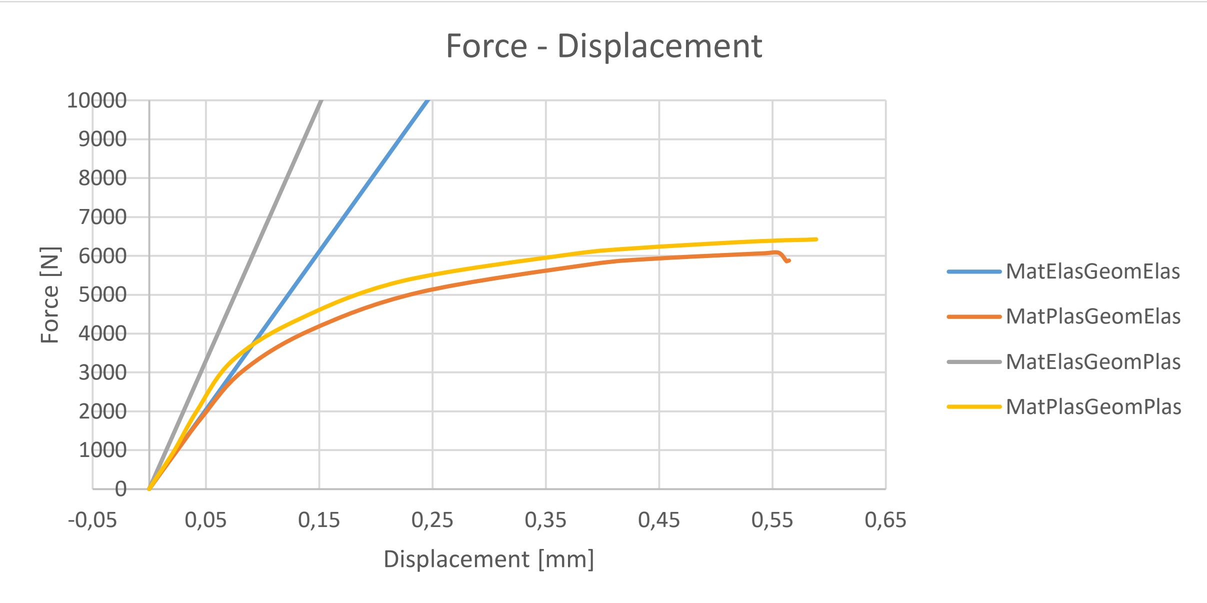

Graph 25: Force-displacement (type of analysis) – close-up

The results of these curves fit more to the reality then the elastic behavior curves. The only difference between these curves is the fact that nonlinear geometry is calculated or not. Although the fact that the difference is neglectable, it is better to take this geometry into account. Since the plate is undergoing a certain amount of deformation and that plastic behavior is occurring, it is best to have NLGeom set to ON. To conclude this analysis, it is best to have plastic behavior of the plate and nonlinear geometry taken into account. Therefore, will these settings be adapted into all of the following models.

5.3 Convergence study

Finite element modelling is based on the number of smaller and simpler elements, called the mesh. As mentioned before the mesh is a crucial part in the good outcome of the results of the model. The finer the mesh, the better the results are with a more accurate solution. Increasing the number of elements however, is also increasing the computation time of the model. That is when a convergence study is made. A convergence study is based on the accuracy-time factor. A more refined mesh typically means a better result but also means a longer computation time. Therefore, it is often better to have a larger mesh with a shorter computation time then a very small mesh with a long computation time. By performing a convergence study it is possible to find the best setup that gives the best accuracy for the least amount of time. For the 1-screw model, 4 different element types have been compared. The element types used for this convergence study are the C-3D elements. These are three-dimensional solid or continuum elements. These elements are best used for linear and complex nonlinear analyses. The solid elements are also best used in problems where contact, plasticity and deformations occur.

1) C3D8R

This is three-dimensional hexahedral element was the first element for the study. It is a linear brick element consisting out of 8 nodes with 1 reduced integration point (R) in the center. The following image gives an example of the structure of this type of element. [18]

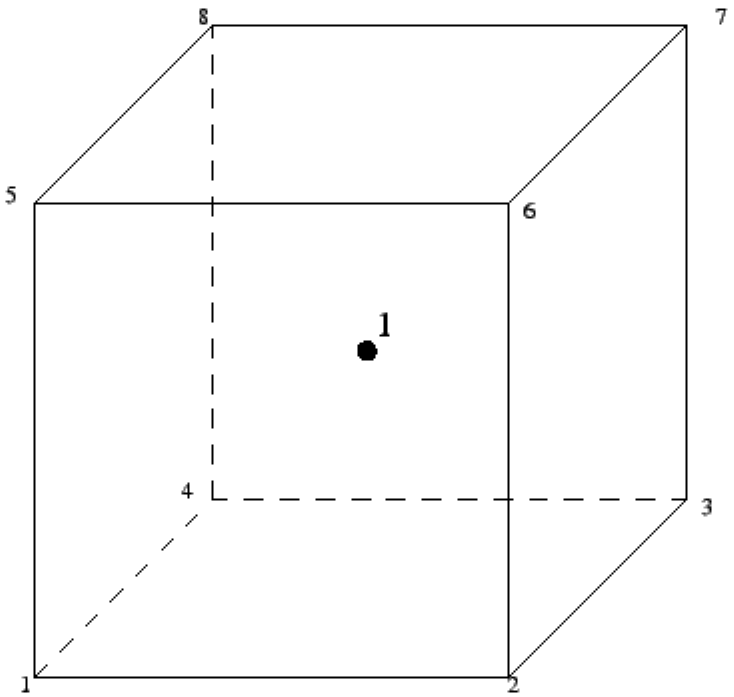

Figure 25: 3D hexahedral element

The following diagram is the result of full analysis of the 1-screw model using the C3D8R element type. The maximum displacement is approximately 0,58 mm and the force is 6,4 kN.

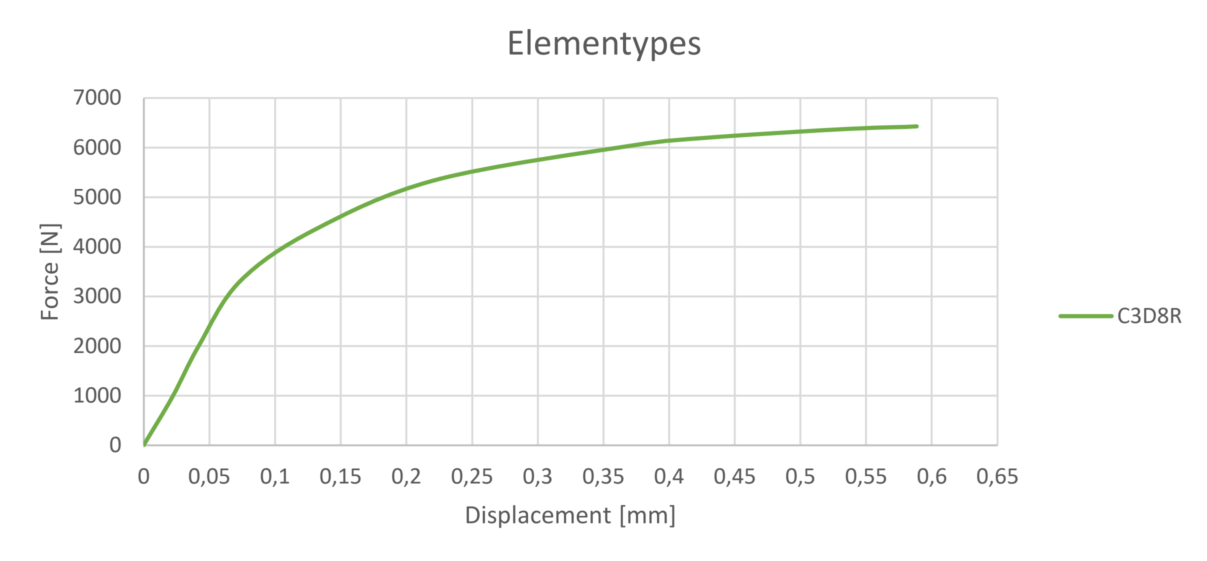

Graph 26: Full analysis of the 1-screw model using the C3D8R element type

2) C3D8

The only difference with the previous C3D8R element type is that for this element there is no reduced integration. For this element there are 2x2x2 integration points. Due to the full integration of the element, this type is not recommended to be used in models with plastic behavior. The following graph gives a comparison between the C3D8 and C3D8R models. The major difference is that the element type without the reduced integration (C3D8), has less displacement then with reduced integration. This is due to the fact that the R-elements are not recommended for models with plastic behavior. [19]

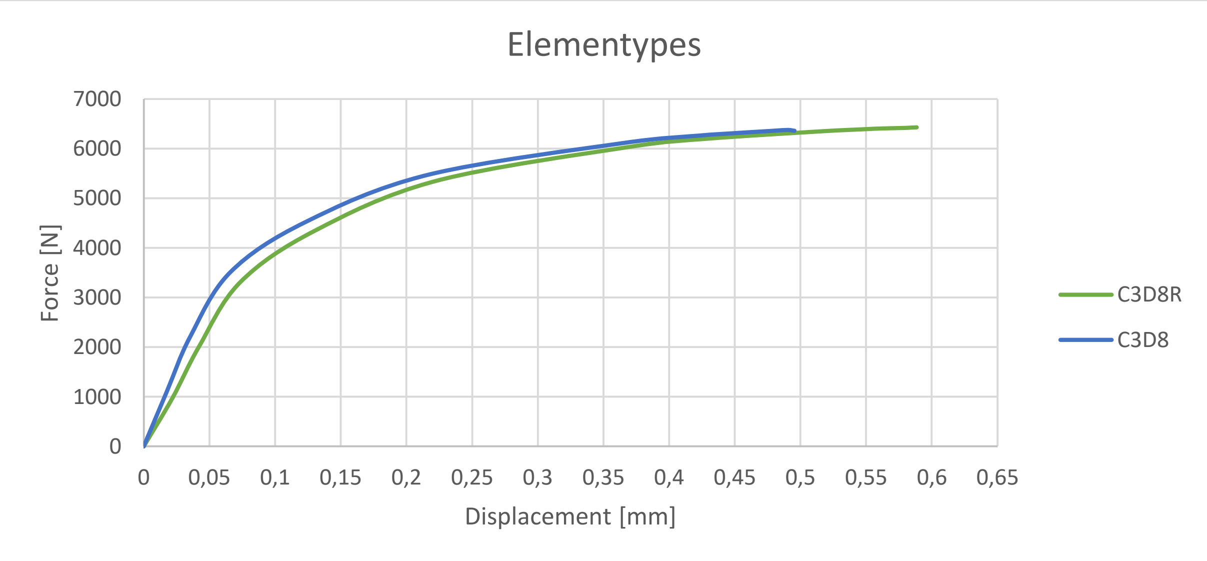

Graph 27: Difference between C3D8R and C3D8

3) C3D20R

The C3D20R element is a quadratic brick element. It has a reduced integration of 2x2x2 integration points. These elements are designed to have a better accuracy then the 8 node models however they are a lot more time consuming. The following image shows the structure with the nodes.

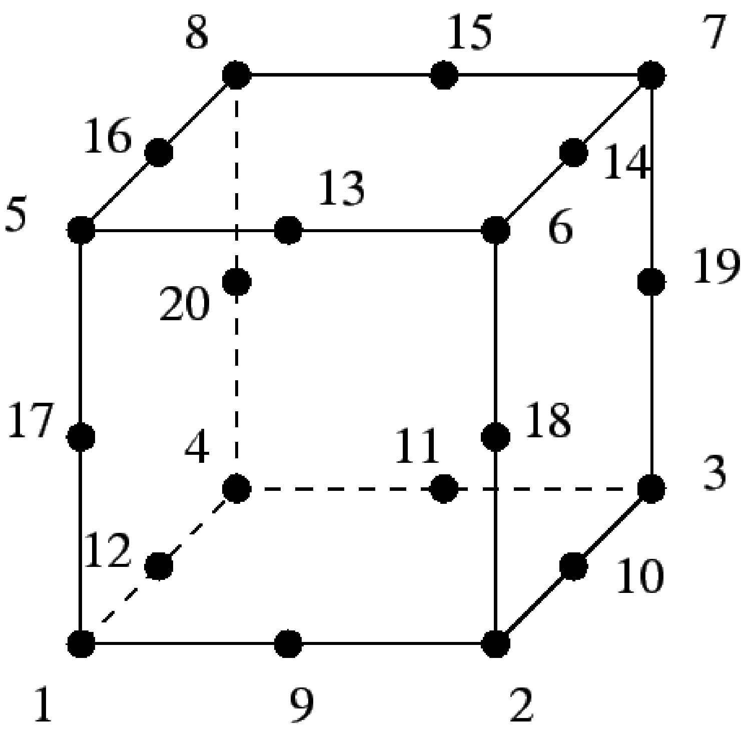

Figure 26: C3D20R element with the nodes

There is one major problem with these quadratic elements however. Models that use some form of contact cause issues when used in combination with the quadratic element types. This problem is also visible in the analysis of the 1-screw model. If compared to the C3D8R model, it is notable that the quadratic model (C3D20R) stops a lot sooner. [20]

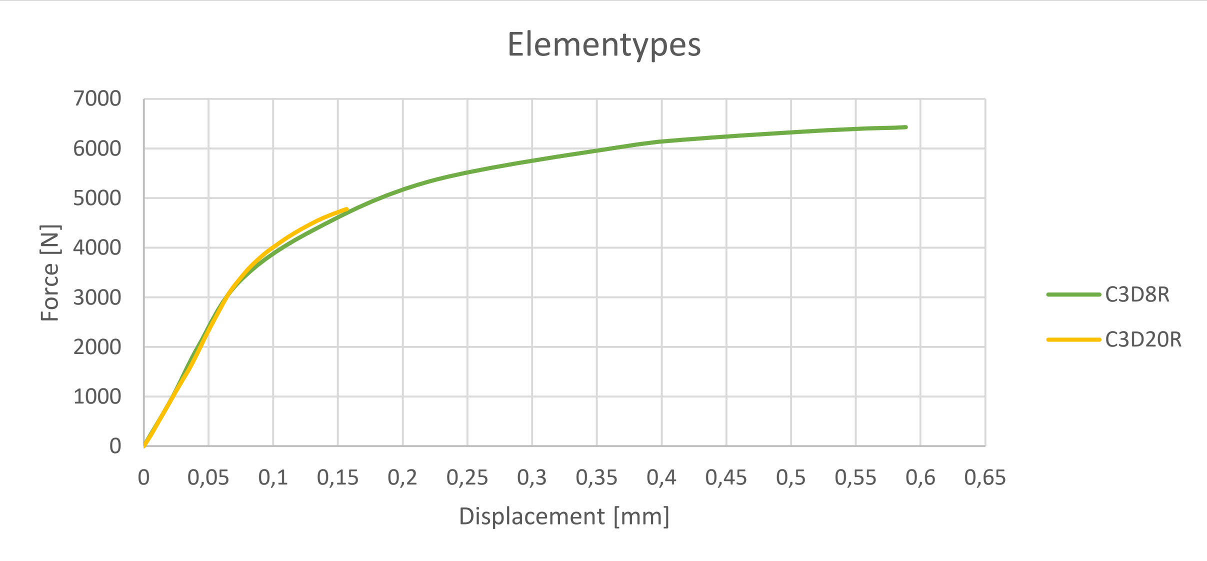

Graph 28: Difference between C3D8R and C3D20R

4) C3D20

The quadratic model without reduced integration is approximately the same as the reduced integration model. Because the quadratic elements have issues with parts in contact, this element type is not recommended for this analysis. The following graphs give an overview of the 4 different element types used for this study.

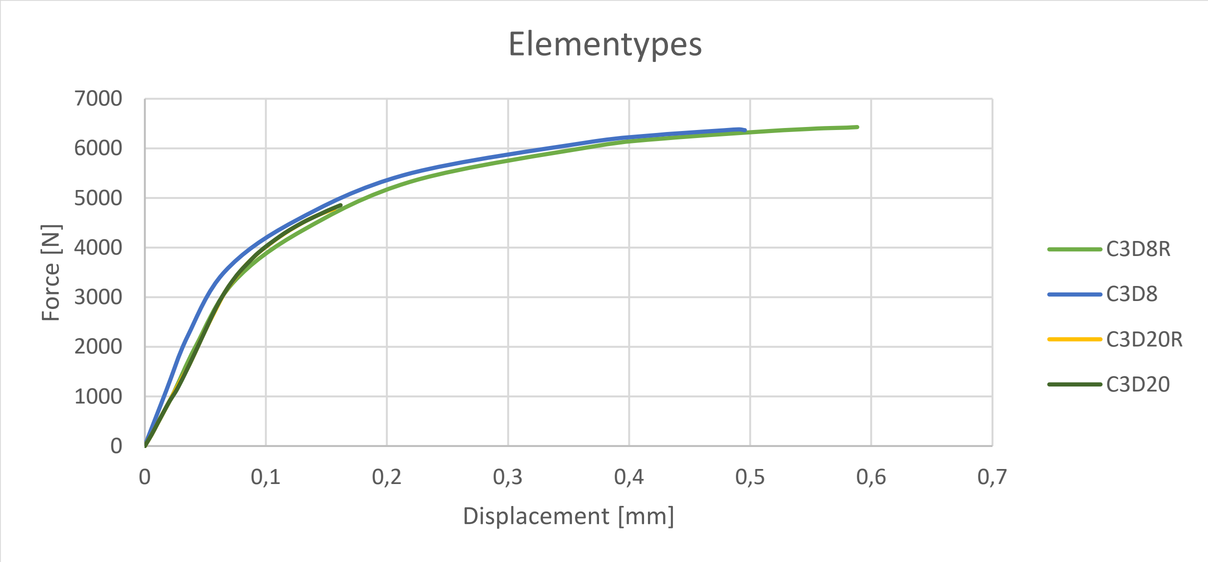

Graph 29: Difference between C3D8R, C3D8, C3D20R and C3D20

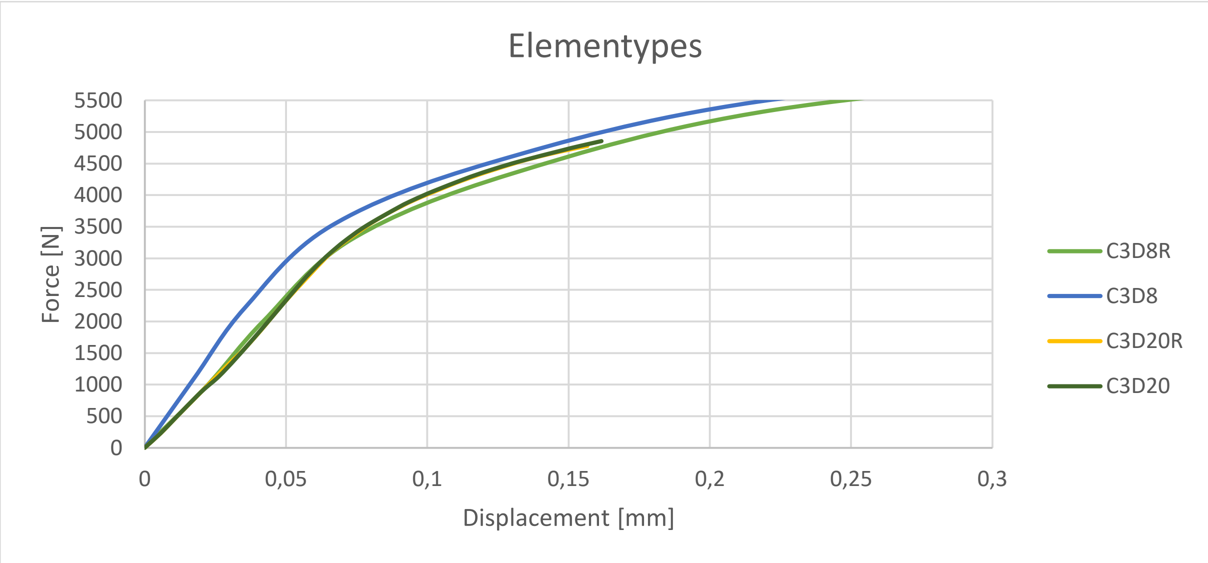

Graph 30: Difference between C3D8R, C3D8, C3D20R and C3D20 – Close-up

As a conclusion it is safe to say that the C3D8R element type gives the best results compared to the other element types. This is mainly due to the results in force and displacement. A convergence study is also based on the time it takes for a model to complete a full analysis. Since quadratic element are more refined then trilinear elements it takes a lot more time to compute these models. The quadratic models took approximately twice as long as the trilinear element models.

5.4 Simulation of the monotonic tests

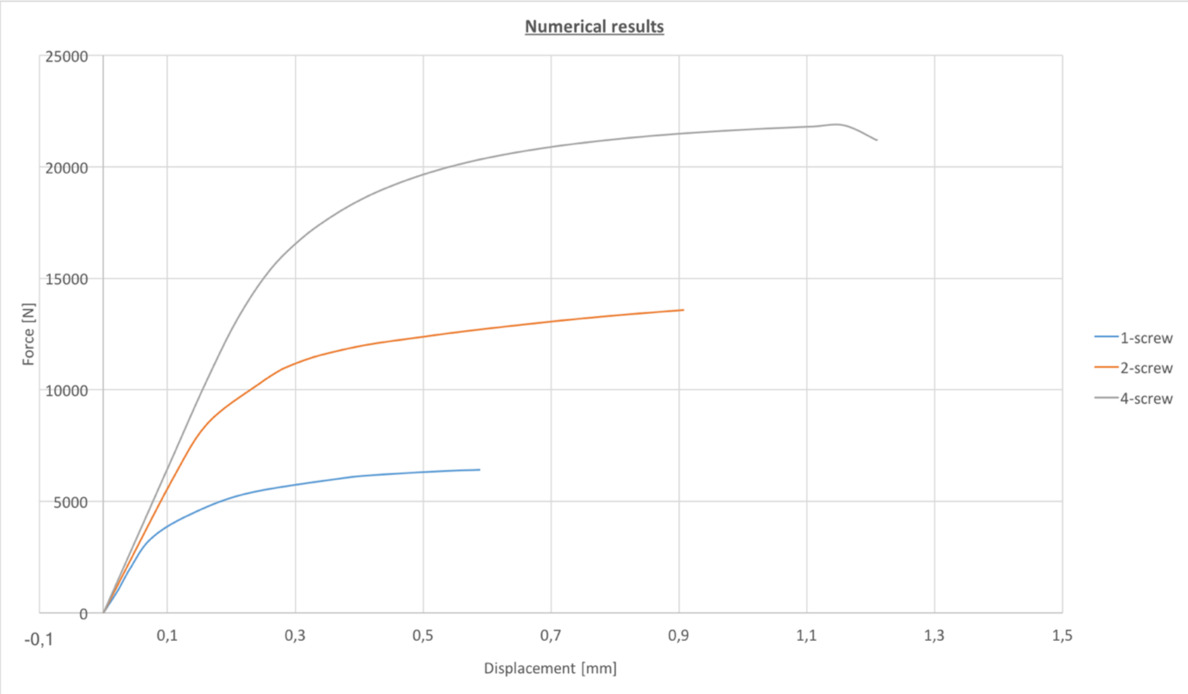

Graph 31: Results of the numerical simulation of the monotonic test

The graph above shows the results of the numerical simulations of the monotonic tests. In this simulation, the screw was simulated without a thread and with two screw heads. Therefore, the connection is going to behave more stiff, the rotation of the screw is limited due to the two heads. The stiffer connection causes to model to reach its maximum strength (which is reached in the tests) but the displacement of the specimens is going to be limited (only the bearing of the plate and the plasticity of the material is simulated).

5.4.1. Summary table

Numerical model (Abaqus)					
Test specimen	Maximum resistance of the connection (kN)	Displacement (mm)	Ratio	Stiffness (N/mm)	Initial stiffness (N/mm)
1 screw, first test	6,426	0,59	1	7261,016949	10891,52542
1 screw, second test	13,59	0,91	2,114845938	9956,043956	14934,06593
1 screw, third test	21,85	1,21	3,400248988	12038,56749	18057,85124

Table 8: Summery of the numerical simulations

5.5 Future works

In this paragraph some improvements and ideas for future works will be explained. Since the models are not perfectly modelled to how the tests are performed, some results deviate from the experimental results. During this thesis, some of these improvements have already been worked on. Due to the limitation in time, these improvements have not been implemented into this thesis as results.

5.5.1. Threaded screw

The biggest difference is the way the screw is modelled compared to the actual screw used in the tests. This simplified model as seen in paragraph 5.1 is a good starting model, but to have more accurate results, it is best that the screw is modelled more in detail. The following image is the model of the screw used in the experimental research.

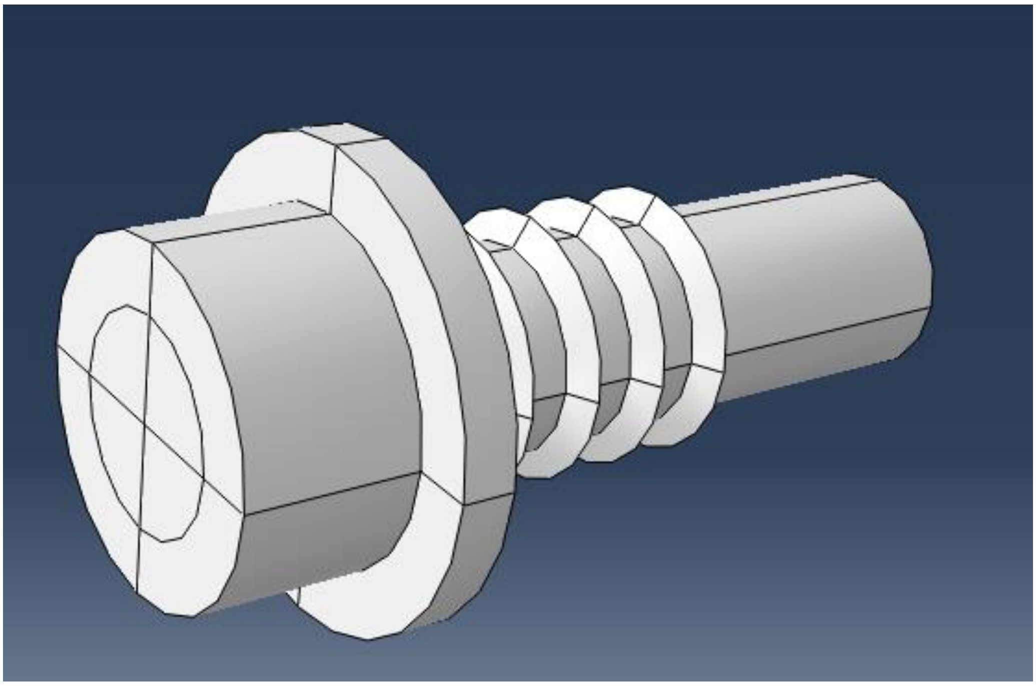

Figure 27: Modelling of the threaded screw

The structure of this part is much more complex than the simplified screw part. To have a perfect fit between the screw and the plate, 2 extra parts had to be made. This ‘rings’ are the parts in the plate which get in contact with the screw. They represent the cut thread in the plate. This is shown in the figure below.

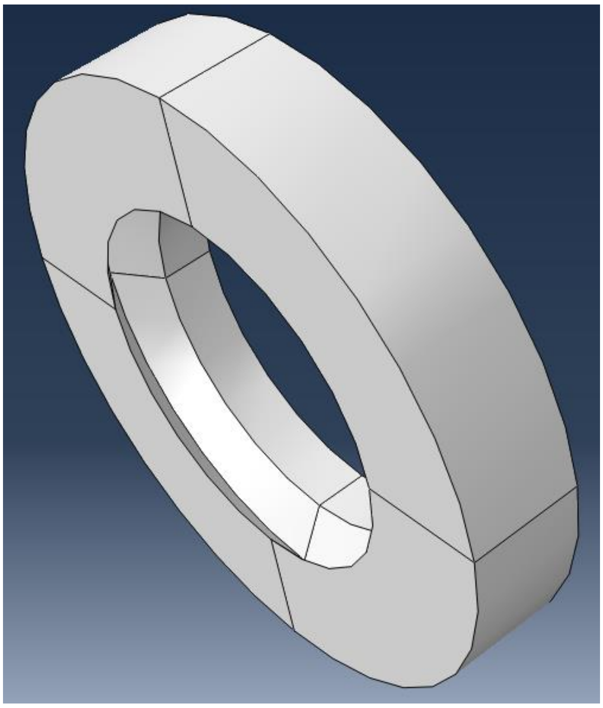

Figure 28: Modelling of the ring

The assembly of the complete model is shown the following image.

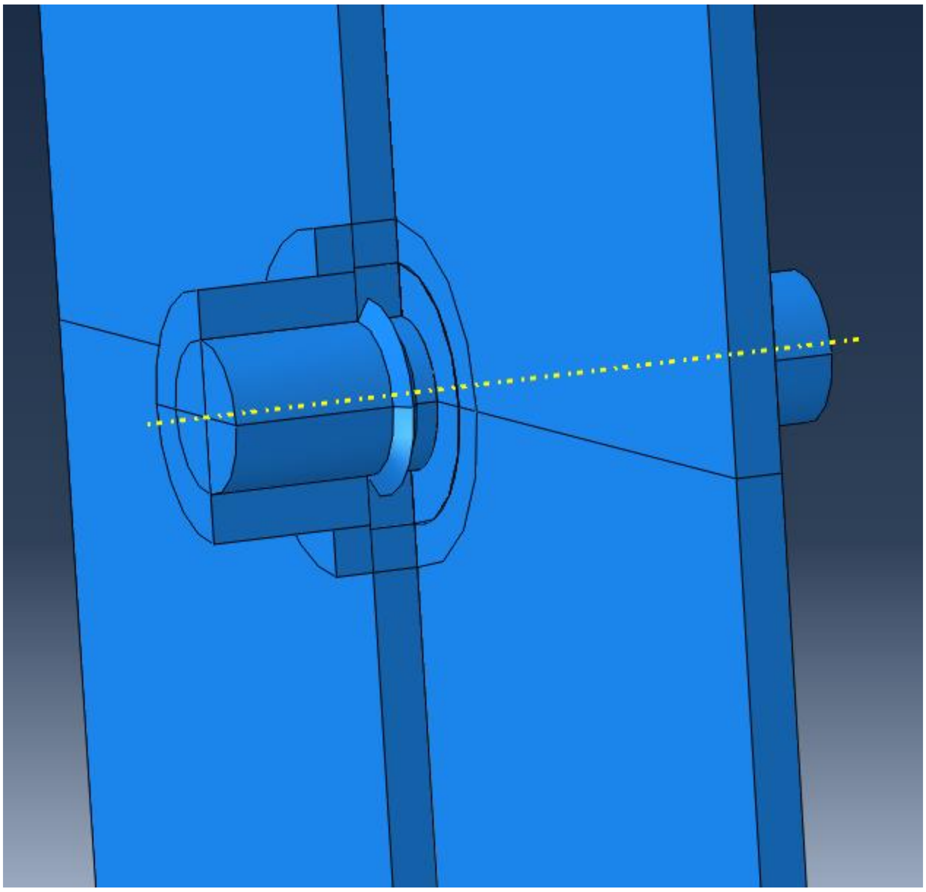

Figure 29: Assembly of the threaded connection

The complete analysis of this model was very time consuming, this is due to the complexity of the model. Since this research is limited in time, the model has not been completed and therefore it is an idea for a future work.

5.5.2. C-profile testing

The experimental testing happened using 1-, 2- and 4-screw connections with simple plate materials. During these experiments both the monotonic and cyclic loading happened with only tensile forces. The plates had a thickness of 1,5 mm which made it impossible to put any compressive forces on them. These forces would lead to buckling of the plate, instead of harming the connection. If c-profiles would have been used instead of plates, the cyclic loading would occur in both tensile and compressive forces. Which will lead to the connection being exposed to not only tensile forces. This may lead to different results and a different conclusion.

Normally the testing of the c-profiles would have been part of the thesis. The analytical calculations have already been made for the connection of the c-profile. The same procedure has been followed as in the 1-, 2- and 4-screw connection using only plates. The analytical approach was made using table 8.2 of the Eurocode EN 1993-1-3 [10].

Material properties

fy =	318	N/mm2	t =	1,5	mm
fu =	370	N/mm2	t1 =	1,5	mm
d =	6,3	mm	b =	100	mm
			A =	150	mm2

Bearing resistance

Fb,Rd = α.fu.d.t

with $\alpha = 3{,}2.\sqrt{(t/d)}$ and $\alpha \leq 2{,}1$ (t = t1)

α =	1,56			
fu =	370	Fb,Rd =	10919,15074	N
d =	6,3		10,92	kN
t =	1,5			
n =	2			

Net-section resistance

Fn,Rd = Anet.fu

with Anet = b.t for 2-screw b = (b - 2d)

2-screw	Anet =	131,1	mm2	
	Fn,Rd =		48507	N
			48,507	kN

Shear resistance

Fv,Rd = Fv,Rk* Fv,Rd = 12,82 kN

* This value can only be obtained by testing the material. According to the manufacturer the value is equal to 6,41 kN

Plasticity resistance

$F_{pl} = (F_y.A)/\gamma_{M0}$ Fpl = 47,70 kN

To make a stiff connection between the L-profiles and the c-profiles, a special part was made. To make sure this accessory had enough strength, some calculations were made. Again for this part, the formulas of the Eurocode table 8.4 of EN 1993-1-3 [10] have been used.

Material properties

(6 bolts of M10 class 8.8 will be used)

fy =	318	N/mm2	αb =	0,37	
fu =	370	N/mm2	kt =	1	for t > 1,25 mm
t =	1,5	mm	γ_{M2} =	1,25	
d0 =	11	mm	n =	6	
d =	10	mm			

Bearing resistance

Fb,Rd = (2,5.αb.kt.fu.d.t)/γ_{M2}

Fb,Rd =	24420	N
	24,42	kN

Shear resistance

Fv,Rd = (0,6.fub.As)/γM2 for strength grade 8.8

with	fub =	800	N/mm2
	As =	58	mm2

Fv,Rd =	133632	N	
	133,632		kN

To make sure that the accessory part could withstand the compressive forces, a calculation has been made to check its buckling resistance. This analytical calculation is done using paragraph 6.3 of the EN 1993-1-1 [21]. The results of the calculation are given below.

6.3 Buckling resistance of members - EN 1993-1-1 (2005)

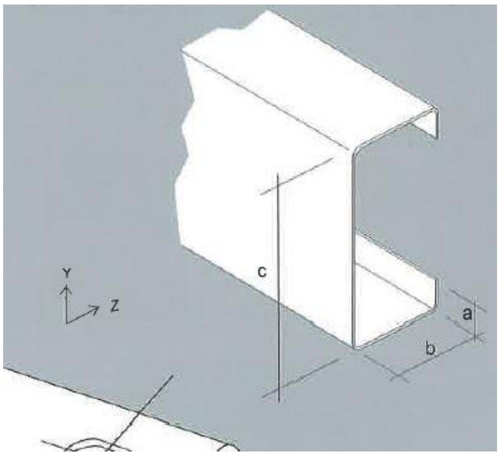

C-profile properties

a =	10	mm
b =	40	mm
c =	100	mm
t =	1,5	mm
A =	291	mm^2
l =	170	mm
f_y =	318	N/mm^2
E =	210000	N/mm^2
L_{cr} =	340	mm
$I_{z,eff}$ =	47130	mm^4
$A_{,eff}$ =	225	mm^2
i_z =	14,47	mm
α =	0,34	

$$\varepsilon = \sqrt{\frac{235}{f_y}} \quad (f_y \text{ in N/mm}^2)$$

ε = 0,85964743

$$\lambda_1 = \pi\sqrt{\frac{E}{f_y}} = 93{,}9\varepsilon$$

λ_1 = 80,720894

$$\bar{\lambda} = \sqrt{\frac{A_{eff} f_y}{N_{cr}}} = \frac{L_{cr}}{i}\frac{\sqrt{\frac{A_{eff}}{A}}}{\lambda_1} \quad \text{for Class 4 cross-sections}$$

λ = 0,256

$$\Phi = 0{,}5\left[1 + \alpha\left(\bar{\lambda} - 0{,}2\right) + \bar{\lambda}^2\right]$$

Φ = 0,542

$$\chi = \frac{1}{\Phi + \sqrt{\Phi^2 - \bar{\lambda}^2}} \quad \text{but } \chi \le 1{,}0$$

χ = 0,980

$$N_{b,Rd} = \frac{\chi A_{eff} f_y}{\gamma_{M1}} \quad \text{for Class 4 cross-sections}$$

$N_{b,Rd}$ =	70125,6302	N
	70,13	kN

Figure 30: Calculation of the buckling resistance

VI. Comparison of the results

6.1 Analytical vs. experimental

Monotonic tests					
Test specimen	Analytical results		Experimental results		Difference (kN)
	Type of failure resistance	Resistance (kN)	Type of failure resistance	Resistance (kN)	
1 screw, first test	Fb,Rd	5,46	Fb,Rd	6,57	1,11
1 screw, second test	Fb,Rd	5,46	Fb,Rd	6,75	1,29
2 screws, first test	Fb,Rd	10,92	Fb,Rd	12,85	1,93
2 screws, second test	Fb,Rd	10,92	Fb,Rd	12,9	1,98
4 screws, first test	Fb,Rd	21,84	Fb,Rd	25,12	3,28
4 screws, second test	Fb,Rd	21,84	Fb,Rd	25,78	3,94

Table 9: Comparison monotonic results

Cyclic tests					
Test specimen	Analytical results		Experimental results		Difference (%)
	Type of failure resistance	Resistance (kN)	Type of failure resistance	Resistance (kN)	
1 screw, first test	Fb,Rd	5,46	Fb,Rd	6,89	26,20%
1 screw, second test	Fb,Rd	5,46	Fb,Rd	6,72	23,10%
1 screw, third test	Fb,Rd	5,46	Fb,Rd	6,89	26,20%
2 screws, first test	Fb,Rd	10,92	Fb,Rd	13,47	23,40%
2 screws, second test	Fb,Rd	10,92	Fb,Rd	13,72	25,60%
2 screws, third test	Fb,Rd	10,92	Fb,Rd	12,5	14,50%
4 screws, first test	Fb,Rd	21,84	Fb,Rd	25,13	15,10%
4 screws, second test	Fb,Rd	21,84	Fb,Rd	25,57	17,10%
4 screws, third test	Fb,Rd	21,84	Fb,Rd	25,39	16,30%

Table 10: Comparison cyclic results

6.2 Numerical vs. experimental

The numerical models, as described in previous paragraphs, will now be compared to the results of the tests. This comparison is a good indication whether the tests have been performed correctly or if the models have been designed properly. The Abaqus models have some limitations concerning the displacement. This is due to the stiff connection and the simplified modelling of the screw. The following diagrams show the numerical models compared to the results of the experimental tests.

6.2.1. One screwed connection

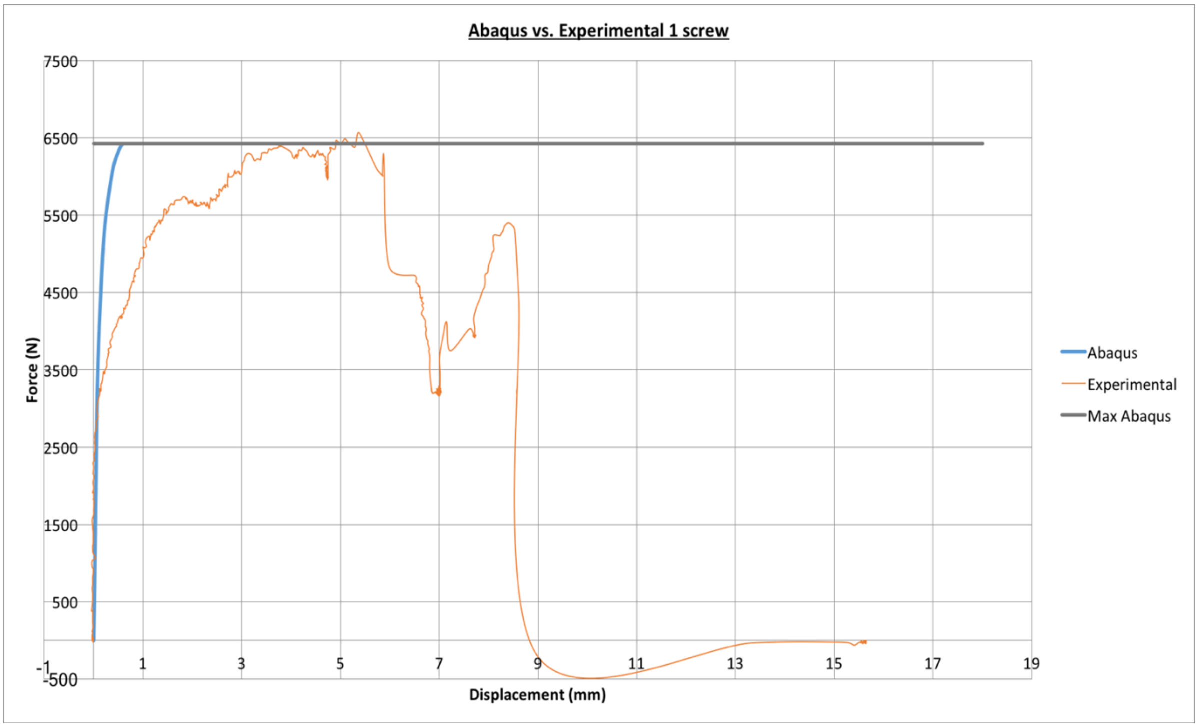

Graph 32: Comparison between Abaqus and the experiments - one screw

As seen in the above graphic, the displacement of the numerical model (Abaqus) stops at approximately 0,6 mm. Whereas the experimental test reaches displacements of 5-6 mm before having a complete failure. This is due to the simplified modelling of the screw. Because the heads are blocking any rotation of the screw, the model is not running as far as it is supposed to go. The maximum force however, is computed properly. The numerical model has its maximum force about the same as the experimental test. The horizontal line represents the maximum force from the numerical model shown as a plateau.

6.2.2. Two screwed connection

The results in the comparison of the 2-screw connection, differ from the 1-screw connection. The biggest difference is the fact that the numerical model is giving a larger maximum force compared to the experimental results. The Abaqus model failed after reaching 13,5 kN whereas the experiments had a maximum force of approximately 12,5 kN. The displacement for the numerical model is again limited due to the simplified screw model. The numerical model being stiffer than the experimental model is visible in the graph shown below. The displacement of the experimental models starts increasing after reaching about 4,5 kN whereas the numerical model only starts having displacement at around 10,5 kN. This is due to the limitation in rotation of the screw in the ‘Abaqus’ model.

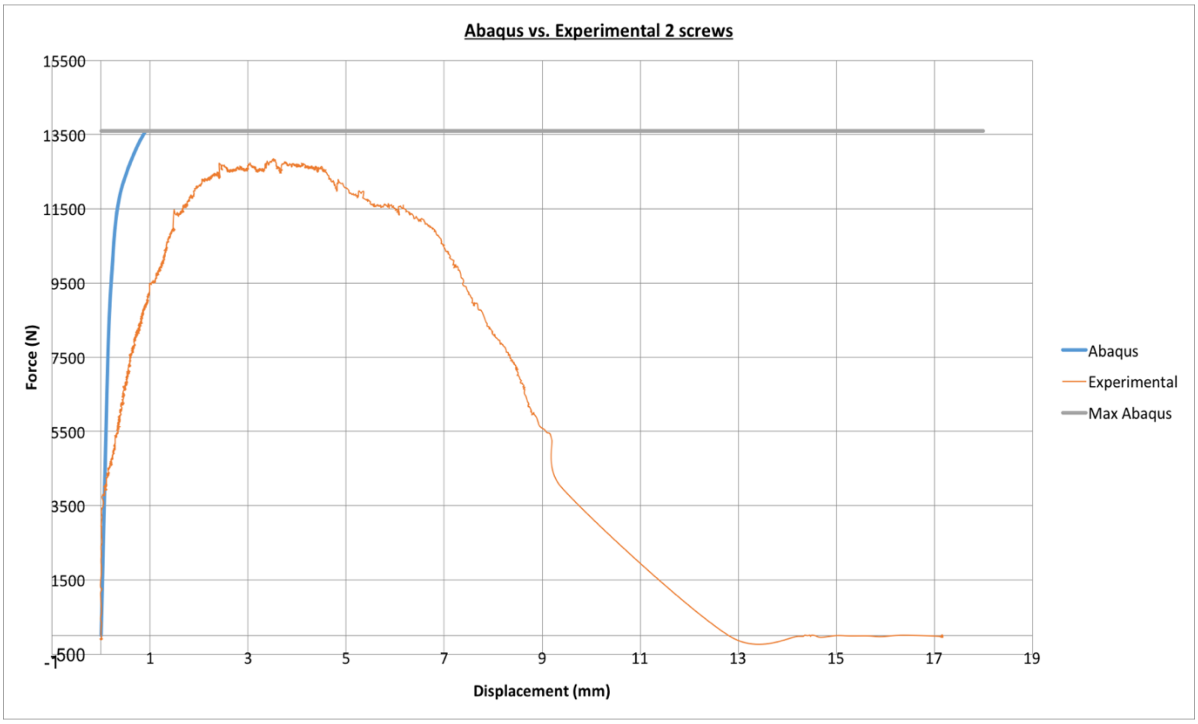

Graph 33: Comparison between Abaqus and the experiments - two screws

6.2.3. Four screwed connection

The numerical model of the 4-screw connection is not reaching the maximum force like it did during the experiments. The numerical model has its maximum force reached after 1,2 mm of displacement with a total of approximately 22 kN. The experiments reached a maximum of about 24,5 kN. There was however, a noteworthy drop in force in the numerical model. After reach its maximum force, it dropped till 22 kN. This reduction did not happen in the 1- and 2-screw models.

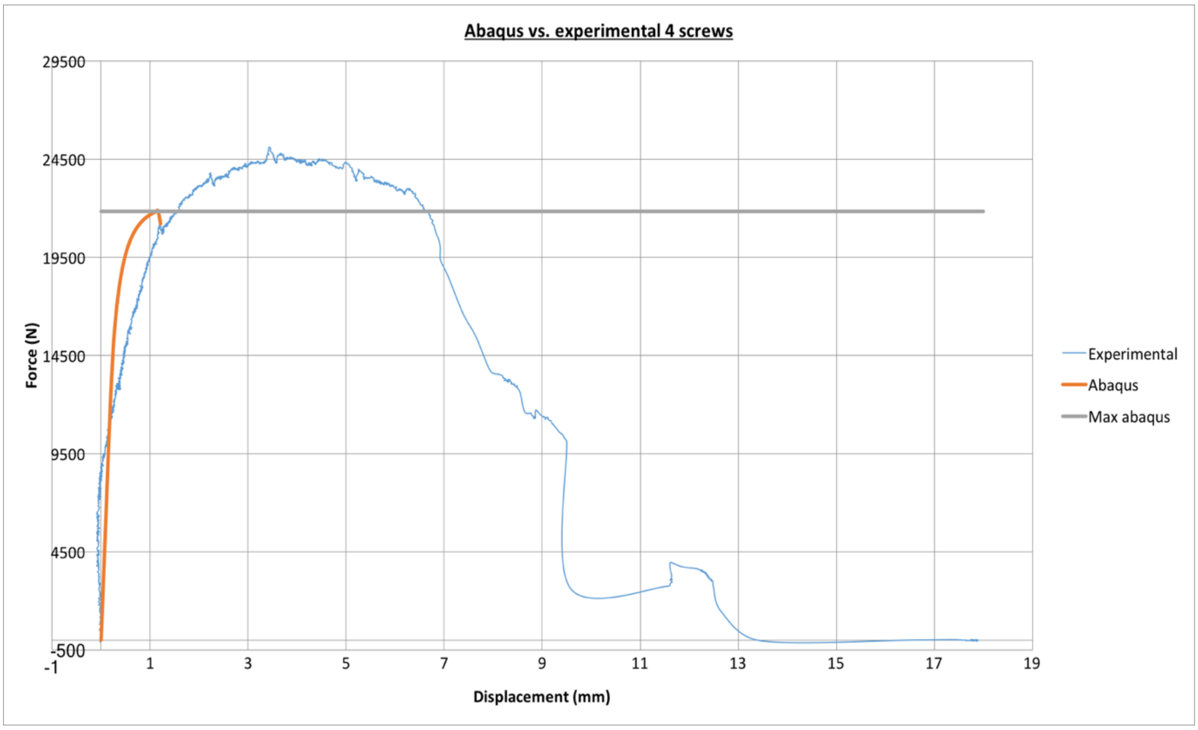

Graph 34: Comparison between Abaqus and the experiments - four screws

6.2.4. Summary table

The following table is a resume of the maximum forces of the experiments and the numerical models. The last column gives the ratio, which is a good indication of the similarity between the numerical and experimental results. The closer this value gets to 1, the closer the numerical results are to the experimental results. The ratios found for the 1- and 2-screw connection are fairly close to the value of 1, whereas the 4-screw connection is having a bit more difference in maximum forces. This table is only based on the maximum forces and does not include for instance the stiffness of the connection. As described in the paragraphs above, is the connection due to the simplified screw model, much stiffer than the actual connection in the experiments. Therefor will the displacement not reach values higher then 1,5 mm since rotation is blocked by the screw heads. So as conclusion it is safe to say that the maximum forces are well computed but the simulation of the displacement has yet to be improved in the Abaqus models.

Test specimen	Experimental results (kN)	Abaqus results (kN)	Ratio
Average 1 screw	6,66	6,426	0,964864865
Average 2 screws	12,875	13,59	1,055533981
Average 4 screws	25,45	21,85	0,858546169

Table 11: Summary between the Abaqus and the experimental results

6.3 Cyclic tests vs. monotonic tests (experimental)

6.3.1. One screwed connection

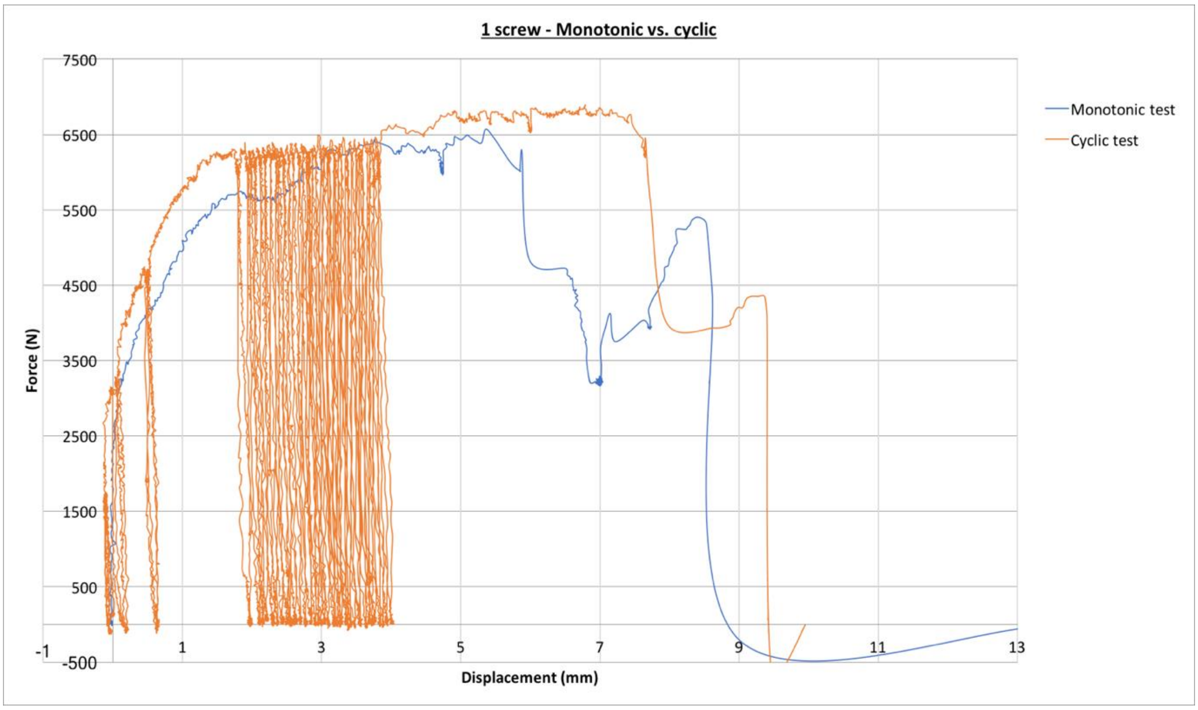

Graph 35: Comparison between cyclic and monotonic tests - one screw

6.3.2. Two screwed connection

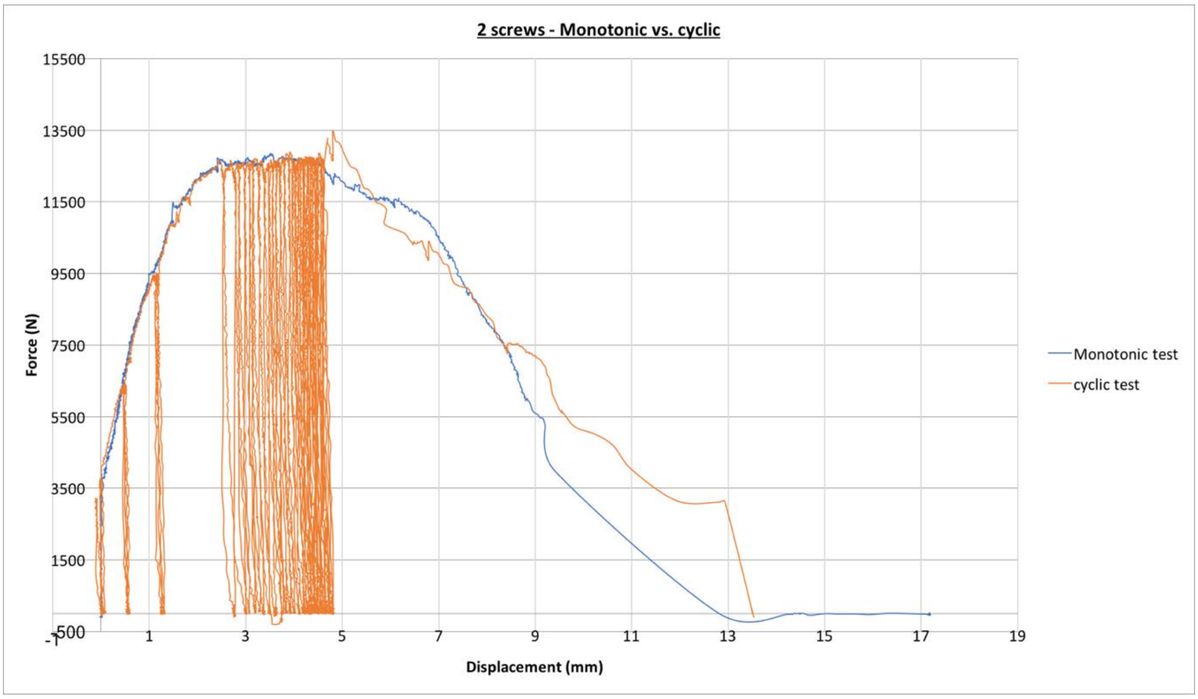

Graph 36: Comparison between cyclic and monotonic tests - two screws

6.3.3. Four screwed connection

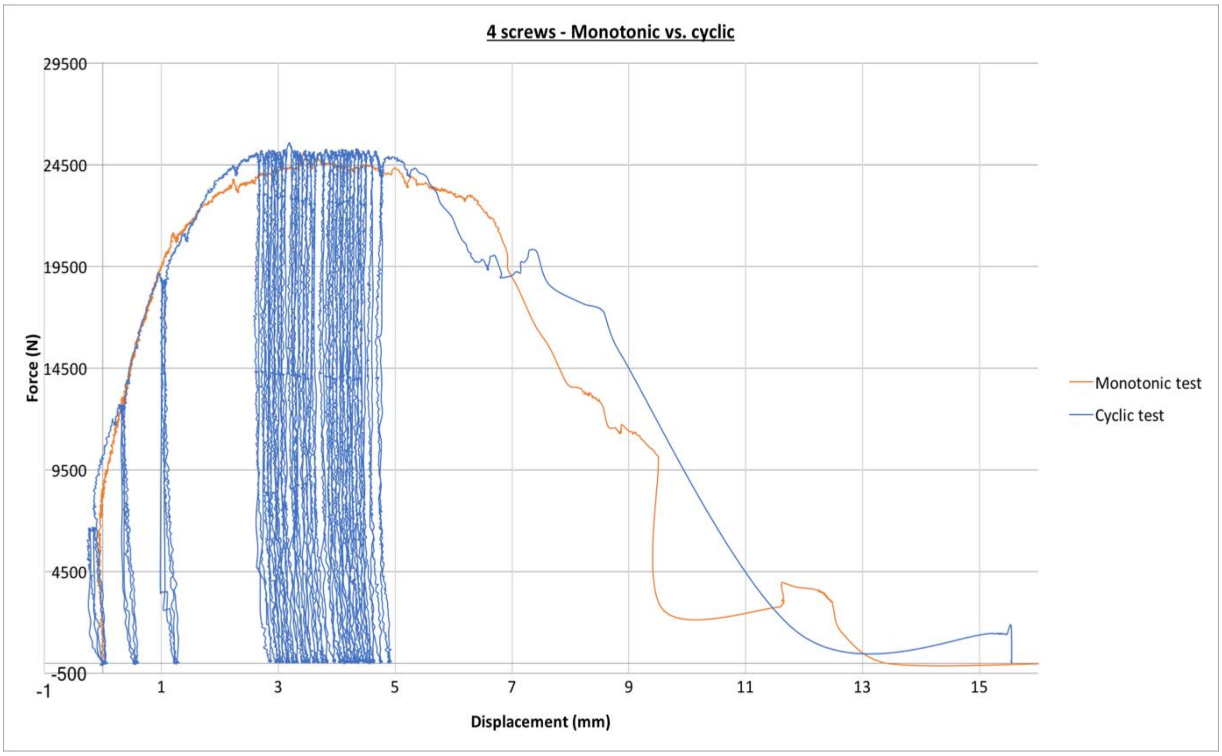

Graph 37: Comparison between cyclic and monotonic tests - four screws

6.3.4. Summary table

Test specimen	Monotonic results (kN)	Cyclic results (kN)	Ratio
Average 1 screw	6,66	6,833333333	1,026026026
Average 2 screws	12,875	13,23	1,027572816
Average 4 screws	25,45	25,36333333	0,99659463

Table 12: Summary of the difference between the cyclic and the monotonic tests

VII. Conclusions

Some general conclusions can be made regarding the results generated by this thesis:

For the experimental approach of the monotonic tests there can be concluded that the maximum force and the displacement of the connections are pretty similar to the results that are given in the analytical approach. The maximum strength of the connection is higher in the experiments due to the safety factor which is used in the analytical approach. The formulae in the Eurocode give a good representation of the behaviour of a screwed connection in LSF structures under a monotonic load. The Eurocode does not yet have a section dedicated to the behaviour of screwed connections under cyclic loading. The compilation of different formulae dedicated to the analytical calculation of LSF structures would be an improvement to the current European standards.

The cyclic tests give a uniform image of the impact of cyclic loading on a screw connection in LSF, in this way of testing, there is no decrease of strength after the cycles have been completed. However, some improvements of the testing procedure can possibly give other results. For example, this thesis only applies cycles in tension, in future experiments the C-profiles can also be tested with tension-compression cycles. The addition of compression can possibly give other results of the impact of cyclic loading on screwed connections. The usage of fully-automatic testing equipment will also give a better understanding of the displacement of the connection, this displacement will probably be more uniform.

Next to the analytical and experimental approach, a numerical study has been made. The results of these numerical models had a decent comparison to the results obtained by the monotonic tests. The displacement however, was not computed properly. This is due to the simplified modelling of the screw. A detailed model of the screw will have an impact on the results and will probably lead to a larger displacement of the models. In this research only monotonic loads have been used in the FEM-tool. By performing cyclic loads on the models in the software, a direct comparison can be made between the results of the cyclic numerical models and the cyclic experimental results. This detailed comparison can lead to a more accurate result.

Lastly it is needed to say that whatever the case is, there is definitely a need for a more detailed approach to the impact of cyclic loading on a screwed connection in light steel framing structures. This thesis is a good basis for future works to improve the knowledge of the impact of cyclic loading.

References

[1] A. Amundarain, „Edinburgh Research Archive," 11 09 2006. [Online]. Available: https://www.era.lib.ed.ac.uk/handle/1842/1409.

[2] Construction knowledge, „Construction knowledge," [Online]. Available: http://www.constructionknowledge.net/metal/metal_cold_formed_steel.php.

[3] Metro plus, „Metro plus design," [Online]. Available: http://www.iliasnotes.info/2015/06/cold-formed-steel-design-structural.html.

[4] ClarkDietrich Engineering Services, „ClarkDietrich," [Online]. Available: http://www.clarkdietrich.com/sites/default/files/imce/pdf/SupportTools/Catalogs/IntroToFraming/CD_IntroToFraming_2-11-14.pdf.

[5] Wikipedia, „Cold-formed steel," 15 September 2016. [Online]. Available: https://en.wikipedia.org/wiki/Cold-formed_steel. [Geopend 6 Oktober 2016].

[6] Steel framing alliance, „Steel framing guide," [Online]. Available: http://www.steelframing.org/PDF/SFA_Framing_Guide_final%202.pdf.

[7] European Light Steel Construction Association, „Stahlbau Zentrum Schweiz," [Online]. Available: http://www.szs.ch/user_content/editor/files/Downloads_Statik/european%20lightweight%20steel-framed%20construction.pdf.

[8] Wikipedia, "Eurocodes," 17 June 2016. [Online]. Available: https://en.wikipedia.org/wiki/Eurocodes. [Accessed 30 November 2016].

[9] Eurocodes, „About the EN Eurocodes," Joint Research Centre, [Online]. Available: http://eurocodes.jrc.ec.europa.eu/showpage.php?id=1. [Geopend 1 December 2016].

[10] The European Union, "EN 1993-1-3," October 2006. [Online]. Available: https://law.resource.org/pub/eu/eurocode/en.1993.1.3.2006.pdf.

[11] European convention for constructional steelwork, *Recommended testing procedure for assessing the behaviour of structural steel elements under cyclic loads,* 1 red., 1986.

[12] Index fixing systems, *Self-drilling screws ABE 6.3,* Index fixing systems, 2012.

[13] LUKAS, „LUKAS Industrial," [Online]. Available: https://industrial.lukas.com/Products/Pumps/Hand+pumps.html.

[14] LUKAS, „LUKAS Industrial," [Online]. Available: https://industrial.lukas.com/Products/Lifting+cylinders/Single_acting+light_alloy+cylinders.html.

[15] HBM, „HBM," [Online]. Available: https://www.hbm.com/nl/2410/u10m-u10s-load-cell-for-static-and-dynamic-tensile-and-compressive-forces/.

[16] Wikipedia, „Wikipedia,” [Online]. Available: https://en.wikipedia.org/wiki/Linear_variable_differential_transformer.

[17] M. A. Sokol, R. A. LaBoube en W.-w. Yu, *Determination of the tensile and shear strengths of screws and the e ect of screw pa erns on cold- formed steel connections,* Center for Cold-Formed Steel Structures Library, 1998.

[18] Wikipedia, „Finite element method,” 9 January 2017. [Online]. Available: https://en.wikipedia.org/wiki/Finite_element_method. [Geopend 10 January 2017].

[19] G. Dhondt, „Eight-node brick element with reduced integration (C3D8R and F3D8R),” 2 March 2014. [Online]. Available: http://web.mit.edu/calculix_v2.7/CalculiX/ccx_2.7/doc/ccx/node27.html.

[20] G. Dhondt, „Eight-node brick element (C3D8 and F3D8),” 2 March 2014. [Online]. Available: http://web.mit.edu/calculix_v2.7/CalculiX/ccx_2.7/doc/ccx/node26.html.

[21] G. Dhondt, „Twenty-node brick element with reduced integration (C3D20R and F3D20R),” 2 March 2014. [Online]. Available: http://web.mit.edu/calculix_v2.7/CalculiX/ccx_2.7/doc/ccx/node30.html.

[22] The European Union, „EN 1993-1-1,” May 2005. [Online]. Available: https://law.resource.org/pub/eu/eurocode/en.1993.1.1.2005.pdf.

[23] The European Union, „EN 1993-1-8,” May 2005. [Online]. Available: https://law.resource.org/pub/eu/eurocode/en.1993.1.8.2005.pdf. [Geopend 15 January 2017].

Attachments

Attachment A: Production drawing 1

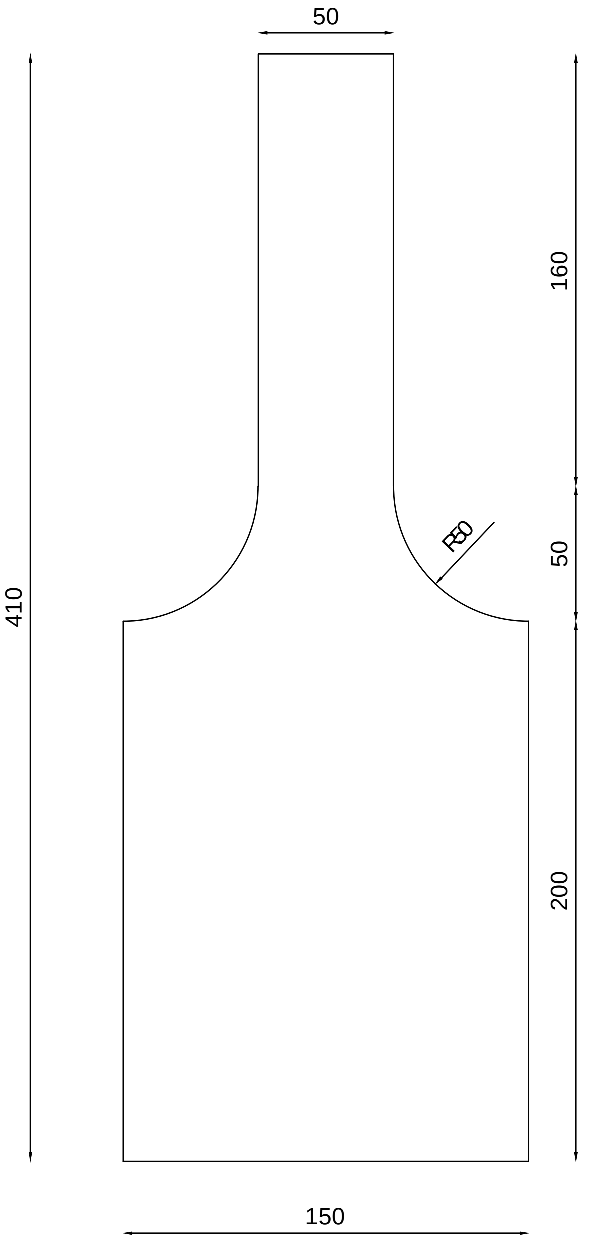

- Alle dimensies in mm
- Totaal stukken: 10
- t=1.5mm

Stuk 1	
designer: Chris Gielen & Karsten Moreels	scale:
date: 06/10/16	

Attachment B: Production drawing 2

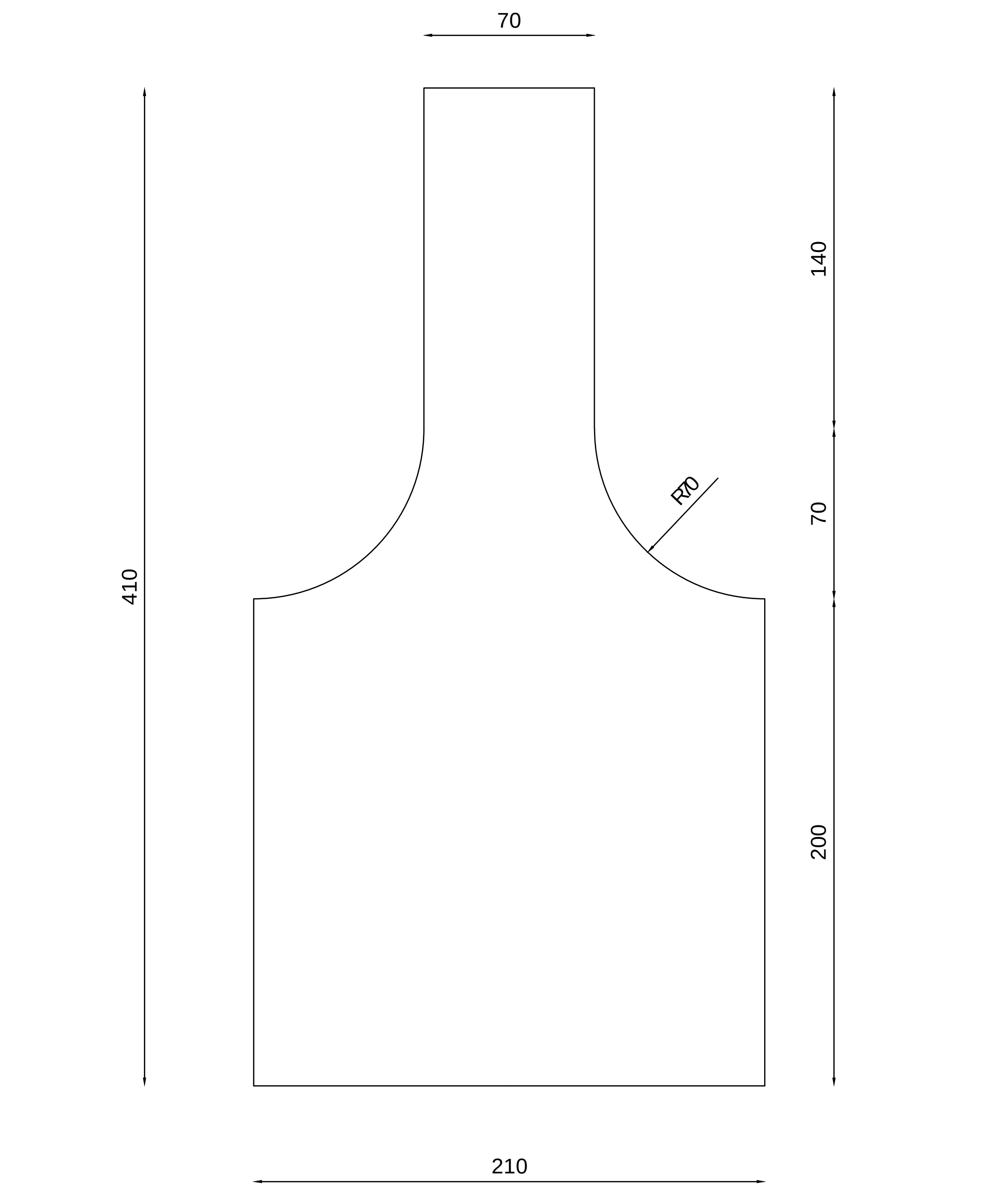

* Alle dimensies in mm
* Totaal stukken: 10
* t=1.5mm

Stuk 2	
designer: Chris Gielen & Karsten Moreels	scale:
date: 06/10/16	

Attachment C: Production drawing 3

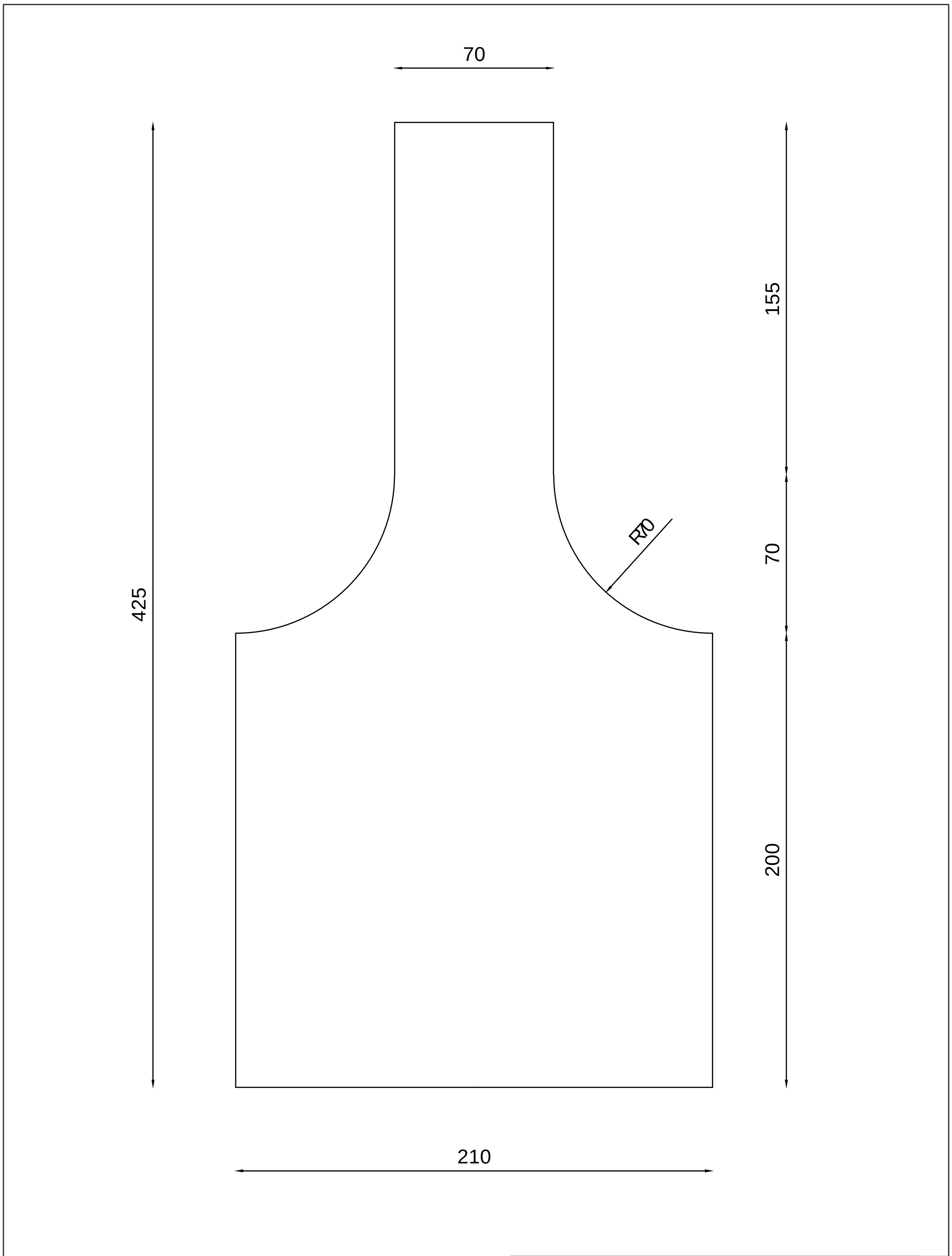

*   Alle dimensies in mm
*   Totaal stukken: 10
*   t=1.5mm

Stuk 3	
designer: Chris Gielen & Karsten Moreels	scale:
date: 06/10/16	

Attachment D: Assembly 1

2X stuk 1

Schroef = Self tapping screw (gat diameter 5.5mm)

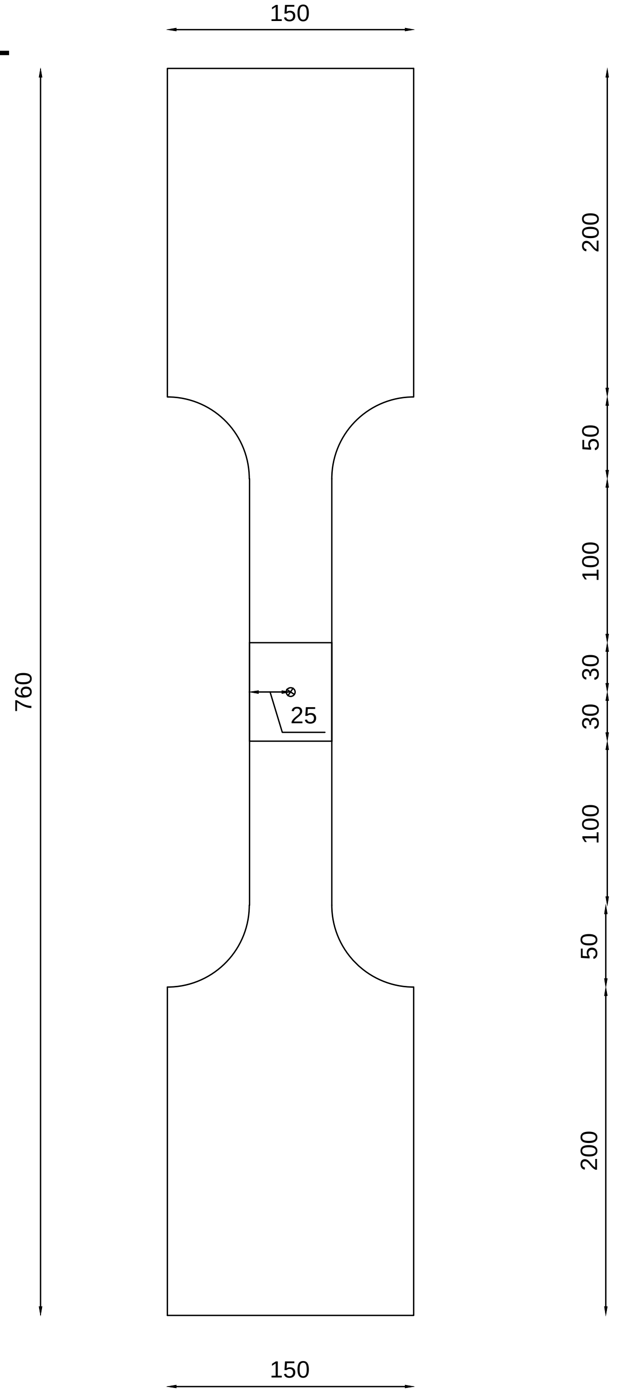

* Alle dimensies in mm

* Totaal stukken: 5

Assemblage 1	
designer: Chris Gielen & Karsten Moreels	scale:
date: 06/10/16	

Attachment E: Assembly 2

2X stuk 2

Schroef = Self tapping screw (gat diameter 5.5mm)

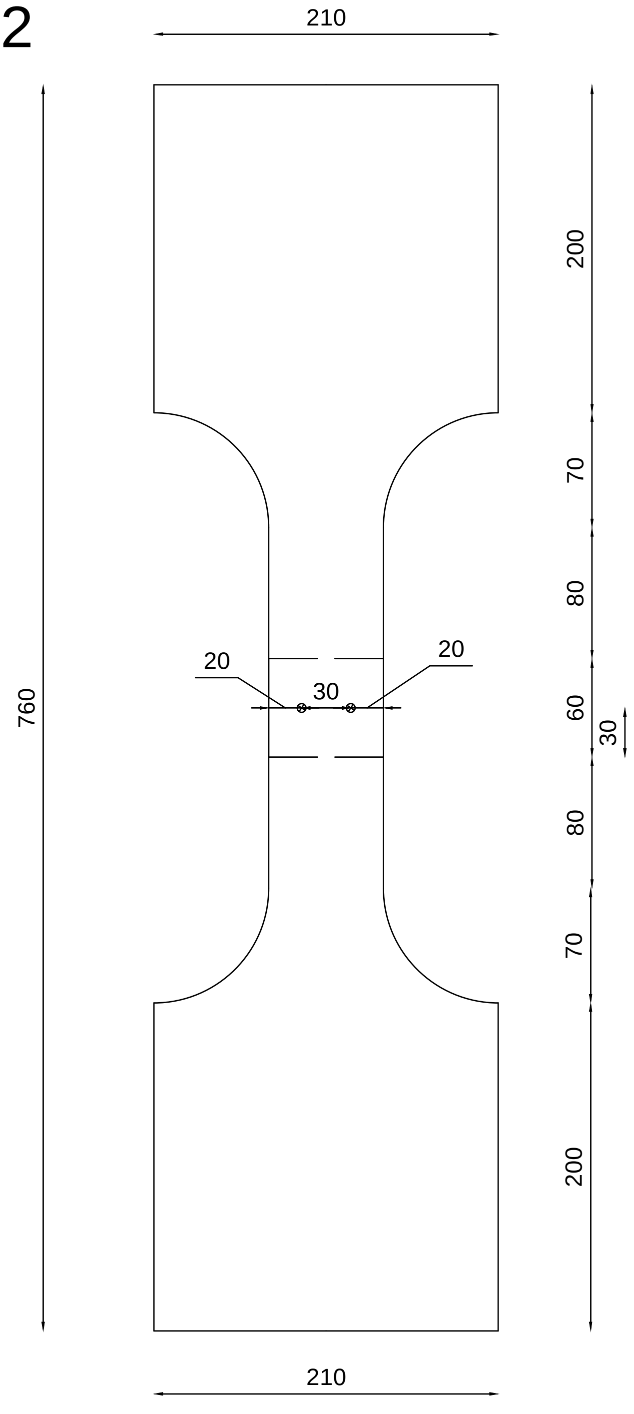

* Alle dimensies in mm

* Totaal stukken: 5

Assemblage 2	
designer: Chris Gielen & Karsten Moreels	scale:
date: 06/10/16	

Attachment F: Assembly 3

2X stuk 3

Schroef = Self tapping screw (gat diameter 5.5mm)

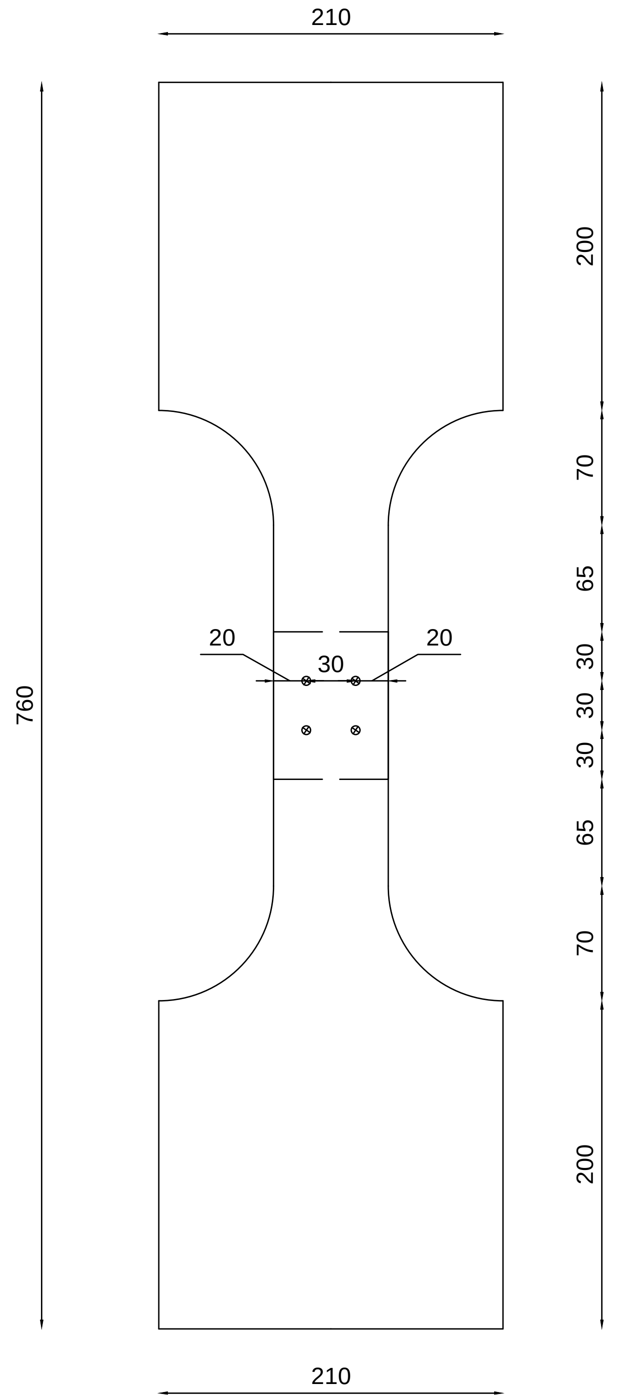

* Alle dimensies in mm

* Totaal stukken: 5

Assemblage 3	
designer: Chris Gielen & Karsten Moreels	scale:
date: 06/10/16	

Attachment G: Sample plate

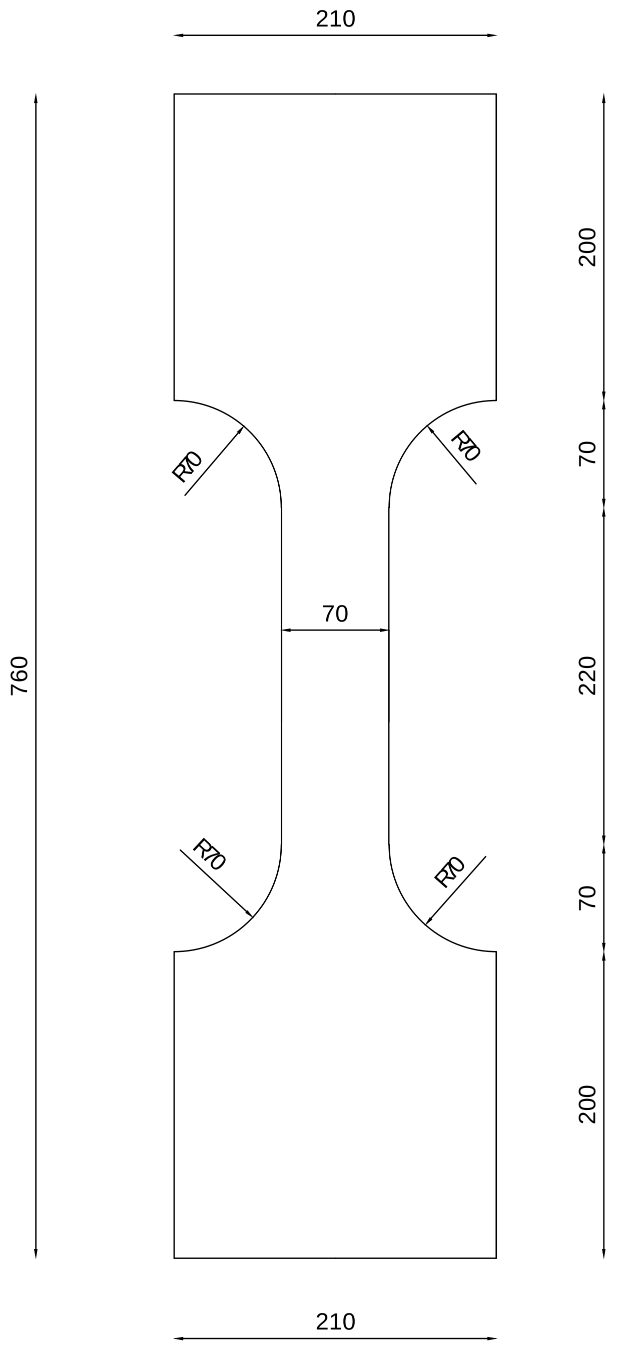

* Alle dimensies in mm
* Totaal stukken: 2
* t=1.5mm

Sample plate	
designer: Chris Gielen & Karsten Moreels	scale:
date: 06/10/16	

Attachment H: L-profile 200x200x20

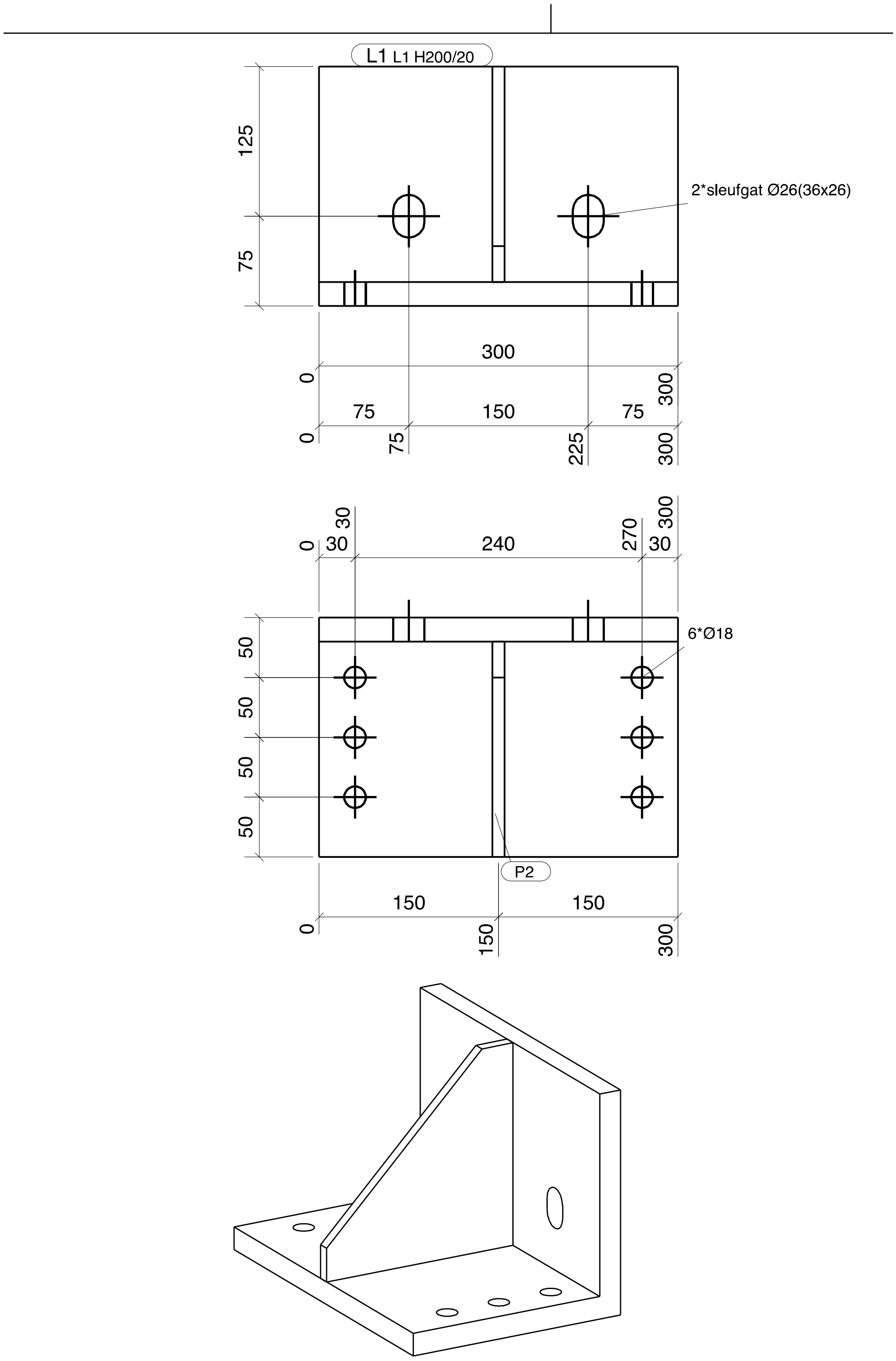

Attachment I: Calculation 1-screw connection

Screw loaded in shear - table 8.2 EN 1993-1-3 (2006)

Material properties

f_y =	318 N/mm^2	t =	1,5 mm
f_u =	370 N/mm^2	t_1 =	1,5 mm
d =	6,3 mm	b =	50 mm
		A =	75 mm^2

Bearing resistance

$F_{b,Rd} = \alpha . f_u . d . t$

with $\alpha = 3{,}2.\sqrt{(t/d)}$ and $\alpha \leq 2{,}1$ $(t = t_1)$

α =	1,56
f_u =	370
d =	6,3
t =	1,5

$F_{b,Rd}$ =	5459,575	N
	5,46	kN

Net-section resistance

$F_{n,Rd} = A_{net} . f_u$

with $A_{net} = b.t$ for 1-screw b = b-d

1-screw A_{net} = 65,55 mm^2

$F_{n,Rd}$ =	24253,5	N
	24,2535	kN

Shear resistance

$F_{v,Rd} = F_{v,Rk*}$

$F_{v,Rd}$ =	6,41	kN

* This value can only be obtained by testing the material. According to a manufacturer the value is equal to 6,41 kN

Plasticity resistance

$F_{pl} = (Fy.A)/\gamma_{M0}$

F_{pl} =	23,85	kN

Attachment J: Calculation 2-screw connection

Screw loaded in shear - table 8.2 EN 1993-1-3 (2006)

Material properties

f_y =	318 N/mm^2	t =	1,5 mm
f_u =	370 N/mm^2	t_1 =	1,5 mm
d =	6,3 mm	b =	70 mm
		A =	105 mm^2

Bearing resistance

$F_{b,Rd} = \alpha.f_u.d.t$

with $\alpha = 3{,}2.\sqrt{(t/d)}$ and $\alpha \leq 2{,}1$ $(t = t_1)$

α =	1,56
f_u =	370
d =	6,3
t =	1,5
n =	2

$F_{b,Rd}$ =	10919,15	N
	10,92	kN

Net-section resistance

$F_{n,Rd} = A_{net}.f_u$

with $A_{net} = b.t$ for 2-screw $b = (b - 2d)$

2-screw A_{net} = 86,1 mm^2

$F_{n,Rd}$ =	31857	N
	31,857	kN

Shear resistance

$F_{v,Rd} = F_{v,Rk*}$

$F_{v,Rd}$ =	12,82	kN

* This value can only be obtained by testing the material. According to a manufacturer the value is equal to 6,41 kN

Plasticity resistance

$F_{pl} = (Fy.A)/\gamma_{M0}$

F_{pl} =	33,39	kN

Attachment K: Calculation 4-screw connection

Screw loaded in shear - table 8.2 EN 1993-1-3 (2006)

Material properties

f_y =	318 N/mm^2	t =	1,5 mm
f_u =	370 N/mm^2	t_1 =	1,5 mm
d =	6,3 mm	b =	70 mm
		A =	105 mm^2

Bearing resistance

$F_{b,Rd} = \alpha . f_u . d . t$

with $\alpha = 3{,}2 . \sqrt{(t/d)}$ and $\alpha \leq 2{,}1$ $(t = t_1)$

α =	1,56
f_u =	370
d =	6,3
t =	1,5
n =	4

→

$F_{b,Rd}$ =	21838,3	N
	21,84	kN

Net-section resistance

$F_{n,Rd} = A_{net} . f_u$

with $A_{net} = b.t$ for 4-screw $b = (b - 2d)$

4-screw A_{net} = 86,1 mm^2

$F_{n,Rd}$ =	31857	N
	31,857	kN

Shear resistance

$F_{v,Rd} = F_{v,Rk*}$ → $F_{v,Rd}$ = 25,64 kN

* This value can only be obtained by testing the material. According to a manufacturer the value is equal to 6,41 kN

Plasticity resistance

$F_{pl} = (Fy.A)/\gamma_{M0}$ → F_{pl} = 33,39 kN

Attachment L: Calculation C-profile (screw-connection)

Screw loaded in shear - table 8.2 EN 1993-1-3 (2006)

Material properties

f_y =	318 N/mm^2	t =	1,5 mm
f_u =	370 N/mm^2	t_1 =	1,5 mm
d =	6,3 mm	b =	100 mm
		A =	150 mm^2

Bearing resistance

$F_{b,Rd} = \alpha.f_u.d.t$

with $\alpha = 3{,}2.\sqrt{(t/d)}$ and $\alpha \leq 2{,}1$ $(t = t_1)$

α =	1,56
f_u =	370
d =	6,3
t =	1,5
n =	2

$F_{b,Rd}$ =	10919,15	N
	10,92	kN

Net-section resistance

$F_{n,Rd} = A_{net}.f_u$

with $A_{net} = b.t$ for 2-screw $b = (b - 2d)$

2-screw	A_{net} =	131,1	mm^2
	$F_{n,Rd}$ =	48507	N
		48,507	kN

Shear resistance

$F_{v,Rd} = F_{v,Rk*}$

$F_{v,Rd}$ =	12,82	kN

* This value can only be obtained by testing the material. According to a manufacturer the value is equal to 6,41 kN

Plasticity resistance

$F_{pl} = (Fy.A)/\gamma_{M0}$

F_{pl} =	47,70	kN

Attachment M: Calculation C-profile (bolt-connection)

Bolt loaded in shear - table 8.4 EN 1993-1-3 (2006)

Material propeties (6 bolts of **M10 class 8.8** will be used)

f_y =	318	N/mm^2	α_b =	0,37	
f_u =	370	N/mm^2	k_t =	1	for t > 1,25 mm
t =	1,5	mm	γM_2 =	1,25	
d0 =	11	mm	n =	6	
d =	10	mm			

Bearing resistance

$F_{b,Rd} = (2,5.\alpha_b.k_t.f_u.d.t)/\gamma M_2$

$F_{b,Rd}$ =	24420	N
	24,42	kN

Shear resistance

$F_{v,Rd} = (0,6.f_{ub}.A_s)/\gamma M_2$ → for strength grade 8.8

with	f_{ub} =	800	N/mm^2
	A_s =	58	mm^2

$F_{v,Rd}$ =	133632	N
	133,632	kN

Attachment N: Buckling resistance

6.3 Buckling resistance of members - EN 1993-1-1 (2005)

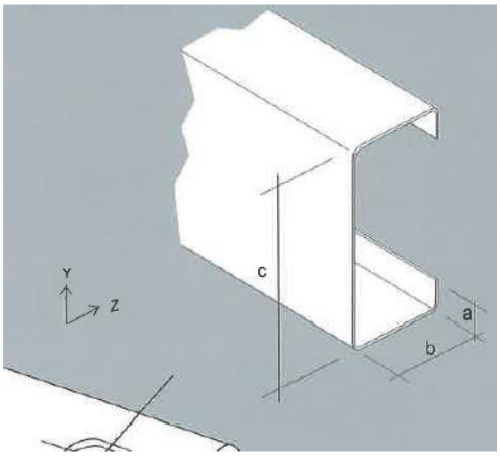

C-profile properties

a =	10	mm
b =	40	mm
c =	100	mm
t =	1,5	mm
A =	291	mm^2
l =	170	mm
f_y =	318	N/mm^2
E =	210000	N/mm^2
L_{cr} =	340	mm
$I_{z,eff}$ =	47130	mm^4
$A_{,eff}$ =	225	mm^2
i_z =	14,47	mm
α =	0,34	

$$\varepsilon = \sqrt{\frac{235}{f_y}} \quad (f_y \text{ in N/mm}^2)$$

ε = 0,85964743

$$\lambda_1 = \pi\sqrt{\frac{E}{f_y}} = 93{,}9\varepsilon$$

λ_1 = 80,720894

$$\bar{\lambda} = \sqrt{\frac{A_{eff} f_y}{N_{cr}}} = \frac{L_{cr}}{i}\frac{\sqrt{\frac{A_{eff}}{A}}}{\lambda_1} \quad \text{for Class 4 cross-sections}$$

λ = 0,256

$$\Phi = 0{,}5\left[1 + \alpha\left(\bar{\lambda} - 0{,}2\right) + \bar{\lambda}^2\right]$$

Φ = 0,542

$$\chi = \frac{1}{\Phi + \sqrt{\Phi^2 - \bar{\lambda}^2}} \quad \text{but } \chi \le 1{,}0$$

χ = 0,980

$$N_{b,Rd} = \frac{\chi A_{eff} f_y}{\gamma_{M1}} \qquad \text{for Class 4 cross-sections}$$

$N_{b,Rd}$ =	70125,6302	N
	70,13	kN

Attachment O: Calculation slip-resistance

3.9.1 Design slip resistance - EN 1993-1-8 (2005)

For the connection of the specimen on the top and bottom part of the construction, **M16 8.8 bolts** will be used

$$F_{p,C} = 0{,}7\, f_{ub}\, A_s$$

f_{ub} =	800	N/mm^2
A_s =	157	mm^2

$F_{p,C}$ =	87920	N
	87,92	kN

$$F_{s,Rd} = \frac{k_s\, n\, \mu}{\gamma_{M3}} F_{p,C}$$

k_s =	1
n =	1
μ =	0,3
γ_{M3} =	1,25

$F_{s,Rd}$ =	21100,8	N
	21,10	kN

This slip-resistance is calculated per bolt. We have a total of 6 bolts so the total slip-resistance will be equal to:

$F_{s,tot}$ =	126,60	kN

3.5 Positiong of holes for bolts - EN 1993-1-8 (2005)
According to table 3.3 p.23, the minimum spacing in mm can be determined as following:

e_1 =	1,2*d0		**M16**
e_2 =	1,2*d0	d0 =	18
p_1 =	2,2*d0		

e_1 =	21,6	mm
e_2 =	21,6	mm
p_1 =	39,6	mm

Attachment P: Determination of the dimensions

Calculations of dimensions (e1, e2, p1 and p2)

e_1	≥	5*d			
e_2	≥	3*d	with d =	6,3	mm
p_1	≥	5*d			
p_2	≥	5*d			

1-screw connection

e_1	≥	31,5	mm
e_2	≥	18,9	mm
b	=	50	mm

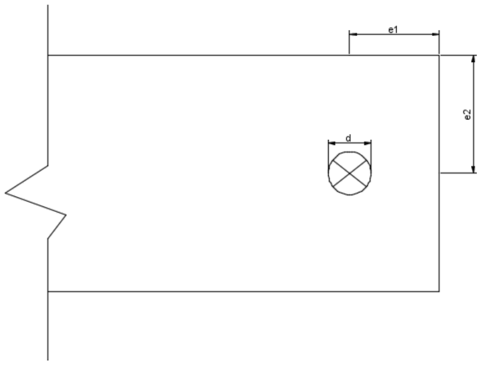

2-screw connection

e_1	≥	31,5	mm
e_2	≥	18,9	mm
p_2	≥	31,5	mm
b	=	70	mm

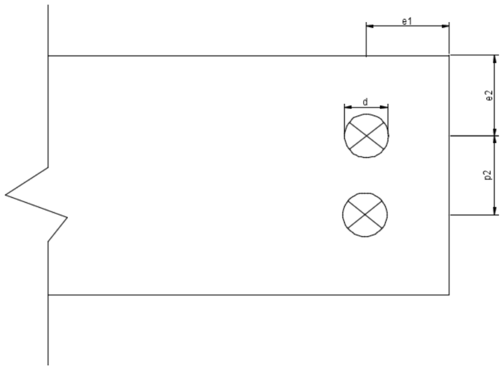

4-screw connection

e_1	≥	31,5	mm
e_2	≥	18,9	mm
p_1	≥	31,5	mm
p_2	≥	31,5	mm
b	=	70	mm

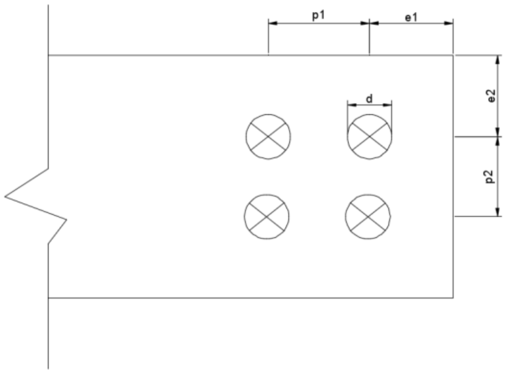

Auteursrechtelijke overeenkomst

Ik/wij verlenen het wereldwijde auteursrecht voor de ingediende eindverhandeling:
Impact of cyclic loading on shear screwed connections used in steel cold-formed structures

Richting: **master in de industriële wetenschappen: bouwkunde**
Jaar: **2017**

in alle mogelijke mediaformaten, - bestaande en in de toekomst te ontwikkelen - , aan de Universiteit Hasselt.

Niet tegenstaand deze toekenning van het auteursrecht aan de Universiteit Hasselt behoud ik als auteur het recht om de eindverhandeling, - in zijn geheel of gedeeltelijk -, vrij te reproduceren, (her)publiceren of distribueren zonder de toelating te moeten verkrijgen van de Universiteit Hasselt.

Ik bevestig dat de eindverhandeling mijn origineel werk is, en dat ik het recht heb om de rechten te verlenen die in deze overeenkomst worden beschreven. Ik verklaar tevens dat de eindverhandeling, naar mijn weten, het auteursrecht van anderen niet overtreedt.

Ik verklaar tevens dat ik voor het materiaal in de eindverhandeling dat beschermd wordt door het auteursrecht, de nodige toelatingen heb verkregen zodat ik deze ook aan de Universiteit Hasselt kan overdragen en dat dit duidelijk in de tekst en inhoud van de eindverhandeling werd genotificeerd.

Universiteit Hasselt zal mij als auteur(s) van de eindverhandeling identificeren en zal geen wijzigingen aanbrengen aan de eindverhandeling, uitgezonderd deze toegelaten door deze overeenkomst.

Voor akkoord,

Gielen, Chris **Moreels, Karsten**

Datum: **17/01/2017**